GREEN SYNTHESIS, CHARACTERIZATION AND ANTIMICROBIAL ACTIVITIES OF SELECTED SCHIFF BASES

JACKLINE NJERI NYAGA

A Thesis Submitted to the Graduate School in Partial Fulfillment of the Requirements for the Award of the Degree of Master of Science in Chemistry of Chuka University

CHUKA UNIVERSITY

OCTOBER, 2024

DECLARATION AND RECOMMENDATIONS

Declaration

This thesis is my original work and has not been presented for an award of diploma or conferment of degree in this or any university

Signature: ..... Date: 22/10/2024

Jackline Njeri Nyaga
SM11/29015/16

Recommendation

This thesis has been examined, passed and submitted with our approval as University supervisors

Signature: ..... Date: 22/10/24

Prof. Gichumbi Joel, PhD
Chuka University

Signature: ..... Date: 22/10/2024

Prof. Njagi Eric, PhD
Chuka University

DEDICATION

This research work is dedicated to my father Mr. John Nyaga, baby sister Miss Stella Wanja Nyaga and all my students at Ugweri Secondary School who wish to provide global solutions through education.

ACKNOWLEDGEMENT

I acknowledge the support and generous guidance accorded to me by my supervisors; Prof. Joel Gichumbi and Prof. Eric Njagi. They made this work achievable. I am grateful for their tireless efforts, professional advice and encouragement.

I would also wish to extend my gratitude to Prof. Ochieng' Ombaka for keeping me up to date with the departmental, school and board of post graduate studies requirements.

Further, I wish to give my regards to all the technical staff at the department of chemistry, Chuka University and my fellow Msc and PhD students for their advice and corrections.

Much love goes to my parents Mr. John Nyaga and Ms. Doris Muthoni for their continued support and love, my sister Miss. Stella Wanja for the continued support in my education journey.

Finally, I am thankful to God for my good health throughout the study duration.

ABSTRACT

Antimicrobial resistance is a serious global health challenge with alarming rates of emergence and spread of resistant microbes necessitating the development of novel antimicrobial agents. Schiff bases, also called imines or azomethines are synthesized from the condensation of aldehydes and amines. They have multiple properties including antibacterial and antifungal properties. Synthetic procedures of Schiff bases often involve the use of catalysts and solvents. The disposal of the latter, often leads to environmental pollution hence the need for the development of novel procedures that are applicable, environmentally friendly and economically realistic. Schiff bases were synthesized through grinding (for the solid aldehydes and amines) and stirring (for liquid aldehydes and amines) techniques without the use of catalysts and solvents in this work. This led to reduced reaction times, clean products, reduced possibility of pollution, no need for extra work up in the removal of solvents and catalysts and easy handling of the reagents. Six Schiff bases were synthesized. Schiff base S_1, from benzaldehyde and 4-aminophenol, S_2 from 4-aminophenol and 4-nitrobenzaldehyde, S_3 from 4-aminophenol and salicylaldehyde, S_4 from aniline and 4-nitrobenzaldehyde, S_5 from aniline and salicylaldehyde and S_6 from aniline and benzaldehyde. The compounds melted at constant temperatures demonstrating their purity. Characterization of the Schiff bases was done using FT-IR, UV-VIS and NMR (proton and carbon NMR) spectroscopy. Sharp IR peaks at 1628.95- 1617.38 cm^{-1} in the IR spectra of the compounds confirmed the formation of the imine bond, C=N. The disappearance of the carbonyl C=O peak at around 1600 cm^{-1} further confirmed the conversion of the aldehydes to imines. Free O-H broad bands were observed at 3447.91-3339.29 cm^{-1}. In compound S_3, the O-H band was shallow and broad which was attributed to keto-enol tautomerism. In the UV-Vis spectra, bands at 261.40- 287.60 nm were observed corresponding to the $n–\pi*$ transitions of the azomethine C=N bond. NMR peaks at 7.26- 7.54 ppm for ^1H NMR and 161.15- 158.34 ppm for ^{13}C NMR further confirmed the presence of the imine protons and imine carbon atoms respectively. The disappearance of free NH_2 peaks which usually occurs at 4.00- 6.00 ppm showed that the amines had been converted to imines. The synthesized compounds were subjected to antibacterial susceptibility tests against three Gram-negative bacteria (*Pseudomonas aeruginosa*, *Escherichia coli* and *Salmonella typhi*), one Gram-positive bacteria (*Staphylococcus aureus*) and one fungi *Candida albicans* at concentrations of 500 ppm, 250 ppm and 125 ppm. The zones of inhibition developed from 7.16- 20.00 mm on all the organisms at all concentrations indicating that all the compounds were biologically active. The data was analyzed using One- Way Anova. Significant difference between the means indicated that compounds with nitro and hydroxyl substitution had greater activity against gram negative bacteria while the compound lacking the substitution had better activity against gram positive bacteria. The compounds also showed better antifungal activity against *Candida albicans* than the positive control. This indicated that the compounds had great potential for development of antibacterial and antifungal drugs.

TABLE OF CONTENTS

LIST OF TABLES

LIST OF FIGURES

LIST OF SCHEMES

CHAPTER ONE
INTRODUCTION

1.1 Background Information

Green synthesis is a set of carefully planned synthetic techniques that aims at the production of essential chemical compounds while minimizing environmental pollution (Anastas and Eghbali., 2010). By definition, green synthesis is the design of chemical products and processes to reduce or eliminate hazardous substances. The most significant aspect of green synthesis is the concept of design, which is largely intentional rather than accidental since it involves planning and systematic conception (Anastas and Eghbali., 2010). Synergies are achieved through proper design of green synthesis procedures (Abdussalam-Mohammed *et al.,* 2020).

Most organic synthetic procedures often use catalysts and organic solvents like benzene, alcohols and chlorinated hydrocarbons which are highly toxic and volatile creating environmental havoc (Sachdeva *et al.,* 2014). Long term exposure to these solvents, especially benzene containing solvents has been linked to harmful effects on the respiratory, haematological and thyroid functioning (Uzma *et al*., 2008). Chemists are therefore constantly faced with the challenge of developing practical processes, reaction media, conditions and utility of materials based on the idea of green chemistry (Gopalakrishnan *et al*., 2006, Jain *et al.,* 2022). Green synthetic approaches are advantageous since they target the use of environmentally benign techniques with the main aim of reducing environmental pollution. In addition to that, they provide shorter reaction times, simple reaction conditions and enhanced yields making them very desirable (Simon and Li, 2012).

The synthesis of Schiff bases through green synthetic approaches can be achieved through several main directions such as use of bio-catalysts, use of renewable raw materials (biomass), alternative reaction solution (such as ionic liquids, supercritical fluids and water), alternative reaction circumstances (such as microwave activation) and new photocatalytic reactions (Abdussalam-Mohammed *et al.,* 2020). Omission of catalysts and solvents (dry media reactions) in the synthesis of Schiff bases in one pot synthetic approaches has been recently explored by various chemists (Simon and Li, 2012). Green synthesis has been achieved through various techniques which include

microwave irradiation, ultrasound sonication, grind stone synthesis and stirring (Kapadnis *et al.*, 2016, Gopalakrishnan *et al.*, 2006, Bendale *et al.*, 2011, Abdussalam-Mohammed *et al.*, 2020).

Schiff bases, also called imines or azomethines, are formed when a primary amine reacts with a carbonyl compound (an aldehyde or a ketone) (Aljamali *et al.*, 2021). They were first discovered by Hugo Schiff in 1864 (Fabbrizzi, 2020). Their synthesis involves a two-step process starting with nucleophilic attack of the primary amine on the carbonyl carbon of the aldehyde followed by a dehydration step. Often, an acid catalyst (including Lewis acids) is employed to serve as the dehydrating agent and also to speed up the nucleophilic attack (Bendale *et al.*, 2011).

Apart from acid catalyzed synthesis of Schiff bases, strong base catalysis and thermal conditions can also be applied. Schiff bases are mostly feebly basic though some form insoluble salts when they react with strong acids (Xavier and Srividhya, 2014). Stepwise, the synthesis of Schiff bases can be shown to take the pathway in Scheme 1.1

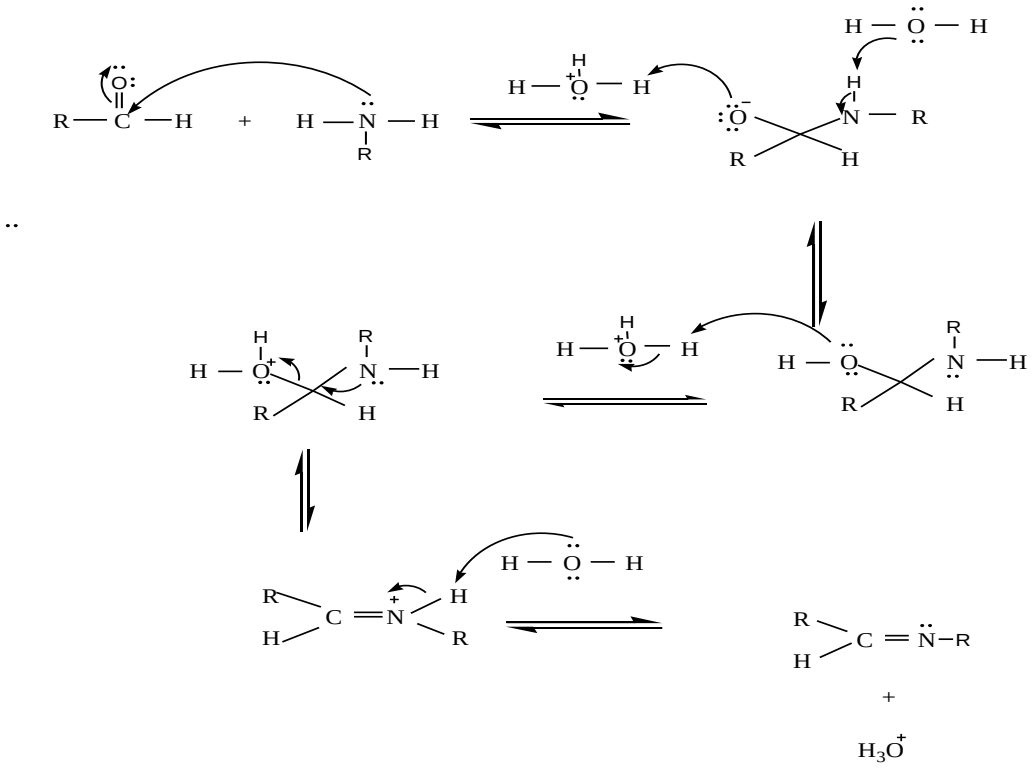

Scheme 1.1: Plausible mechanism of formation of a Schiff base
Bendale *et al.*, 2011

The conventional method of Schiff base preparation involves refluxing a mixture of amine and carbonyl compounds in organic solvents under azeotropic conditions (Jain *et al.,* 2022, Bendale *et al.,* 2011). This method (reflux) requires extra work up in the removal of solvents from the reaction mixture (Sachdeva *et al.,* 2014). Synthesis of Schiff bases can be carried out through stirring, microwave irradiation (Kapadnis *et al.,* 2016) ultrasound sonication, (Bendale *et al.,* 2011) grinding and handball milling methods (Cai and Luo, 2014) with minimal or total avoidance of use of solvents and catalysts in green synthetic procedures, a direction most chemists are recently taking (Bendale *et al.,* 2011). The appearance of brightly coloured products (bright yellow, red or orange) and amber coloured products characterizes Schiff base synthesis since it indicates conversion of the carbonyl compounds and amines into Schiff bases (Bendale *et al.,* 2011).

Dry media reactions are worth the attention they receive from chemists since they involve the use of solid acids, acid treated clays, zeolites, ion-exchange resins and metal oxides replacing highly corrosive, hazardous and polluting acids. Better regio-and stereo selectivity has been realized with solid acids in many organic synthesis approaches (Gopalakrishnan *et al.,* 2006). However, the removal of catalysts, supports, solvents (especially aprotic dipolar solvents with high boiling points) (Savalia *et al.,* 2013) and other auxiliaries is avoided through omission of the use of catalysts and solvents (Cai *et al.,* 2008).

The use of a microwave to irradiate amines and aldehydes or ketones has been widely applied in the synthesis of a variety of Schiff bases by speeding up the condensation process (Gopalakrishnan *et al.,* 2006). Panda (*et al.,* 2013), made reports on the synthesis of Schiff bases from isatin derivatives through microwave irradiation resulting in purer products (Panda *et al.,* 2013). Schiff bases from salicylaldehyde and aromatic amines have been synthesized by microwave irradiation (Chakraborty *et al.,* 2012). Similarly, water based synthesis of Schiff bases from substituted benzaldehydes and 3-chloro-4-fluoro aniline through microwave irradiation has been reported with a 73- 86% yield in 3- 6 minutes of reaction time (Naqvi *et al.,* 2009). In addition to that aromatic anilines and substituted benzaldehydes have been used to prepare Schiff bases under microwave irradiation using ß-ethoxyethanol as the wetting agent. ß-

ethoxyethanol is a polar molecule and it quickly absorbs microwaves thereby heating the mixture fast and effectively (Bhusnure *et al.,* 2015). Also, imidazole Schiff base derivatives have been synthesized under microwave irradiation in 2-4 minutes with a 90-98% yield once again proving the potency of microwave irradiation in Schiff base synthesis (Eftekhari *et al.,* 2020).

Ultrasonic irradiation has been used in the synthesis of Schiff bases by dipping an ultrasonic processor at an operating frequency of 16 kHz with a manually adjusted output of 104 watts directly in the reaction mixture (Venkatesan *et al.,* 2011). Similarly, reports of synthesis of Schiff bases from vaniline and *p*-toludine in a sonicator at 45^{o}C with and without the use of an acetic acid catalyst have been made. In the presence of the catalyst, the reaction took 9- 10 minutes while in the absence of the catalyst, the reaction took 13-15 minutes (Bendale *et al.,* 2011). Sonochemistry approach provides excellent yield, reduced reaction times and operational lucidness. This is attributed to the occurrence of acoustic cavitation that leads to creation, enlargement and caving in of gaseous and vaporous cavities in the irradiated substance. In the cavitation bubble, high local temperature and pressure is produced as it collapses thereby speeding up the rate of reaction (Arafa and Shaker, 2016). Synthesis of a Schiff base with great antiurease activity from 4-methylaniline and 4-nitrobenzaldehyde was achieved in 1.5 minutes at an optimum temperature of 50^{o}C with a yield of 89% by ultrasound sonication showing the supremacy of this method over reflux which took 16 hours to synthesize the Schiff base (Mermer *et al.,* 2019).

Under grindstone synthesis in a mortar and a pestle, Schiff bases from substituted benzaldehydes and 3-chloro-4-fluoro aniline was reported with a 53- 70% yield (Naqvi *et al.,* 2009). A mixture of vaniline and *p*-toludine was triturated in a mortar using a pestle for 10-12 minutes to prepare a Schiff base (Bendale *et al.,* 2011). An equimolar mixture of 2-chloro-4-nitroaniline and 5-bromo-2-hydroxybenzaldehyde were grinded in a mortar using a pestle in the presence of glacial acetic acid without a solvent for 3 hours. Thin layer chromatography indicated the conversion of the mixture to the Schiff base 4-bromo-2- (2-chloro-4-nitrophenyl) imino) methyl) phenol (Zulfiqar *et al.,* 2020). Garlic (a biocatalyst) assisted synthesis of Schiff bases from *p*-toluidine and a variety of aromatic aldehydes through grindstone technique in a mortar using a pestle has also

been reported (Bedi *et al.,* 2020). Mechano-synthesis has been widely used in green synthesis of Schiff bases and worth noting is the synthesis of Schiff bases using L-proline (an organocatalyst) showing the potency of this method in Schiff base synthesis (Majeed *et al.,* 2023).

Condensation of a mixture of an amine and a carbonyl compound can also be done through stirring. Uniform stirring is achieved through the use of a magnetic stirrer (Yadav and Mani, 2015). A Schiff base from aniline and benzaldehyde under natural acid catalysis was synthesized through stirring at room temperature for 5- 10 minutes. Grape juice, lemon juice and mango extracts were used as the natural acid catalysts at volumes ranging from 0.5 ml to 2.5 ml. Yields in grape juice were the highest followed by those in mango extracts then lemon juice (Yadav and Mani, 2015). A chitosan based Schiff base was prepared by dissolving 1 g of chitosan in 100 mL of 2% acetic acid. After stirring for 30 minutes in a magnetic stirrer to get a homogenous mixture, 1 mL of salicylaldehyde solution in ethanol was added with further stirring for 30 minutes more to obtain the Schiff base (Alharthi *et al.,* 2022). Stirring can also be coupled with reflux to improve the reaction outcome, reduce reaction time and attain pure products (Taj *et al.,* 2011, Alharthi *et al.,* 2022).

The main techniques in the characterization of Schiff bases are elemental analysis, ultra violet visible (UV/Vis) spectroscopy, infrared (IR) spectroscopy, nuclear magnetic resonance (NMR) spectroscopy and mass spectrometry (Raafat *et al.,*2005, Issa *et al.,* 2008, Nagesh and Mruthyunjayaswamy, 2015). In all the techniques, the presence of C=N (imine bond) confirms the formation of the Schiff base (Muhammad Kaleem *et al.,* 2015). In IR spectroscopy a band at around 1620- 1628 cm^{-1} corresponds to the imine bond stretch while the π-π* absorption bands of C=N appear at 224- 365 nm in the UV/Vis spectrum. Further, in the ^{1}H NMR spectrum, the imine protons occur at 8.00- 9.00 ppm while in the ^{13}CNMR the imine carbons occur between 155.65- 168.83 ppm (Gichumbi *et al.,* 2016).

The increase and spread of multidrug-resistant pathogens has necessitated the search for novel antimicrobial agents (Terreni *et al.,* 2021). Globally, it is estimated that 8.22 million deaths attributable to antimicrobial resistance could occur by the year 2050

million deaths attributable to antimicrobial resistance (Naghavi *et* al., 2024). Common pathogens include *Bacillus subtilis* (Gram positive bacteria) which is found in the soil and vegetation and causes ropiness. *Staphylococcus aurues* (Gram positive bacteria) found in the soft tissue, skin, wound infections and endovascular bone joint and cause pneumonia, scaled skin, toxic shock syndrome and sepsis. *Escherichia coli* (Gram negative) found in the lower intestines of warm-blooded animals and causes chloecystitis, bacteremia, urinary tract infections, bloody diarhoea and food poisoning (Aslam *et al.,* 2012). Globally, it is estimated that *Escherichia coli* causes 1.7 billion diarrhea cases with over 400,000 children under the age of five loosing their lives (Thystrup *et al.,* 2024). This organism is responsible for 17 million deaths globally every year. *Salmonella typhi* (Gram negative bacteria) that causes typhoid and enteric fever. *Pseudomonas aeruginosa* causes lung infections and kidney infections (Aslam *et al.,* 2012).

Antibiotics can be classified according to the mode of action. β-lactam antibiotics (penicillin, carbapenems, cephalosporins and monobactams) are known to bind to penicillin binding proteins which are responsible for peptidoglycan (PG) biosynthesis. PG is a key component in bacterial cellwalls. Aminoglycosides and tetracyclines block the bacterial ribosome at 30 S subunit inhibiting protein biosynthesis. Quinolone blocks bacterial DNA replication while sulfa drugs block folate coenzyme biosynthetic pathway (Kumar and Varela, 2013, Upmanyu and Malviya, 2020).

Antibacterial resistance is known to occur through various pathways which include enzymatic inactivation through destruction of the drugs reducing the drugs to a form that is inexpedient in bacterial inhibition (Kumar and Varela, 2013). Production of β-lactamases enzymes that render β-lactam antibiotics (penicillin, carbapenems, cephalosporins and monobactams) ineffective is one classical example of enzymatic inactivation. Genes encoding β-lactamases (*bla)* are either on the plasmids or the chromosomes (Dowling *et al.,* 2017). The TEM-1 and SHV (sulphydril variable active site) β-lactamase (plasmid bound) were discovered on *E. coli* and are together called extended spectrum β-lactamases (ESBLs) due to their ability to hydrolyze the β-lactam ring in many β-lactam antibiotics including a broad range of extended spectrum cephalosporins. Cefotaxime degrading enzyme CTX-M type was also discovered in

1990 in *E. coli*. Previously only gram-negative bacteria were known to be ESBLs producers but gram-positive bacteria have also developed this type of resistance raising the number of producers to more than 200 recently (Kumar and Varela, 2013). Enterobacteriaceases produce antibiotic hydrolyzing enzymes such as macrolide esterases and fosfomycin epoxidases which inactivate erythromycin A and oleandomycin by hydrolyzing the lactone ring. Although less studied, hydrolysis of the carbon-phosphorous (C-P) bond in the epoxide antibiotic fosfomycin by the C-P lyase enzyme complex is a resistance mechanism by many soil bacteria (Kumar and Varela, 2013).

Another pathway of antimicrobial resistance is through structural modification of the drug through transfer of a functional group (acyl, ribosyl, phosphoryl or thiol group) in an irreversible reaction is a mechanism known to affect aminoglycosides, fosfomycin, macrolides, lincomycin and chloramphenicol (Kumar and Varela, 2013). Ribosome protection preventing binding of tetracycline to microbial ribosomes was discovered in *Streptococcus spp.* Biofilm formation is one more mechanism of resistance especially in catheters, teeth paques, water environments and in wounds (Dowling *et al.,* 2017, Kumar and Varela, 2013)

Also, antimicrobial resistance is known to occur through variation of the drug target leading to its inability to bind to the biological targets. The biological drug targets include; protein synthesis machinery, nucleic acid synthesis proteins, cell wall synthesis apparatus and metabolic pathway enzymes. Alteration of the molecular targets occurs in many ways such as in DNA gyrase, a quinolone target, RNA polymerase, a rifampicin target and targets of other antimetabolite drugs such as sulfonamides (Kumar and Varela, 2013).

Similarly, reduced permeability through the presence of lipopolysaccharide (LPS) and porin channels in bacterial cell walls is another pathway of antimicrobial resistance. This consists of lipid A, polysaccharide and O-antigen. Bacteria that have LPS moiety are resistant to erythromycin, roxithromycin, clarithromycin and azithromycin. These include *Vibrio cholerae, Pseudomonas aeruginosa* and *Salmonella enterica. Klebsiella pneumoniae, Pseudomonas aeruginosa, Enterobacter aerogenes* and *Serratia*

marcescens exhibit resistance to β-lactams, aminoglycosides, chloramphenicol and fluoroquinolones via porin channels (McManus, 1997, Kumar and Varela, 2013, Guardabassi and Courvalin, 2005).

Moreover, *Escherichia coli* and *Staphylococcus aureus* exhibit antimicrobial resistance to tetracyclines and quartenary ammonium compounds through efflux pumps by either adenosine triphosphate (ATP) hydrolysis or ion gradient to efflux the drugs (Kumar and Varela, 2013). Often, resistance to a drug results from microbial variants that carry transferable multidrug resistance determinants (Kumar and Varela, 2013). The increase and spread of antimicrobial resistant pathogens can be attributed to overuse and misuse of drugs due to lack of awareness on antimicrobial use, hazards and resistance, overuse of antibiotics in agriculture, increased income levels leading to easy travel routes and biological factors related to the pathogen evolution (Dadgostar, 2019). Furthermore, discreet resistance spread patterns are supported by the lack of systematic data collection. Globally, only 42 countries systematically gather data regarding antibiotics in livestock (Dadgostar, 2019). Selection of appropriate antifungal agent(s) on individualized level is limited by poor prognosis associated with invasive fungal infections, understanding the activity and efficacy of the drugs and limited available drugs making treatment of fungal infections difficult in most parts of the world especially where resistance occurs (Miceli *et al.,* 2011). The azoles and polyenes are the most common antifungal agents especially for treatment of *Candida* and *Cryptococcus* infections (Kangogo *et al.,* 2011).

Schiff bases have been synthesized in large numbers due to their ease of preparation, high solubility in common solvents, variety of structures, specific features, high stability in different chemical fields, magnetic, spectral, redox and catalytic properties (Lemilemu *et al.,* 2021). They are also known to possess antibacterial, antifungal, anti-inflammatory, antioxidant and antiviral properties among other biological properties. Schiff bases from aldehydes and amines containing electron withdrawing groups such as the nitro group have shown greater potential as antimicrobial agents (Lemilemu *et al.,* 2021). The nitro group plays an important role in controlling synthesis, reactivity and enantioselectivities (Nunez *et al.,* 2013). In addition to that, Schiff bases from aromatic aldehydes with effective conjugation are particularly stable due to resonance

compared to those from aliphatic ones. Imines from aliphatic aldehydes readily polymerize affecting their activity (Sharif *et al.,* 2015).

Owing to their ease of preparation and biological activity against common disease causing microbes, Schiff bases have been considered as potent antimicrobial agents as well as promising molecules in drug development (Ceramella *et al.,* 2022, Gichumbi *et al.,* 2016). Schiff bases have chelating ability leading to formation of their metal complexes which also have widespread biological activities, catalytic properties as well as inhibitory action (Gichumbi *et al.,* 2016). Similarly, complexation is an important mechanism that can be used to remove heavy metals that are potentially harmful from biological systems thereby preventing some major conditions like tumor formation in cells (Sinicropi *et al.,* 2022). The azomethine functional group (C=N) is associated with biological activity due to its chelating ability (Ejidike and Ajibade, 2016).

Further, Schiff bases have free radical scavenging ability, can bind oxygen to redox systems exerting their ability to oxidize the DNA of the disease-causing microorganisms and have many other specific mechanisms of action against disease causing pathogens which if studied can lead to development of a new class of antimicrobial agents (El-Sayed *et al.*, 2013). In addition to that, the activity of these compounds is also attributed to their ability to form hydrogen bonds at the azomethine nitrogen with the active centers of various cellular constituents interfering with normal cellular processes of the microbes (Aslam *et al.,* 2012). Consequently, the interference of the synthesis of cellular walls leading to altered permeability of into the microbial cells, deactivation of various cellular enzymes that play vital roles in metabolic pathways and denaturing of cellular enzymes leading to death of the bacterial cells are some of the inhibitory mechanisms of Schiff bases (Aslam *et al.,* 2012).

Presence of various substituents in the aldehydes and amines precursors that are used in the synthesis of Schiff bases has led to increased activity against bacteria and fungi and the specific mechanism of inhibition of each Schiff base against various microorganisms should be studied (Hisaindee *et al.,* 2015, Aslam *et al.,* 2012). Compounds containing -OH substituents were found to be more active than those containing halogen substituents. However, chloride substituted compounds were found

to be active against gram negative bacteria (*Escherichia coli*, *Pseudomonas aeruginosa* and *Proteus mirabilis*) while o*rtho* and *para*-OH and -SH substituted compounds were found to be active against both gram negative and gram positive bacteria (*Escherichia coli*, *Pseudomonas aeruginosa*, *Proteus mirabilis*, *Staphylococcus aureus*, *Bacillus subtilis*, *Serratia marcescens* and *Staphylococcus epidermidis*) and fungi (*Aspergillus niger, Alternaria alternate, Penicillium roqueforti* and *Saccharomyces cerevisiae*) (Hisaindee *et al.,* 2015). *Ortho* sulfhydryl group and *para* -OH on aniline site had moderate inhibitory effect on bacteria and good antioxidant action hence the influence on fungal permeability (Hisaindee *et al.,* 2015).

Various reports indicate that Schiff bases derived from aromatic aldehydes and ketones are more stable than those from straight chain compounds while those having nitro and halo derivatives had greater antibacterial activity than those having furan and phenyl substituents (Salama *et al.,* 2015). Schiff bases from arylpyrazole and chitosan have shown considerable activity against a vast number of both gram negative (*Escherichia coli* and *Helicobacter pylori)* and gram-positive bacteria (*Streptococcus pneumoniae, Bacillus spp.,* and *Staphylococcus aureus*) as well as different fungi (*Aspergillus fumigates, Geotricum candidum, Trychophyton gypseum, Candida albicans* and *Syncephalastrum racemosum*) (Salama *et al.,* 2015). Their level of antimicrobiall activity is also influenced by the type of solvent used for *in vitro* analysis. A study by Shanty and Mohanan (2018) showed that Schiff bases that were dissolved in methanol (polar protic solvent) had greater activity than those that were dissolved in polar aprotic solvents (ethyl acetate, chloroform, acetonitrile and acetone) (Shanty and Mohanan, 2018). Generally, the compounds are very promising antimicrobial agents (Parekh *et al.*, 2005).

1.2 Statement of the Problem

Schiff base synthetic procedures involves the use of catalysts (like acetic acid, sulfuric acid and other mineral acids) and solvents (like hexane, benzene, dimethyl sulfoxide and chlorinated hydrocarbons) which lead to environmental pollution necessitating development of safer procedures that are applicable, environmentally and economically friendly. Green synthesis of Schiff bases has been done using various techniques such as microwave irradiation, ultrasound sonication, grinding and stirring with minimal use

of catalysts and solvents or using naturally sourced catalysts like citric acid from citrus fruits, mango extracts and tartaric acid from grapes. However, these methods have not been harmonized to come up with a standard procedure for use in green synthesis of Schiff bases. Solvent and catalyst free procedures have not been extensively explored as a standard pathway to green synthesis of Schiff bases.

Antimicrobial resistance is a major challenge to disease management and cure with constant emergence and spread of resistant microbes globally. In order to address antimicrobial resistance, development of novel antimicrobial agents is necessary. Most researchers who deal with green synthesis of Schiff bases stop at the possibility of synthesis and the antimicrobial activity of the compounds synthesized without further structure activity relationships studies to deduce the mode of antimicrobial activity of these compounds.

1.3 General Objectives

The general objective was to synthesize selected Schiff bases using a green chemistry approach, characterize the Schiff bases and investigate their antibacterial activity against *Escherichia coli, Pseudomonas aeruginosa, Salmonella typhi, Staphylococcus aureus* and antifungal activity against *Candida albicans*.

1.4 Specific Objectives

i. To synthesize selected Schiff bases using green synthetic approaches by grinding (for solid precursors) and stirring (for liquid precursors) in the absence of catalysts and solvents.
ii. To characterize the synthesized compounds using infra-red spectroscopy, UV/Vis spectrometry, melting points and nuclear magnetic resonance spectrometry.
iii. To determine the antibacterial and antifungal activities of the synthesized compounds against selected bacteria and fungi.

1.5 Research Questions

i. Can Schiff bases be synthesized through solvent and catalyst free grinding and stirring procedures?

ii. Can the Schiff bases synthesized be characterized through infra-red spectroscopy, UV/Vis spectrometry and nuclear magnetic resonance spectroscopy?
iii. Do the Schiff bases synthesized have significant antimicrobial (antibacterial and antifungal) activity?

1.6 Significance of the Study

The main focus of the study was to synthesize novel Schiff bases using green chemistry approaches so as to reduce environmental pollution that often accompanies most organic synthetic processes. In this study, solvent and catalyst free procedures were used in the synthesis of the Schiff bases through grinding techniques for the Schiff bases that were synthesized from solid amines and aldehydes. Stirring was done for the Schiff bases that were synthesized from liquid amines and aldehydes. The procedures used were environmentally safe, time saving, had high yields (greater than 70%) and produced highly pure compounds. Moreover, this study was a contribution to the existing knowledge on green synthesis of Schiff bases.

Worth noting is that characterization of the synthesized compounds was done using infra-red spectroscopy, UV/Vis spectrometry and nuclear magnetic resonance spectroscopy to elucidate their structure and for possible structure activity relationship studies.

The antibacterial and antifungal activity of the synthesized compounds was investigated with the aim of dealing with the emerging and rapidly spreading drug resistant microbes which has led to the increase in the demand for novel antimicrobial agents hence increasing the burden of disease. This is in line with the development plan by the Kenyan government aimed at reducing the burden of drug imports in realization of vision 2030. This was also meant to stop long exposure periods of the human population to the resistant microbes which has negative implications on the cells and could potentially cause non communicable diseases increasing the country's burden of disease further.

CHAPTER TWO
LITERATURE REVIEW

2.1 Green Chemistry Synthesis of Schiff Bases

The principles of green chemistry include prevention of pollution by avoiding the use of solvents and catalysts, designing of safer chemicals and solvents (preferably natural solvents like water), one-pot synthesis, multicomponent reactions, continuous processing and final waste reduction (Kar *et al.,* 2023). Tremendous efforts have been made by modern pharmaceutical industries towards identifying organic solvents with reduced ecological footprints in comparison to traditional approaches. Green solvents, which include water, lipid polymers, bio-ethanol, supercritical fluids and ethyl lactate are majorly applied in green organic synthesis (Talaviya and Majmudar, 2012).

In the synthesis of Schiff bases and other organic molecules, simple alkanols (methanol and ethanol) and alkanes (hexane and heptanes) are preferred while solvents like dioxane, acetonitrile, acids, formaldehyde and tetrahydrofuran are avoided. Alcohol-water solutions are also preferred compared to pure alkanols or propanol-water solutions (Talaviya and Majmudar, 2012). Ethanol is the most preferred solvent in the synthesis of Schiff bases through reflux method. Reflux involves heating of the reaction mixture and possible oxidation of ethanol to carbon (II)oxide and carbon (IV)oxide occurs with the latter being a major environmental pollutant (Camara and Iwasita, 2005). Also, ethanol can undergo parallel reactions forming acetaldehyde, acetic acid as well as carbon (IV)oxide (Camara and Iwasita, 2005) during reflux. Acetaldehyde and other carbonyl compounds such as formaldehyde are environmental pollutants. They are known to be carcinogenic and cause eye and nasopharyngeal irritation (Pal *et al.*, 2008). In order to avoid pollution, extra work in removing solvents and catalysts and production of extra unnecessary products, green chemistry is applied in the synthesis of Schiff bases (Naqvi *et al.,* 2009).

2.1.1 Grinding and Hand Ball Milling

In mechanochemistry, the mechanical energy produced by the shock or friction between two different surfaces is utilized in synthesis (Sachdeva *et al.,* 2012). Although grinding in a mortar with a pestle is used to generate enough mechanical energy to achieve desired synthesis, hand ball milling is preferred because it provides shorter reaction

times since the reactant particles collide leading to their fracture and activation and subsequent reaction through an intense energy exchange (Boruah *et al.,* 2021). Moreover, better trituration outcomes, such as homogeneity, is achieved by the use of a ball mill (Sachdeva *et al.,* 2012). The reaction leading to the formation of Schiff bases is exothermic (Naqvi *et al.,* 2009) and high yields can be accomplished by grindstone chemistry technique (Vibhute *et al.,* 2009).

Solid state, solvent free reaction are carried out using reactants alone (Liu *et al.,* 2019) or incorporating them with clays, zeolites, silica, alumina or other matrices (Naeimi *et al.,* 2006). Tight and regular arrangement of the molecules in the solid state enables reactions to occur more selectively when grinding technique is applied as opposed to solution state (Sachdeva *et al.,* 2012). Higher yields and reduced reaction times have been achieved through this method in comparison to reflux method (Naqvi *et al.,* 2009, Vibhute *et al.,* 2009). Schiff bases have been synthesized from 3-chloro-4-fluoroaniline and substituted benzaldehydes through grinding in a mortar and pestle for 5-10 minutes giving a 53-70% yield after recrystallization in absolute ethanol (Naqvi *et al.,* 2009). Higher yields (78-96%) from condensation of a series of 3,5-dichloro-2,4-dihydroxy benzaldehyde with substituted aniline was achieved in grindstone technique in a mortar and pestle at relatively shorter reaction times compared to conventional method (60-70% yield) (Vibhute *et al.,* 2009).

The formation of Schiff bases involve a two step process starting from addition leading to formation of carbinolamine followed by elimination of water (Scheme 2.1). The elimination of water is necessary so as to avoid hydrolysis of the imines to aldehydes or ketones and amines since the reaction leading to formation of Schiff bases is easily reversible. The removal of water is analogous to E_2 elimination of alkyl halides except that it is not concerted (Xavier and Srividhya, 2014).

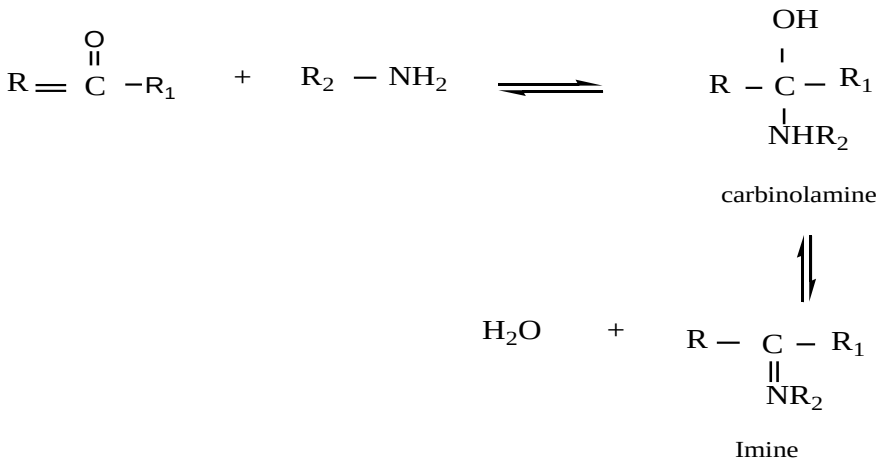

Scheme 2.1: A two-step solvent free synthetic procedure of a Schiff base
Xavier and Srividhya, 2014

Mild acidic conditions are maintained in Schiff base synthesis to prevent them from reacting with the acidic catalysts and also to prevent amine protonation that would make it a non-nucleophile shifting the equilibrium away from carbinolamine formation (Xavier and Srividhya, 2014). Rigorously anhydrous conditions are maintained during synthesis of imines to prevent them from hydrolysis by water (Xavier and Srividhya, 2014).

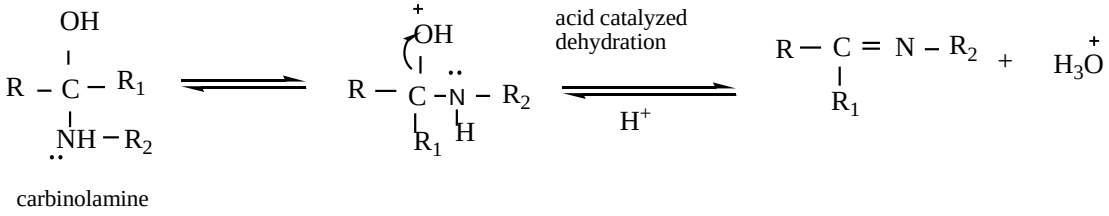

Scheme 2.2: Dehydration of carbinolamine
Xavier and Srividhya, 2014

2.1.2 Stirring

This is a method that involves mixing equimolar amounts of amines and carbonyl compounds to form imines (Yusuf *et al.,* 2020, Chigurupati, 2015, Sun *et al.,* 2017, Sachdeva *et al.,* 2014). Uniform stirring is achieved using a magnetic stirrer (Sachdeva *et al.,* 2014). Lesser reaction time is involved as the Schiff bases can be formed within 30 minutes of stirring (Sun *et al.,* 2017). Schiff bases from 5-fluorosalicylaldehyde with N-ethylethane-1,2-diamine and N, N-dimethylethane-1,2-diamine in methanol have

been prepared by stirring for 30 minutes at room temperature (Sun *et al.,* 2017). A Schiff base of 2-hydroxy-1-napthaldehyde and glycine has been prepared by stirring for 5 minutes then refluxing for 3 hours (Shinde *et al.,* 2014).

Reports of synthesis of a series of Schiff bases from substituted vanillin and various aromatic substituted amines in the presence of triethylamine, a basic catalyst have been made. Equimolar concentrations of vanillin and the amines with anhydrous ethanol as the solvent was used with stirring at 60- 70^{o}C for 6 hours in a water bath. The sample was evaporated at 65^{o}C using a rotary evaporator. Those with aryl substituents were more stable and were readily synthesized while those with alkyl substituents were relatively unstable. Those from aliphatic aldehydes were unstable and were readily polymerizable while those from aromatic aldehydes having effective conjugation were more stable (Chigurupati, 2015).

2.1.3 Microwave Irradiation

Molecules having dipole moments interact with microwaves leading to a sharp rise in temperature (Chemchem *et al.,* 2020). Microwave irradiation provides more precise and controlled volumetric heating, faster heating rates, lower energy consumption, improved quality and properties of the processed materials (Chakraborty *et al.,* 2012), amelioration of reproducibility (Chemchem *et al.,* 2020) reduced reaction time, minimized by products, reduced pollution, lower cost, improved yields and easier work up (Chemchem *et al.,* 2020).

Avoidance of toxic and low boiling solvents that could lead to accidents is afforded using microwave irradiation making the method safe, efficient and environmentally benign (Shinde *et al.,* 2014, Abirami & Nadaraj, 2014). Through microwave irradiation, Schiff bases of azetidinones have been synthesized using N,N-dimethyl formamide as a reaction mediator since it efficiently absorbs microwave energy through dipole rotation and can retain the water formed in the reaction thus avoiding the need for water separator. Shorter reaction times are afforded by this method compared to reflux method. A product that requires four hours to form under reflux typically takes three-four minutes in a microwave to form. For example, the reaction between 2-amino-4-(coumarin-3-yl)thiazole and substitute aldhydes took 2-3 minutes under microwave

irradiation and 5-6 hours under reflux (Naik and Desai., 2006). Formation of a Schiff base from salicyladehyde and *p*-aminophenol took $3^1/_2$ minutes under microwave irradiation while under reflux 4 hours were required for complete reaction (Savalia *et al.*, 2013).

Equimolar concentrations of the aldehyde and amine are used to prepare Schiff bases through microwave irradiation and heating is done at various temperatures for reproducibility (Chemchem *et al.,* 2020). Solid supports (montmorillonite clay), calcium oxide catalyst, cerium (III)-catalyzed synthesis of Schiff base as well as activated fly catalyzed synthesis of Schiff bases under microwave irradiation has been reported (Sachdeva *et al.,* 2012). Microwave synthetic yields are dependent on the amount of solvent used, temperature and microwave power (Chakraborty *et al.*, 2012).

The formation of Schiff bases is also influenced by the presence of electrondonating and electronwithdrawing groups (El-Gammal *et al.,* 2021). For example, in 4-methoxyaniline, resonance reduces the electrophilicity of the amine while in 4-nitroniline, the electron withdrawing property of the nitro group reduces the nucleophilicity of the amine group in the synthesis of Schiff bases through microwave irradiation (El-Gammal *et al.*, 2021).

Schiff bases of salicylaldehyde and substituted aromatic ketones were prepared at 300W microwave power and 80^{o}C temperature requiring 30 seconds to 2 minutes for the reaction to be complete (Chakraborty *et al.*, 2012). Activated fly ash catalyzed nucleophilic attack on carbonyl group of amine and final step dehydration leading to the formation of a Schiff base from 3,4-dimethoxybenzaldehyde and 4-nitroaniline through microwave irradiation (Gopalakrishnan *et al.*, 2006). The yield in microwave based synthesis depends on amount of solvent used, temperature and microwave power. Increase in temperature from 80^{o}C to 120^{o}C has shown increase in the yield of Schiff bases from 48% to 72% with further increase in temperature to 140^{o}C showing a decrease in yield in some studies (Chakraborty *et al.*, 2012).

Bis-Schiff bases from condensation of propane-1,3-diamine and halogen substituted aldehydes under microwave irradiation have been prepared as new, potent, selective

and less toxic antimicrobial agent. The synthetic procedure involved making a homogenous mixture of propane-1,3-diamine, halogen substituted benzaldehyde, acetic acid and ethanol which was then introduced into the microwave with the magnetic stirrer and irradiated at 50 W intermittently at 30 seconds intervals for 3 minutes. The solid formed was washed with water and recrystallized from ethanol to give bis-Schiff bases (Shinde *et al.,* 2014). The single mode technology assures safe and reproducible experimental procedures (Abirami & Nadaraj, 2014). 2-[(3-Methylquinoxalin-2-yl)oxy]acetohydrazide dissolved in dimethyl formamide (DMF) was added to heterocyclic/ aromatic aldehydes with a few drops of glacial acetic acid and the mixture transferred to a microwave oven to prepare a Schiff base (Achutha *et al.,* 2013).

2.1.4 Ultrasound Sonication

Ultrasonic sonication technique involves the use of an ultrasonic processor to synthesize Schiff bases (Venkatesan *et al.,* 2011). In the synthesis of Schiff bases, ultrasound sonication is often accompanied by shock cooling to obtain the product (Venkatesan *et al.,* 2011). According to hot spot theory, explosion of bubbles in solution cause local and instant increase in temperature and pressure leading to homolytic bond breakage (Bendale *et al.,* 2011). Reaction times are reduced by up to more than 80% by the use of this technique (Venkatesan *et al.,*2011). Equimolar aldehydes and primary amines have been used to prepare Schiff bases by placing them in an Ehlenmeyer flask and placing the flask in an ultrasonic water bath and adjusting the temperature to 40 ^{o}C (Chemchem *et al.,* 2020).

Mild conditions and easily controlled reactions are achieved using ultrasound sonication (Venkatesan *et al.,*2011). The accelerated reaction rate is ascribed to solid fragmentation and efficient mixing enabling mass transfer. In liquid- liquid phase transfer reactions, ultrasound sonication leads to homogenization which greatly increases the reactive interface and subsequently the reaction rate (Ooi *et al.,* 2000). Sonochemistry equipment that are most common are ultrasonic cleaning bath and ultrasonic probe. In ultrasonic cleaning bath, the flask containing the reagents is placed in a water bath and acoustic energy emitted by a transducer propagates through water to the reaction mixture where chemical changes occur while in ultrasonic probe, energy

is transmitted directly to the reaction mixture. This makes ultrasonic probe more efficient than ultrasonic cleaning bath (Chemchem *et al.*, 2020).

The presence of a catalyst in ultrasonic sonication procedures reduces the reaction times even further. Synthesis of Schiff bases through ultrasound sonication at 45^{o}C required 10-12 minutes while in the presence of an acetic acid catalyst the reaction was complete in 9-10 minutes (Bendale *et al.,* 2011). Generally, in organic synthesis, sonochemistry greatly improves the reaction outcomes, reduces reaction times and improves yields. For instance, improved yields in the epoxidation of α-β-unsaturated ketones and alkylation of carbonyl substrates were achieved through ultrasound sonication compared to mechanical stirring. Reduced reaction times and improved yields were also attained in the alkylation of isoquinoline Reissert compound and in 1,3-dipolar cycloadditions of pyridium ylides under liquid- liquid phase transfer conditions (Ooi *et al.,* 2000).

Solid state supersonic gas impacting at low temperature (from room temperature to 100^{o}C is increasingly being used for green chemistry due to simple manipulation, high selectivity and productivity and low cost that is associated with the technique (Cai & Luo, 2014). The technique eliminates possibilities of cross contamination, produces high yields in short times, uses solvent free procedures and the product is in submicron particle sizes hence do not require time consuming treatments (Guo *et al.,* 2020).

2.2 Conventional Method of Schiff Base Synthesis

2.2.1 Reflux Method

Reflux is a classical method that involves the use of catalysts and solvents. An ethanolic solution of an aldehyde and a primary amine were placed in the reaction mixture and the pH adjusted using an alkali (Khalil *et al.,* 2012, Al Zoubi *et al.,* 2017). The mixture was then refluxed with controlled heating for three to six hours and recrystallized in water and ethanol to obtain the solid that is then dried at room temperature (Al Zoubi *et al.,* 2017). An ethanolic solution of tryptamine hydrochloride and ethanolic solution of 4-amino-1,5-dimethyl-2-phenyl-3-pyrazol-5-one was heated at 40-50^{o}C for 14 hours and had a 53.59% yield after reflux in nitrogen and recrystallizing in water and ethanol (Al Zoubi *et al.,* 2017). Reflux under nitrogen gas has been applied in synthesis of Schiff bases followed by recrystallization in water and ethanol with a yield of 53% as

a greener version of this conventional method (Al Zoubi *et al.*, 2017). Schiff base synthesis by reflux under nitrogen gas using ethylenediamine and bisaldehyde in dimethyl sulfoxide (DMSO) has been reported. The solid mass formed was collected and washed in diethyl ether and crystallization was done in ethanol and dried over calcium chloride. This method is simple, low cost and gives desired products with precise control over reaction parameters. DMSO can also be used in this method to dissolve the aldehyde and amine. Washing of the product can also be done using diethyl ether and drying done using anhydrous calcium chloride (Khalil *et al.,* 2012). Often, thin layer chromatography is used to monitor the reaction progress in reflux (Shinde *et al.,* 2014).

In the view of reducing pollution, recyclable reaction media and catalysts have been used. The synthesis of Schiff bases under solvent free conditions and in polypropylene glycol as a recyclable reaction media has been reported. Water based synthesis has also been reported (Sachdeva *et al.,* 2014).

2.3 Characterization of Schiff Bases

2.3.1 Solubility Test

The solubility of the products is determined by dissolving the product to the solvent in a 1:2 ratio mass to volume respectively (Xavier and Srividhya, 2014). Schiff bases solubility has been tested in water, ethanol, acetone, benzene, dichloromethane, dimethyl sulfoxide (DMSO) and chloroform. They were mostly soluble in DMSO and DMF (Xavier and Srividhya, 2014). Investigations of the solubilities of chitosan based Schiff bases as a function of pH has shown that the solubility of Schiff bases highly depends on the molecular weight and the degree of substitution with hydrophilic groups (Barbosa *et al.,* 2019). Turbidity measurements with transmittance measured at 566 nm at different pH values showed that Schiff bases containing hydrophilic groups like the hydroxyl (-OH) are more soluble in protic solvents. They showed a transmittance close to 100% over the entire pH range. Increased solubility implies better penetration in biological systems hence better biological activity (Barbosa *et al.,* 2019). For substituted Schiff basess, keto-enol tautomerism equilibrium is greatly influenced by proticity and polarity of the solvents with organic solvents favouring formation of keto-

enol forms as opposed to polar solvents. Medium acidity causes dissociation of the keto-enol forms hence influencing the tautomeric equilibrium (Ferrari *et al.,* 2011).

2.3.2 Melting Points

A digital melting point apparatus is used to determine the melting points of the synthesized products so as to ascertain their purity (Fugu *et al.,* 2013). The melting points of various Schiff bases was tested by placing a little amount in a small capillary tune with one end fused. A thermometer was used to measure the temperature at which the substance begun to melt (Xavier and Srividhya, 2014). Sharp melting points indicate that compounds are pure (Fugu *et al.,* 2013, Mohamed *et al*., 2006). Compounds containing two hydroxyl (-OH) groups tend to form intramolecular hydrogen bonds increasing their melting points while keto-enol tautomerism in Schiff bases tend to lower their melting points (Cinarli *et al.,* 2011). Hydrogen bonding occurs between nitro and hydroxyl groups in Schiff bases that contain hydroxyl substitution thus increasing their melting points. However, generally Schiff bases tend to have low melting points ranging below 150 ^{o}C (Cinarli *et al.,* 2011.

2.3.3 Infra-red Spectroscopy

The bonds in a molecule vibrate through stretching and bending movements. The vibrations are in certain allowed vibration states. Infra-red (IR) radiation causes vibrational excitation of the bonds causing them to vibrate at higher vibrational states. This forms the basis of IR spectroscopy (Klein 2012, Stuart, 2004). The energy gap between vibrational states depends on the nature of the bond. For instance, C-H bond has a larger energy gap than a C-O bond and therefore will absorb a higher energy photon, a characteristic frequency. Samples are irradiated with IR radiation to determine which frequencies are not absorbed generating an IR spectrum via a mathematical operation called Fourier transform (Klein 2012). An IR spectrum is a plot of frequencies absorbed by the sample against the wave number (an absorption spectrum). The wave number is directly proportional to the frequency and its units are in cm^{-1}. IR spectrum ranges from 400- 4000 cm^{-1}. The left hand side of the frequency represents the higher energy radiation while the right hand side represents the lower energy radiation (Klein., 2012).

2.3.3.1 Sample preparation for IR Spectroscopy

Salt plates comprising sodium chloride, are used to prepare the sample for IR spectroscopy. Solid samples are dissolved in a suitable solvent and placed between two salt plates. A drop is placed between two salt plates for liquid samples and is called a neat sample. Samples that are not soluble are mixed with potassium bromide (KBr) and pressed into a thin transparent film called a KBr pellet (Klein., 2012). Schiff bases have been prepared for IR analysis by mixing 1.5 mg of the Schiff bases previously dried overnight at 60^{o}C with 100 mg of previously dried KBr mechanically. A disc was prepared from the mixed powder and dried for 15 hours at 110^{o}C under reduced pressure and introduced into the spectrometer (Santos *et al.,* 2005). Similar preparations for IR analysis of other Schiff bases have been done and a resolution of 2 cm^{-1} with 15 scans at a range of 4000-400 cm^{-1} in KBr pellet and in tetrachloromethane (CCl_4) solution (Ebrahimi *et al.,* 2014).

2.3.3.2 IR Spectrum

The wave number at which a bond absorbs IR radiation depends on the strength of the bond. Strong bonds absorb IR radiation at higher wave numbers. Single bonds, except those involving hydrogen, X-H; C-H, C-O, N-H, appear on the right hand side of the spectrum at wave numbers below 1500 cm^{-1}. Double bonds appear between 1600 and 1850 cm^{-1} while tripple bonds appear at 2100- 2300 cm^{-1} (Klein., 2012). In the characterization of Schiff bases the absence of the aldehyde characteristic band at around 1665 cm^{-1} confirms conversion of the aldehydes and amines to imines (Santos *et al.,* 2005). The imine bond stretch should occur at wave numbers of 1620-1628 cm^{-1} further confirming the condensation of the carbonyl compounds and amines forming imines (Gichumbi *et al.,* 2016). The $\tilde{\nu}_{max}$ for C=N of 2-methoxy-6-(4-methylphenyl) imino) methyl) phenol was found to be at 1626 cm^{-1} using the 8400s Shimadzu FTIR spectrophotometer (Bendale *et al.,* 2011). The IR spectrum of biopolymeric Schiff bases have been shown to have a strong absorption band corresponding to the C=N vibration band at around 1621-1627 cm^{-1} (Santos *et al.,* 2005). More reports of strong bands at 1620-1626 cm^{-1} corresponding to the imine C=N bond have been made (Uddin *et al.,* 2020).

Compounds with –OH substitution, especially salicylaldehyde based Schiff bases have shown bands at around 3340- 3386 cm^{-1} corresponding to the O-H bond (Uddin *et al.*,2020, Santos *et al.*, 2005). The amide band also appears at around 1655 cm^{-1}. Angular deformations of the N-H band at 1602 cm^{-1}, CH_3 at 1381 cm^{-1}, C-N at 1422 cm^{-1} as well as C-N axial deformation at 1323 cm^{-1} indicate intramolecular hydrogen bond interaction. In other reports by Uddin *et al.,* (2020), medium stretching vibration band attributed to C-N at 1235 to 1244 cm^{-1} is also observed. Formation of new bands that were absent in the precursors confirms conversion of the aldehydes and amines to imines. In the characterization of Schiff bases from chitosan and aromatic aldehydes, a new band at around 1540- 1590 cm^{-1} corresponding to a C=C aromatic ring that was not present in the original chitosan and a weak stretching vibration at 1575-1584 cm^{-1} attributed to C=C is observed also (Santos *et al.,* 2005, Uddin *et al.,* 2020).

2.3.4 Ultra-violet Visible Spectroscopy

Ultra violet visible (UV/Vis) spectroscopy provides information about conjugated double bonds in a compound. The basic principle of UV-Vis spectrophotometry is based on the measurement of wavelength and intensity of UV and visible light absorbed by a sample as a function of wavelength. Absorption of UV light by a molecule causes promotion of electrons from ground state to excited state in the orbitals of the chromophores (functional groups) and the easier it is to excite electrons the greater the wavelength that is absorbed (Pratiwi and Nandiyanto, 2022).

UV/Vis spectroscopy is carried out with solutions, vapours and gases and the standard cuvette contains pure solvent that does not absorb in the region. The choice of solvent to use in UV/Vis spectroscopy is dependent on the solubility of the sample in consideration since the sample must be converted into a clear solution. Some commonly used solvents are *n*-heptane, water, trifluoroethanol and hexafluoroisopropanol. The solvents are suitable since they are colourless (Perkampus, 1992, Pratiwi and Nandiyanto, 2022). In addition to being colourless, a good solvent must be pure, must not contain conjugated double bonds and must not interact with the molecules of the sample (Pratiwi and Nandiyanto, 2022).

2.3.4.1 UV/Vis Spectrum

Spectroscopy of organic compounds mostly are based on n – π* and π-π* transitions and for absorption in the UV/Vis region to occur, a chromophore (functional group that absorbs in the UV/Vis region) is required in the test compound (Gichumbi *et al.*, 2016). Absorption in the region causes electronic transitions, rotational transition and bonding electron vibrations in molecules. Carbonyl and nitro groups and associated systems do not show peaks in the UV/Vis region. n – π* transitions associated with C=O, C=N, N=N, -NO_2, -COOR, -COOH or -$CONH_2$ non conjugated chromophores occur at wave numbers 250- 360 nm. Arene-ruthenium complexes show absorption bands attributed to the n – π* and π-π* transitions respectively (Gichumbi *et al.*, 2016). The π-π* absorption bands of C=N appear at about 224-365 nm in acetronitrile (Gichumbi *et al.*, 2016). On a Perkin-Elmer Lambda 4B using silica glass cuvette with 1 cm path length at the range 200- 600 nm the C=N bands were observed at 275- 353 nm in another synthetic procedure (Issa *et al.*, 2008).

2.3.5 Nuclear Magnetic Resonance (NMR) Spectroscopy

Nuclear magnetic resonance **(**NMR) spectroscopy is based on the fact that a nucleus with an odd number of protons or an odd number of neutrons possesses a nuclear spin. A spinning proton can be viewed as a rotating sphere of charge which generates a magnetic field. When subjected to an external magnetic field the magnetic moment aligns with (α) or against (β) the external magnetic field and is quantized. The two spin states have an energy gap and when a nucleus occupying the α state is subjected to an electromagnetic radiation with photons of energy equivalent to the energy gap then an absorption can occur and the nucleus can flip to the β state. The frequency of radiation required for NMR falls in the radio frequency. Due to surrounding electrons, all nuclei do not absorb the same frequency of radiation (Klein., 2012, Ebrahimi *et al.*, 2014).

The sample is irradiated with short pulse covering the entire range of relevant radio frequencies. All the protons are excited and begin to return to their original spin states (decay) releasing energy in a particular way generating an electrical impulse in a receiver coil which records a complex signal called free induction decay (FID). The FID is then converted to a spectrum via a mathematical technique called the Fourier transform (Klein, 2012). The ^{13}C NMR and ^{1}H NMR spectra of Schiff bases has been

obtained by scanning with a field gradient operating at 500.14 MHz for proton observation and trimethylsilane (TMS) as internal standard and referenced 0.00 ppm with DMSO-d_6 and deuterated chloroform ($CDCl_3$) solvents. The experiments were done in unlock mode with enough scans to achieve a signal- to- noise ratio of 200:1 (ca). The spectra were obtained at a probe temperature of about 298 K (Ebrahimi *et al.,* 2014).

2.3.5.1 NMR Spectrum

An NMR spectrum is characterized by the number of signals, the location of the signals, the area under each signal and the shape of the signal (Vicha, 2014, Muhammad Kaleem *et al.,* 2015). Nuclear magnetic spectroscopy gives information about the protons and carbon present in the compounds. ^{1}H NMR provides information about the chemical environment of the proton involved through the chemical shift of the peak, number of protons through the intensity of the peak and information about the number of neighboring protons through the multiplicity (Muhammad Kaleem *et al.,* 2015).

^{13}C NMR spectroscopy basically shows interactions between electrons and the magnetic moments of atomic nuclei, or between two or more atomic nuclei (Vicha, 2014). ^{13}C NMR provides information to assign magnetically non-equivalent carbon atoms (example those of methyl, ethylene, aromatic, imine e.t.c) present in compounds. Imine carbons show peaks at 168.83- 155.65 ppm in deutrated DMSO (Muhammad Kaleem *et al.,* 2015). The ^{1}H NMR spectra of compounds in deutrated solvents show the absence of chemical shifts for amino protons which confirms the formation of the final product (Sharaby *et al.,* 2017). The imine protons show singlets a range of about 8.32-9.71 ppm (Issa *et al.,* 2008).

^{1}H NMR and ^{13}C NMR confirms formation of complexes by monitoring the imine proton and carbon signals in the ligand and the complex (Gichumbi *et al.,* 2016). The -CH=N protons for a novel bis-Schiff base appeared at 8.00- 9.00 ppm in the ^{1}H NMR spectra while in the ^{13} C NMR spectra, the imine carbons appeared within 160.00 to 165.00 ppm (Shinde *et al.,* 2014).

2.4 Applications of Schiff Bases

Synthesis of a large number of Schiff bases has been done due to their important properties such as the ability to reversibly bind oxygen, catalytic activity in hydrogenation of olefins, photochromic properties and complexing ability towards toxic metals (Khalil *et al.*, 2012). They are highly useful as antibacterial, antifungal, antiviral (Berhanu *et al.,* 2019), anti-inflammatory, anticancer and antipyretic agents (Uddin *et al.,* 2020).

The imine functional group (C=N) is known to be responsible for most of the activity shown by Schiff bases since the lone pair of electrons on the nitrogen atom is known to interact with other molecules through hydrogen bonding and other mechanisms (Aljamali *et al.,* 2021).

2.4.1 Antioxidant Properties

Schiff bases also show great scavenging activity on free radicals. The presence of hydroxyl groups in Schiff bases is known to improve their scavenging activity. Those with more than one hydroxyl group showed better scavenging properties (Miar *et al.,* 2021). A study on 1,1-diphenyl-2-picryl hydrazyl (DPPH) showed greater antioxidant properties due to the presence of 2,3 di-hydroxyl groups compared to compounds having 3-hydroxyl, 2,5- di-hydroxyl and 2,4,6-trihydroxyl groups. Compounds containing one or more hydroxyl groups showed better activity than those containing methoxy groups (Miar *et al.,* 2021).

Quantum mechanics calculations showed that the Highest Occupied Molecular Orbital (HOMO) and the Lowest Unoccupied Molecular Orbital (LUMO) energies, electronegativities and chemical softness of the molecules are effective on the explanation of their antioxidant activities (Miar *et al.,* 2021). Chitin from armors of crustaceans (*Astacus leptodactylus*) from lake Sevan, Armenia was converted to chitosan (the deacetylated derivative) and was used to synthesize novel Schiff bases and their metal which were biocompatible, biodegradable, nontoxic and had excellent antioxidant properties (Gavalyan, 2016).

2.4.2 Antifungal Properties

Common pathogenic fungi in humans include *Aspergilus niger* and *Candida albicans.* Fungi not only affect the skin but internal organs too. A human adult's skin produces sebum, a natural antifungal agent. This substance prevents regular and common fungal attacks (Shinde *et al.,* 2014). Antifungal agents include; propionic acid and its salts, benzoic acid caprylates and the azole antifungals (fluconazole, clotrimazole, ketoconazole e.t.c) (Kangogo *et al.,* 2011). Schiff bases are known to exhibit antifungal properties. The imine derivatives of quinazolinones are known to possess antifungal properties against *Candida albicans, Trichophyton rubrum, Trichophyton mentagrophytes, Aspergillus niger* and *Microsporum gypseum*. Benzothiazole or phenyl-azo-thiazole derived Schiff bases and complexes with benzoylpyridine as well that of copper (II) with benzoylpyridine show antifungal properties against a number of pathogenic fungi (Kumar *et al.,* 2009).

The antifungal activity of Schiff bases is influenced by the substituents on the compounds. Halogen substituted Schiff bases such as fluoro substituted benzophenone imines showed greater antifungal activity than those substituted differently (Muhammad Kaleem *et al.,* 2015, Shinde *et al.,* 2014). Structural changes in fungi due to mutations have made their targeting by antifungal drugs harder leading to many cases of resistance especially in HIV/Aids patients making the synthesis of novel Schiff bases necessary as potential antifungal agents (Kangogo *et al.,* 2011).

2.4.3 Antifungal Resistance by *Candida albicans*

A worldwide study involving 205,329 *Candida spp* and other yeast isolates from 40 countries between the year 1997 and 2005 showed reduced susceptibility to fluconazole and voriconazole. There has since been a continued trend in resistance to antifungal agents with HIV/AIDS patients being the most affected (Pfaller *et al.,* 2013). Poor therapeutic outcomes and high minimum inhibitory concentrations have been reported in *Candida albicans* and the mechanism of resistance is through reduction of ergosterol content in the cell membrane (Perlin *et al.,* 2017).

An increase in resistance toward fluconazole by *Candida albicans* was noted in Ecuador and Colombia (Pfaller *et al.,* 2013). Treatment with azole antifungals lower

the cellular sterol and can confer polyene resistance (Perlin *et al.,* 2017). In Boston (USA) two tertiary care cancer centres reported fluconazole resistance in *Candida spp.* while in France resistance to caspofungin was reported 30 days after treatment with fluconazole, a case of cross resistance (Perlin *et al.,* 2017).

Emergence and spread of non *albicans Candida* infections arising from increasing age, long duration of catheter use, recent gastrointestinal surgeries, glucocorticoid therapy, candiduria, diabetes and intravenous drug use is a major concern cross resistance of azole and echinocandins has been demonstrated in *Candida albicans, Candida tropicalis, Candida parapsilosis and Candida glabrata*. MDR *Candida glabrata* is beginning to emerge (Sanguinetti *et al.,* 2015). All *Candida albicans* and *Candida glabrata* isolated in South Africa in a study showed susceptibility to micafunginand, intermediate resistance to caspofungin and complete resistance to anidulafungin. 50% of *Candida albicans* showed resistance to azoles in Cameroon and South Africa. A further resistance to amphotericin B and 5-flucytosine in *Candida albicans* was reported in South Africa (Sanguinetti *et al.,* 2015).

In Cameroon and Kenya, susceptibility of *Candida albicans, Candida krusei* and *Candida tropicalis* to echinocandins was reported but resistance was reported in *Candida glabrata* (Dos Santos Abrantes *et al.,* 2014). Antimicrobial resistance can be reduced and eradicated through combinatory drug therapy, discovery of novel antimicrobial agents and use on novel drug delivery systems such as use of nano particles (Khameneh *et al.,* 2019).

2.4.4 Antibacterial Activity

Schiff bases show moderate to excellent antibacterial activity due to the lone pair of electrons on the imine nitrogen atom. In an attempt to identify potent and safer antibacterial agents, efforts have been focused in the synthesis of novel Schiff bases. Compounds containing aromatic rings show better antibacterial activity against common bacteria like *Escherichia coli* and *Staphylococcus aureus* (Sharif *et al.,* 2015) and stability than those containing allylic substituents (Rani *et al*., 2015). Pyridine-2,6-carboxamide derived Schiff bases showed higher antibacterial activity against *Escherichia coli, Staphylococcus aureus* and *Bacillus subtilis* bacteria than

streptomycin and those that had methoxy, chloro, fluoro and thienyl substituents showing better activity that the unsubstituted one (Al-Omar and Amr, 2010).

Substitution majorly influences the activity of Schiff bases and keto-enol tautomerism can occur at the imine bond in Schiff bases containing *ortho*-hydroxyl groups leading to tautomers of different activities (Ceramella *et al.,* 2022). *Bis* Schiff bases showed good to moderate inhibition at 12.5- 200 mg/mL in DMSO with better activity being exhibited in Gram negative than Gram positive bacteria. The good activity was attributed to the pharmacologically active -Cl, -OH, -OEt and -Ome groups attached to the phenyl group in addition to the C=N group (Shinde *et al.,* 2014). Schiff bases containing -OH, chloro and cyano substituents close to the imine group show good antibacterial activity against *Staphylococcus aureus* and *Escherichia coli* (Shinde *et al.,* 2018). Schiff bases having sulphur atoms are known to exhibit good antibacterial activity against, *Escherichia coli* and *Bacillus subtilis* while those with nitrogen atoms show good activity against *Staphylococcus aureus* and *Salmonella enteritidis* (Rani *et al.,* 2015).

Although studies show that Schiff bases with heteroatoms such as oxygen and nitrogen have better antibacterial activity, a compound with a cyclopentane ring showed better activity against two gram positive bacteria (*Bacillus subtilis* and *Staphylococcus aureus*) and two gram negative bacteria (*Escherichia coli* and *Pseudomonas fluorescence*) showing that simpler and smaller alicyclic rings gave better activity (Shinde *et al.,* 2014).

Schiff bases also exhibit auto florescence, which is attributed to the $n \rightarrow \pi^*$ transition of the $C{=}N_{imine}$ bond, a property that is useful in monitoring the efficacy of pharmacological carriers *in vivo* thereby avoiding the use of fluorochromes (Aragon-Muriel *et al.,* 2022). The stability of imines decreases with increase in pH because the imine bond prevents reversibility against external factors such as pH, a very useful characteristic at the time of drug release (Aragon-Muriel *et al.,* 2022).

Schiff base activity in biological systems is sometimes enhanced by complexation with metal ions (Liu and Hamon., 2019). This can be explained on the basis of Overtone's

concept and Tweedy's chelation theory. Often, there is a decrease in polarity of the central metal atom after chelation due to partial sharing of the positive charge with the donor groups (Schiff bases) and due to the π-electron delocalization on the whole chelate ring as is the case in Zirconium-Schiff bases. This favours the interaction of the complexes with the lipids and polysaccharides making up the microbial cell walls and membranes breaking down the permeability barrier and obstructing normal cell processes (Mounika *et al.,* 2010). Moreover, complexes exhibit high values of electric dipole moment, which may favour their dipole- dipole and dipole- induced interactions with high dipole moment species in biological systems. A large dipole moment and a higher polarizability of the target site leads to greater strength of interaction or affinity. A zinc (II) ceftriaxone based Schiff base complex with a dipole moment (10.225 Debye) showed very high biological activity against *Staphylococcus aureus* and *Escherichia coli* compared to the free ceftriaxone antibiotic (Anacona *et al.,* 2021).

Staphylococcus aureus and *Escherichia coli* are the leading cause of postpartum infections. Postpartum endometritis is the most common nosocomial infection leading to high morbidity and difficulty in recovery after delivery (Anacona *et al.,* 2021). Ceftriaxone based Schiff base, which was synthesized by a reaction between ceftriaxone and 2,6-diamino pyridine and its metal complexes showed inhibitory zones of 40- 42 mm and 46- 48 mm for *Escherichia coli* and *Staphylococcus aureus* respectively. Most compounds showed greater activity against *Staphylococcus aureus (*gram positive) than *Escherichia coli* (gram negative) (Anacona *et al.,* 2021). This could be explained by the differences in the cell membrane structure and the cell wall composition influencing bacterial permeability as well as on the differences in ribosome of microbial cells. The cell walls of gram negative bacteria are more complex than that of gram negative bacteria (Kim *et al.,* 2015). In addition, differences in the antibacterial activity may arise due to steric, electronic, pharmacokinetic factors along with mechanistic pathways (Anacona *et al.,* 2021).

2.4.5 Antibacterial Resistance by selected Bacterial strains

The emergence of drug resistant bacteria has been attributed to the changing structures of bacteria rendering the drugs in the market less effective in targeting the bacteria (Petty *et al.,* 2014). Bacteria cells can either be Gram positive (having a cell wall

thickness of about 20-40 nm and give a positive result for the Gram stain test appearing purple under the microscope) or Gram negative (having a cell wall thickness of about 2-7 nm and do not retain the crystal violet stain hence appearing pink under the microscope) (Kim *et al.*, 2015). Gram negative bacteria have in addition to the cell wall, a lipopolysacharides membrane that makes it quite difficult for them to be targeted by antibacterial agents (Kim *et al.*, 2015). Some of the Gram negative bacteria include *Escherichia coli, Pseudomonas aeruginosa, Helicobacter pylori, Salmonella typhi* and *Klebsiella pneumoniae,* while some of the Gram positive include *Staphylococcus aureus, Bacillus anthracis* and *Mycobacterium spp* (Bharti *et al.*, 2010). Schiff bases synthesized from thiosemicarbazide and carbonyl compounds were found to contain moderate to strong antibacterial against Gram negative bacteria *Escherichia coli, Salmonella typhi, Pseudomonas aeruginosa, Klebsiella pneumoniae* and *Vibrio cholerae* (Bharti *et al.*, 2010).

Centre for disease control and prevention (CDC) (Dadgostar, 2019) reports that more than two million people in the United States become ill with antibiotic-resistant diseases every year, resulting in a minimum of 23,000 deaths (Dadgostar, 2019). Most antibiotics contain the β-lactam (*beta*-lactam) ring in their structure. These include penicillin, cephalosporins and carbapenems. This ring is known to be responsible for their activity. However, the emergence of bacterial strains that can hydrolyse the β-lactam ring by producing β-lactamase enzyme renders the drug ineffective in eliminating the bacteria leading to antibacterial resistance. Schiff bases are important intermediates in the synthesis of β-lactam antibacterial agents and their presence in the drug structure enhances the activity of the drugs (Figure 2.3 and Figure 2.4) (Petty *et al.*, 2014).

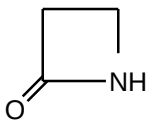

Figure 2.1: Structure of the β-lactam ring
Petty et al., 2014

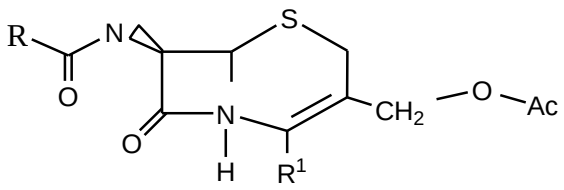

Figure 2.2: Structure of a cephalosporin antibiotic
Petty et al., 2014

In India, the Philippines, Russia and South Africa, tuberculosis (TB) infection rates have always been high and multi-drug resistant TB is projected to escalate significantly by 2040 (Dadgostar, 2019). Drug resistance in HIV/Aids patients in Sub-Saharan Africa is at 60% threatening the global goal of putting an end to Aids by 2030 (Dadgostar, 2019). A 1% economic loss in the USA and a 5-7 % loss for developing countries is estimated by 2050 resulting from loss in productivity due to death and hospitalization, use of combinatory drug regimens to combat resistance and loss of exports from labor intensive sectors is estimated by 2050 (Dadgostar, 2019).

Modern treatment procedures, which include transplants, technical surgeries, hospitalization and Intensive Care Unit (ICU) depend on antimicrobial agents that help in the healing and recovery processes (Bajpai *et al.*, 2013, Chalmers and Pletz, 2017). Antimicrobial resistance contributes to different complications for chemotherapy, dialysis, surgery and joint replacement especially for people with chronic illnesses like diabetes, asthma and rheumatoid arthritis patients forcing the use last-resort classes of medicines such as the carbapenems and polymyxins which are not readily available in developing countries and have many undesirable side effects (Chalmers and Pletz, 2017).

Antibacterial agents can be classified according to their mode of action. Sulphonamides and sulphones, example cotrimazole inhibit cell metabolism, penicillin and cephalosporins (*β-lactams*) inhibit cell wall synthesis, aminoglycosides, tetracyclines and chloramphenicol inhibit protein synthesis, quinolones inhibit nucleic acid transcription and replication and valinomycin, polymyxin and gramicidin interfere with the activity of the plasma membrane (Coates *et al.*, 2011).

Existing drugs mainly target enzymes, membranes and the DNA of the disease causing microorganisms inhibiting cell metabolism, cell wall synthesis, protein synthesis and nucleic acid transcription and replication (Bajpai *et al.,* 2013). Antibacterial resistance originates from innate resistance or through acquisition of resistant genes through transferable genetic elements like plasmids, transporons and integrons, mutations of chromosomal DNA (Petty *et al.,* 2014, Bello-Lopez *et al.,* 2019) biofilm formation (Perlin *et al*., 2017), ribosomal protection, decrease in porin, enzymatic inactivation, DNA deletion and modification of the cell membrane and cell walls leading to drug efflux (El-Garch *et al.,* 2010). Although vaccines such as pneumococcal conjugate vaccines (PCVs) have significantly reduced the carriage of vaccine type pneumococci, increased exposure to the vaccines on non-vaccine type serotypes has led to acquired resistance (Hackel *et al.,* 2013). The introduction of PCVs has highly contributed to the emergence and spread on nonencapsulated *Streptococcus pneumoniae* (NESP) through mutations. NESPs are difficult to target using common antibiotics (Keller *et al.,* 2016). Antifungal resistance is largely attributed to drug pharmacokinetics, host factors, site of infection, the pathogen itself and its susceptibility to the drug and prophylactic treatment (Pfaller *et al.,* 2013, Mane *et al.,* 2016). The rising incidences of systemic opportunistic fungal infections especially in Sub Saharan Africa is associated to AIDs pandemic, prolonged antimicrobial therapy, invasive procedures and immunosuppressive therapy (Kangogo *et al.,* 2011).

2.4.5.1 *Klebsiella pneumoniae*

The recent increase of identification and spread of carbapenemase producers is alarming as these have been considered as the drugs of last resort. *Klebsiella pneumoniae* carbapenemase (KPC) producer was first identified in 1996 in the Eastern United States of America and has since spread to the contiguous parts of the states particularly Puerto Rico, Columbia, Greece, Israel and the People's republic of China. Outbreaks of KPC have been reported in South America and in many European countries with limited treatment options since KPC producers are multidrug resistant leading to 50% death rates after infections (Nordmann *et al.,* 2011). New Delhi metallo-β-lactamase-1 (NDM-1) producers have also been identified in *E.coli* ST-131 and *Klebsiella pneumoniae* and since its discovery from an Indian patient in 2008 in Sweden, it has been identified in all continents except Central and South America with

most cases having a direct link to the Indian subcontinent. The *bla*NDM-1 gene is not associated with a single clone and can be found in plasmids harboring other carbapenemases genes like OXA-48, macrolide resistant genes, aminoglycoside resistant genes etc., leading to multidrug resistance (Nordmann *et al.,* 2011).

2.4.5.2 *Escherichia coli*

Escherichia coli sequence type 131 (ST131) arose from a single progenitor *Escherichia coli* and diverged into three sub lineages before the year 2000 (Petty *et al.,* 2014, Pfaller *et al.,* 2013). It is a multidrug resistant (MDR) clone responsible for resistance towards fluoroquinolones, aminoglycosides, trimethoprim-sulfamethoxazole and carbapenems. It is globally disseminated in Canada, Australia, India, Spain, United Kingdom and New Zealand and is responsible for high proportion of urinary tract and bloodstream infections (Petty *et al.,* 2014). Metallo- β-lactamases producing *Escherichia coli* strains have been identified in Japan and spread quickly to Taiwan and Greece. The strain was then identified in Sweden from an Indian patient who was previously hospitalized in New Delhi and the strain has since been identified in all continents except Central and South America (Pfaller *et al.,* 2013). *Escherichia coli* strains that produce carbapenenamases (β-lactamase enzymes) that hydrolyses the carbapenems have been identified in Puerto Rico, Colombia, Greece, Israel, the people's republic of China and South America since it was first discovered in the United States of America (Nordmann *et al.,* 2011).

In Africa, two hundred and seventy-three isolates of *Escherichia coli* obtained from seven hospitals in Lagos, Nigeria were screened for fluoroquinolone resistance and showed a 22.3% increase from the 0-2% rates that were present between 1994 and 1999 (Okeke *et al.,* 2007, Shah *et al.,* 2016). Data collected from the urban areas of Kenya and non-urban areas of Ghana and Zimbabwe showed antibacterial resistance by *Escherichia coli* towards ampicillin, oxytetracyclin, ciprofloxacin and trimethoprim. Higher levels of resistance were recorded from the data obtained from the urban areas than that from the non-urban areas (Okeke *et al.,* 2007).

Multidrug resistance by *Escherichia coli* has been recorded in Gabon, Kenya, Nigeria, Senegal and Tanzania and the failure to contain these resistant organisms and genes

causes adverse consequences if infection occurs making it hard to contain childhood diarrhea, persistent infections and diarrheal pathogens in AIDS patients (Okeke *et al.,* 2007, Shah *et al.,*2016). In Kenya, diarrheagenic *E. coli* (DEC) is the leading cause of diarrhea in children, which in turn is the second leading cause of deaths for children below five years. Data collected from the pediatric unit of Kiambu County Hospital showed some resistance to carbapenems, quinolones cephalosporins and major resistance to amoxicillin erythromycin and sulfonamides with multidrug resistance patterns (Shah *et al.,* 2016).

Tetracycline was the drug of choice in Africa for the treatment of *Escherichia coli* related infections until the end of 1970's when incompatible group C tetracycline resistant plasmids were isolated in Tanzania, Kenya and other parts of Africa necessitating the replacement of tetracycline with trimethoprim-sulfamethoxazole. Further replacement has since been made to quinolones due to further emergence of resistant strains (Okeke *et al.,* 2007). Samples from Kenya, Ghana and Zimbabwe showed resistance to ampicillin, oxytetracycline and trimethoprim and the gene encoding resistance in the three drugs for each country was found to be located on the same plasmid (Nys *et al.,* 2004) indicating the spread of resistant microbes in Africa.

2.4.5.3 *Helicobacter pylori*

A global study conducted between January 2006 and December 2009 showed that *Helicobacter pylori* was resistant to clarithromycin, amoxicillin, metrinidazole, tetracycline, rifabutin with increased resistance towards metrinidazole, clarithromycin and levofloxacin in Europe, America and Africa. Patients with non-ulcer dyspepsia showed higher resistance towards clarithromycin while those with peptic ulcer had higher resistance to metronidazole (De Francesco *et al.,* 2010). *Helicobacter pylori* resistance to clarithromycin, metrinidazole and cevofloxacin in 18 European countries was at 17,5%, 34.9% and 14.1% between year 2008 and 2009. A rise in resistance from 18.9% to 27.7% in Japan has been recorded and although the rates of resistance in the United States of America remains relatively constant due to immunization, the methods of eradicating the bacteria are on the decline (Thung *et al.,*2016). A potential antibiotic, furazolidone was declared by Thung *et al.,* (2016) but *Helicobacter pylori* resistance was reported at 16.8% in China, 13.8% in India and 21.6% in Iran related to six

mutations in porD and oorD genes on the chromosome of *Helicobacter pylori* (Thung *et al.,* 2016).

Helicobacter pylori resistance in Africa was detected through a study on 324 isolates and associated to mutations on A2143G gene. This conferred to clarithromycin and quinolone resistance. Out of the 324 isolates, 41 were resistant to metronidazole and tetracycline (Jaka *et al.,* 2018). Africa has the highest prevalence of up to 70.1% to *Helicobacter pylori* with Nigeria topping at 87.7% (Smith *et al.,* 2019). DNA transformation and sequencing was used to determine the role of rdxA in metronidazole susceptibility showing up to 69% resistance to at least 8 μg of metronidazole per millilitre in African *Helicobacter pylori* strains (Secka *et al.,* 2013). The bacteria is responsible for 90% of duodenal ulcers and 70% of gastric ulcers. Apart from metronidazole, clarithromycin, amoxicillin and tetracyclines are also used for the treatment of *Helicobacter pylori* conditions but studies from Cameroon, Nigeria, Ethiopia and Kenya have shown reduced susceptibility towards these antibiotics by *Helicobacter pylori* (Tanih *et al.,* 2009). 100% resistance to amoxicillin, tetracycline and metronidazole has been recorded in Nigeria (Tanih *et al.,* 2010, Tanih *et al.,* 2009). Cross resistance to clarithromycin (an expensive macrolide) was detected in Nigeria and was linked exposure to less expensive macrolides. Higher resistance was reported in isolates from female patients due to use of nitroimidazole derivatives for treatment of protozoal and gaenaecological problems. Kenya, Cameroon and Ethiopia recorded averagely similar antibacterial susceptibility results with 80% clarithromycin, 72.5% gentamycin, 67.5% tetracycline and 55.5% erythromycin susceptibility on average (Tanih *et al.,* 2010).

2.4.5.4 *Staphylococcus aureus*

Plasmid borne resistance for Staphylococcus is abundantly demonstrated for β-lactamase mediated penicillin resistance with more that 60% resistance rates in human *Staphylococcus aureus* isolates (Becker *et al.,* 2018). Vancomycin remains a drug of choice for severe methicillin Resistant *Staphylococcus aureus* infections but Vancomycin intermediate resistant *Staphylococcus aureus* (VISA) has been isolated with its basis of resistance involving stepwise mutations in genes encoding molecules predominantly involved in all envelope biosynthesis (Will *et al.,* 2017). The dominant

community acquired methicillin resistant *Staphylococcus aureus* (CA-MRSA) USA 300 North American (USA300-NA) descended from ancestral USA500 just like methicillin sensitive *Staphylococcus aureus* (MSSA) strain by acquisition of various mobile genetic elements (MGEs) and shows a very recent clonal expansion. Recent multiple studies show its spread to South America, Middle East, Western Pacific and Europe (Glaser *et al.,* 2016). Circulation of USA300-NA was also reported in Africa (Strauβ *et al.,* 2017). The use of pneumococcal conjugate vaccines (PCVs) in Japan in 2012-2014 saw an increase in resistance to penicillin, macrolide and meropenem by pneumococcal isolates of serotype 15A-ST63 which is not covered by PCV 13. The spread of 15A-ST 63 has been reported in the United Kingdom, USA and Canada (Nakano *et al.,* 2018).

A study involving 1440 isolates of *Staphylococcus aureus* showed methicillin resistance in 213 strains. High methicillin resistant *S. aureus* (MRSA) was reported in Nigeria, Kenya and Cameroon at 21-30% and below 10% in Tunisia, Malta and Algeria (Kesah *et al*., 2003). More than 80% of MRSA were resistant to at least four classes of antibiotics (Shittu *et al*., 2006). Isolates form sub-Saharan African countries showed more than 50% resistance to trimethoprim sulfamethoxazole with Gabon, Nigeria and Tanzania showing 96-100% resistance habored in a drfG gene. In Namibia drfG gene prevailed but drfA gene was also common. In Gabon spa t1476 and spa CC064 were positive for drf G and drfK. Two genes of trimethoprim resistant (TMP-R) *Staphylococcus aureus* (spa t1045) were drfA, drfG and drf K negative but F98Y mutation positive. Several drfB mutations were identified in TMP-R *Staphylococcus aureus*. More than half of *Staphylococcus aureus* was isolated from travelers returning from Sub Saharan Africa and suffering from skin and soft tissue infections (SSTIs) were TMP-R and also carried the drfG gene (Shittu *et al*., 2006).

2.4.5.5 *Streptococcus pneumoniae*

Streptococcus pneumoniae has atleast 92 known serotypes all with the ability to cause invasive disease and drug resistance. A global study on *Streptococcus pneumoniae* isolates showed serotypes 19F and 6B which were commonly found in Latin America showed resistance to penicillin and erythromycin at 64.3% and 23.8% respectively. In the Asian and Pacific region, serotype 14 had higher resistance to erythromycin. Serotype 14 was found in Africa, Latin America, Middle East and North America. In

South Africa the highest resistance to penicillin was due to serotypes 6A, 6B, 9V, 15A and 19A (Hackel *et al.*, 2013). Increased isolation of Nonencapsulated *Streptococcus pneumoniae* (NESP) is a major concern since the susceptibility of the bacteria is highly dependent on its capsule. Prevalence of NESPs has been reported in Portugal, Spain, Brazil, Italy, Southern France, Israel, Poland and Thailand with increasing trends. NESP resistance to penicillin was recorded in Portugal, Brazil and Southern France while resistance to erythromycin was recorded in Portugal and Southern France. Resistance to clindamycin, tetracycline, sulfamethoxazole-trimethoprim was recorded in Portugal with MDR being a common feature in NESPs (Keller *et al.,* 2016).

CHAPTER THREE
MATERIALS AND METHODS

3.1 Study Area

This research work was conducted at Chuka University which is located in Chuka Town in Tharaka Nithi County along Meru-Nairobi highway. Schiff base synthesis, FT-IR and UV-Vis characterization was done at the chemistry laboratory while antimicrobial activity was determined at the Animal Science laboratory in Chuka University. NMR spectroscopy was done at the University of KwaZulu-Natal University in South Africa

3.2 Chemicals and Materials

All chemicals used were of analytical grade and were used as received from suppliers without any further purification. Benzaldehyde, aniline, salicylaldehyde, 4-aminophenol and 4-nitrobenzaldehyde were purchased from Sigma-Aldrich. Ethanol, methanol, nutrient agar and DMSO were obtained from ASPET school suppliers. The bacterial and fungal strains were obtained from Kenya Medical Research Institute (KEMRI). Other bench apparatus used were from Chuka University laboratory.

3.3 Synthesis of the Schiff Bases

The Schiff bases were prepared according to literature methods with a few modifications (Scheme 3.1-3.6) (Liu *et al.*, 2019, Yusuf *et al.*, 2020). Grinding (for the Schiff bases prepared from solid amines and aldehydes) and stirring (for the Schiff bases that were prepared from liquid amines and aldehydes) methods were used in the absence of catalysts and solvents. The methods led to reduced time of reactions, clean products, easy handling of the reagents, reduced possibility of pollution from the synthesis and no extra work up in the removal of solvents and catalysts after synthesis (Sachdeva *et al*., 2014, Liu *et al.*, 2019, Yusuf *et al.*, 2020).

3.3.1 Synthesis of Schiff Base S_1

Schiff base S_1 was synthesized from 0.01 mol of 4-aminophenol and (0.01 mol) benzaldehyde according to the method used by Yusuf *et al.*, (2020) with a few modifications (Yusuf *et al.*, 2020). The mixture of 4-aminophenol and benzaldehyde was stirred using a magnetic stirrer for 20 minutes. The yellow paste formed was dried

overnight at room temperature forming a solid. The solid was ground into powder and recrystallized in ethanol.

3.3.2 Synthesis of Schiff Base S_2

Schiff base S_2 was synthesized from 0.01 mol 4-aminophenol and 0.01 mol of 4-nitrobenzaldehyde according to the method used by Liu *et al.,* (2019) with a few modifications (Liu *et al.,* 2019). The mixture of 4-aminophenol and 4-nitrobenzaldehyde was triturated in a mortar using a pestle for about 20 minutes. The amber coloured product formed was recrystallized using ethanol.

3.3.3 Synthesis of Schiff Base S_3

Schiff base S_3 was prepared by reacting 0.01 mol of 4-aminophenol and 0.01 mol salicylaldehyde according to the method used by Yusuf *et al.,* (2020) with a few modifications. The mixture of 4-aminophenol and salicylaldehyde was stirred in a magnetic stirrer for 19 minutes. The bright yellow product formed was allowed to dry overnight into solid at room temperature and then it was recrystallizeed in ethanol (Yusuf *et al.,* 2020).

3.3.4 Synthesis of Schiff Base S_4

Schiff base S_4 was prepared from 0.01 mol aniline and 0.01 mol 4-nitrobenzaldehyde according to the method used by Yusuf *et al.,* (2020) with a few modidifications. The mixture of aniline and 4-nitrobenzaldehyde was stirred in a magnetic stirrer for 30 minutes. The bright orange product formed was allowed to dry overnight into solid at room temperature then it was recrystallizeed in ethanol (Yusuf *et al.,* 2020).

3.3.5 Synthesis of Schiff Base S_5

Schiff base S_5 was synthesized using 0.01 mol aniline and 0.01 mol salicylaldehyde according to the method used by Yusuf *et al.,* (2020) with few modifications. The mixture of aniline and salicylaldehyde was stirred in a magnetic stirrer for 23 minutes. The bright orange product formed was allowed to dry overnight at room temperature forming a solid which was then recrystallizeed in ethanol (Yusuf *et al.,* 2020).

3.3.6 Synthesis of Schiff Base S_6

Schiff base S_6 was prepared by reacting 0.01 mol aniline and 0.01 mol benzaldehyde according to the method used by Yusuf *et al.,* (2020) with a few modifications. The mixture of aniline and benzaldehyde was stirred in a magnetic stirrer for 20 minutes. The amber coloured product was allowed to dry overnight at room temperature forming a solid which was then recrystallizeed in ethanol (Yusuf *et al.,* 2020).

3.3.7 Limitation of the selected synthetic method

Although the synthesis of the Schiff bases through solvent and catalyst free grinding and stiriing procedures has numerous advantages such as reduced times, reduced pollution, easy work up, clean products and reduced times compared to reflux, the time of synthesis is however longer than that afforded by microwave irradiation (Chakraborty *et al.,* 2012, Savalia *et al.,* 2013, Shinde *et al.,* 2014). Grinding and stirring techniques were chosen for this study since the procedures are energy saving compared to microwave irradiation (Liu *et al.,* 2019, Yusuf *et al.,* 2020)

3.4 Characterization of the Schiff Bases

3.4.1 Melting Points

The melting points of the synthesized products were determined in an mrc MPA-12 melting point apparatus from Chuka University according to the method used by Bendale *et al.,* (2011). A capillary tube was closed on one end by heating it on a non-luminous flame for about 3 minutes. The sample was crushed into a fine powder in a tile. The sample was then picked through the open end of the capillary tube and tapped to pack to a height of about 1- 2 cm. The capillary tube was introduced into the melting point apparatus through the closed end. The initial melting point, when the solid began to melt and the final melting point when all the solid had melted were recorded and averaged to obtain the actual melting point of the solid. (Bendale *et al.,* 2011).

To obtain consistent melting points, open capillary method was used to confirm the values obtained from the melting point apparatus. This was done according to the method used by Xavier and Srividhya (2014) using a liquid paraffin bath . The capillary tubes, closed on one end by heating on a non luminous flame for 3 minutes were used. The samples were crushed on a tile to a fine powder and packed into the capillary tube

through the open end and tapped to fill the capillary tube to a height of 1-2 cm. The capillary tube was attached to a 10-360^{o}C thermometer using a string, clamped on a stand and dipped into a 250 ml beaker half full with liquid paraffin making sure that the bulb of the thermometer and the closed end of the capillary tube were dipped into the liquid paraffin up to a length of about 2 cm. The beaker containing the paraffin was heated on a non-luminous flame. The temperature of the liquid paraffin was observed carefully as it rose up to the point where the solid initially melted (Xavier and Srividhya, 2014). This was recorded as $T_{1.}$ The temperature was monitored until up to the point where all the solid melted and this was recorded as $T_{2.}$ The average of the two temperatures was calculated using Equation 3.1 and assigned as the melting point of the solid:

$$\text{Melting Point} = \frac{T1 + T2}{2} \quad \text{.....Equation 3.1}$$

3.4.2 Percentage Yield

The actual yield of the product (Schiff base) was obtained by accurately weighing the crystallized product using an analytical balance. The theoretical yield was calculated by multiplying the stoichiometric moles of product and the molar mass of the product. The percent yield was expressed as a percentage of the ratio of the actual yield to the theoretical yield according to Equation 3.2. This was done according to the method used by Xavier and Srividhya (2014).

$$\text{Percent Yield} = \frac{\text{Actual Yield}}{\text{Theoretical Yield}} \text{ x } 100\% \quad \text{.....Equation 3.2}$$

3.4.3 Infrared Spectroscopy

The functional groups present in the synthesized Schiff bases were determined using a Shimadzu IRAffinity-1S Fourier Transform infrared spectrophotometer. This was done according to the method used by Singh *et al.*, (2017). A milligram of the solid sample was mixed with 100 mg of potassium bromide (KBr). The mixture was ground into powder and mechanically pressed into a thin transparent pellet. The pellet was then placed in the spectrophotometer and absorption measured in the 4000-400 cm^{-1} range. Liquid samples were allowed to dry overnight and recrystallized in ethanol before preparing them for analysis (Singh *et al.*, 2017).

3.4.4 Ultra-Violet Visible Spectroscopy

UV/Vis spectra were obtained using a Shimadzu UV-1800 spectrophotometer according to the method used by Holthoff *et al* (2012). For S_1, 0.0013 g was dissolved in 30 mL methanol. A 1 mL volume of the solution was diluted in 10 mL methanol. For S_2, 0.0017 g were dissolved in 30 mL methanol and 1 mL of the solution formed was further diluted in 10 mL methanol. For S_3, 0.0024g was dissolved in 30 mL methanol and 1mL of the resulting solution was diluted in 10 mL methanol. For S_4, 0.0031g was dissolved in 30 mL methanol and 1 mL of the resulting solution was diluted in 10 mL methanol. Similarly, 0.0037 g of S_5 was dissolved in 30 mL methanol and 1 mL of the resulting solution was diluted in 10 mL methanol. Finally, 0.0008g of S_6 was dissolved in 30 mL methanol and 1 mL of the resulting solution was diluted in 10 mL methanol. Further dilution was done to reduce the intensity of the colour of the samples for clear analysis. The diluted samples were transferred into quartz cuvettes (1 cm path length) and analyzed in the range of 200-600 nm (Holthoff *et al.,* 2012).

3.4.5 Nuclear Magnetic Resonance Spectroscopy

^{1}H-NMR and ^{13}C-NMR spectra was recorded at KwaZulu-Natal University in South Africa using a Bruker Avance III 400 instrument set at 400MHz. This was done according to the method used by Gichumbi *et al.,* (2016). Deuterated chloroform ($CDCl_3$) was used as the solvent and trimethylsilane (TMS) as the internal standard (Gichumbi *et al*., 2016).

3.5 Antimicrobial Activity

Antibacterial studies were performed using disc diffusion method modified from Zaidan *et al.,* (2005) and Gichumbi *et al.,* (2016). The gram negative bacteria *Pseudomonas aeruginosa*, *Escherichia coli* and *Salmonella typhi* and gram positive bacteria *Staphylococcus aureus* and *Candida albicans* fungi were used for tests.

3.5.1 Experimental Design

Four bacterial strains; *Pseudomonas aeruginosa*, *Escherichia coli, Salmonella typhi* and *Staphylococcus aureus* and one fungi species; *Candida albicans* were analyzed using completely random design (CRD) with the six synthesized compounds diluted to the concentrations of 500 mg, 250 mg and 125 mg. Three replicates were analyzed and

the zones of inhibition measured. Gentomycin was used as the standard control drug and DMSO as the negative control (Gichumbi *et al.*, 2016).

3.5.2 Preparation of Culture Media

To prepare 1 L of Muller-Hinton Agar medium, 38 g of Muller-Hinton Agar powder (HiMedia Laboratories) was used as per the manufacturer instructions. The medium was carefully weighed and placed in a sterile container. Subsequently, 1,000 mL of distilled water were added to the container, and the mixture was stirred with a magnetic stirrer until the agar powder was fully dissolved (Gichumbi *et al.,* 2016). The container was then covered, ensuring it was not tightly sealed, to allow steam to escape during autoclaving. The medium was sterilized in an autoclave at 121°C and 15 psi for 15 min (Model; X280A; China). After autoclaving, the agar was left to cool to 45°C. This cooling process could be expedited by placing the medium container in a water bath. Once the agar reached a suitable temperature, it was poured into sterile Petri dishes. 10 mL of the agar was poured into each petri dish. The agar was then left undisturbed to solidify at room temperature. Upon solidification, a cork borer with a 3 mm diameter was used to create evenly spaced wells in the agar, providing designated locations for placing the synthetic compounds (Zaidan *et al.,* 2005, Gichumbi *et al.,* 2016,).

3.5.3 Preparation of Microbial Inoculums

For the preparation of the bacterial inoculum, a McFarland Standard was employed to standardize the bacterial density. A 0.5 McFarland Standard was prepared by combining 0.5 mL of 1% sulfuric acid with 99.5 mL of distilled water in a glass container. Using a sterile loop or swab, several colonies of the bacterial culture to be tested were collected and transferred into a tube containing the McFarland Standard. The mixture was thoroughly blended to achieve a uniform suspension. The turbidity of the bacterial suspension was then compared to the 0.5 McFarland Standard, and adjustments were made by adding more bacterial colonies or more McFarland Standard until the turbidity closely matched the standard. This ensured the creation of a standardized bacterial inoculum, which was subsequently used for spreading on the Muller-Hinton Agar plates containing the synthetic compounds (Zaidan *et al.,* 2005, Gichumbi *et al.,* 2016).

3.5.4 Incubation and Measuring of Zones of Inhibition

Following the preparation of Muller-Hinton Agar plates with synthetic compounds, as well as the inoculation of bacterial cultures using the standardized McFarland Standard and spreading of the bacterial strains on the plates containing synthetic compounds, the plates were sealed with Parafilm® to prevent contamination. They were then placed in an incubator (Model Memmert UNB) 400 set at a controlled temperature of 37°C. This incubation period lasted for a duration of 12 h. After the designated incubation time elapsed, the plates were carefully removed from the incubator, taking care to maintain sterility. Zones of inhibition, characterized by regions where bacterial growth was inhibited around the wells containing synthetic compounds, were visually inspected. To quantify the size of these zones, a ruler was used to measure the diameter in millimeters. The measurements were recorded for each compound against the respective microorganism (Zaidan *et al.,* 2005, Gichumbi *et al.,* 2016).

3.6 Data Analysis

The data underwent analysis of variance using the general linear model procedure in SAS version 9.4. To discern significant differences among the means, the least significant difference (LSD) test was employed at a significance level of $\alpha = 0.05$ within the SAS software (Dianat *et al.,* 2015).

3.7 Ethical Considerations

This work upheld honesty, objectivity and integrity in data reporting, results analysis and methodology avoiding bias in experimental design and data analysis. The contribution from other people was acknowledged. Should there be need for use of the outcome for policy matter the information will be released to requesting institution upon consultation with Chuka University.

CHAPTER FOUR

RESULTS AND DISCUSSION

4.1 Physical Properties of the Synthesized Schiff Bases

The physical properties of the synthesized Schiff bases are shown in Table 1. The compounds were soluble at room temperature in solvents with relatively low dielectric constant such as methanol, ethanol, acetonitrile, dimethyl formamide, dichloromethane and acetone. The colours of compounds S_1 and S_6 were amber yellow; S_2 and S_3 were bright yellow while S_4 and S_5 were orange. The colours were close to those of Schiff bases synthesized by Xavier and Srividhya, (2014) and those synthesized by Naqvi *et al.,* (2009).

Table 4.1: Physical properties of synthesized Schiff bases

Ligand	Colour	MP (°C)	MF	Calculated Molecular Mass	Mass (g)	Yield (%)
S_1	Amber yellow paste	236	$C_{13}H_{12}NO$	198	16.9	85
S_2	Bright yellow powder	156	$C_{13}H_{11}N_2O_3$	243	20.1	83
S_3	Bright yellow paste	220	$C_{13}H_{12}NO_2$	214	16.0	75
S_4	Orange liquid	240	$C_{13}H_{11}N_2O_2$	227	20.4	89
S_5	Orange paste	216	$C_{13}H_{12}NO$	198	16.8	88
S_6	Amber yellow liquid	110	$C_{13}H_{12}N$	182	13.8	76

The melting points (MP) of compounds S_2 and S_6 were significantly lower (156 and 110°C respectively) than those of S_1, S_3, S_4 and S_5 (236, 220, 241 and 216°C respectively). The melting points were in close range with those obtained by Bendale *et al.,* (2011) and Xavier and Srividhya, 2014. The compounds melted at sharp well-defined temperatures indicating that they were of high purity (Mohamed *et al.,* 2006, Fugu *et al.,* 2013). The calculated molecular masses (MM) of the compounds ranged from 182-243 g/mol based on the proposed molecular formulae (MF). The compounds were obtained in substantial yields (75-89%) which was in agreement with the amounts obtained by Xavier and Srividhya, (2014) in the preparation of Schiff bases by catalyst free stirring procedures and Yusuf *et al.,* (2020) in the preparation of Schiff bases by solvent and catalyst free grinding procedures (Xavier and Srividhya, 2014, Yusuf *et al.,* 2020).

4.2 Infrared Spectra Analysis

Selected bands of diagnostic importance are shown in Table 2. Free O-H broad bands were observed at 3447.91- 3339.29 cm^{-1} (Al Zoubi *et al.,* 2017). In compound S_3, the O-H band was broad extending from 3405.47 to 3343.74 cm^{-1} which was attributed to existence of keto-enol forms of the compound (Issa *et al.,* 2008) (Appendix 1(b)). A sharp peak at 1628.95-1617.38 cm^{-1} was attributed to C=N bond (Cinarli *et al.,* 2011, Muhammad Kaleem *et al.,* 2015, Ejidike and Ajibade, 2016). C-H stretching vibrations occurred at 1374.21-1364.70 to cm^{-1} while out of plane C-H deformations were observed at 870-630 cm^{-1}(Barbosa *et al.,* 2019). Other notable bands were C=C aromatic ring vibrations at 1577.56-1502.61cm^{-1} and C-O band at 1278.86- 1230.64 cm^{-1} (Barbosa *et al.,* 2019). Compounds S_5 showed broad bands at around 2400- 2700 cm^{-1} indicating the possibility of intramolecular hydrogen bonds formation and this was backed by its high melting point (216^{o}C) (Cinarli *et al.,* 2011). Solvent interference (solvent used during recrystallization) was attributed to the O-H band shown by compound S_6 (Issa *et al.,* 2008). This is as shown in Appendix 1(a) to 1(e). Worth noting was the disappearance of the C=O band at around 1600 cm^{-1} confirming the conversion of the aldehydes to imines (Barbosa *et al.,* 2019).

Table 4.2: Selected absorption bands (cm^{-1}) of the synthesized Schiff bases

Ligand	ν(O-H)	ν (C=N)	ν (C-O)	ν (C=C)
S_1	3341.82	1620.27	1238.35	1507.43
S_2	3339.29	1617.38	1231.60	1502.61
S_3	3405.47	1617.38	1257.64	1507.43
S_4	-	1625.31	1237.39	1577.56
S_5	3447.91	1621.24	1278.86	1575.91
S_6	3425.72	1628.95	1237.39	1505.30

A representative IR spectrum is shown in Figure 5 and the rest of the spectra are shown in Appendix 1.

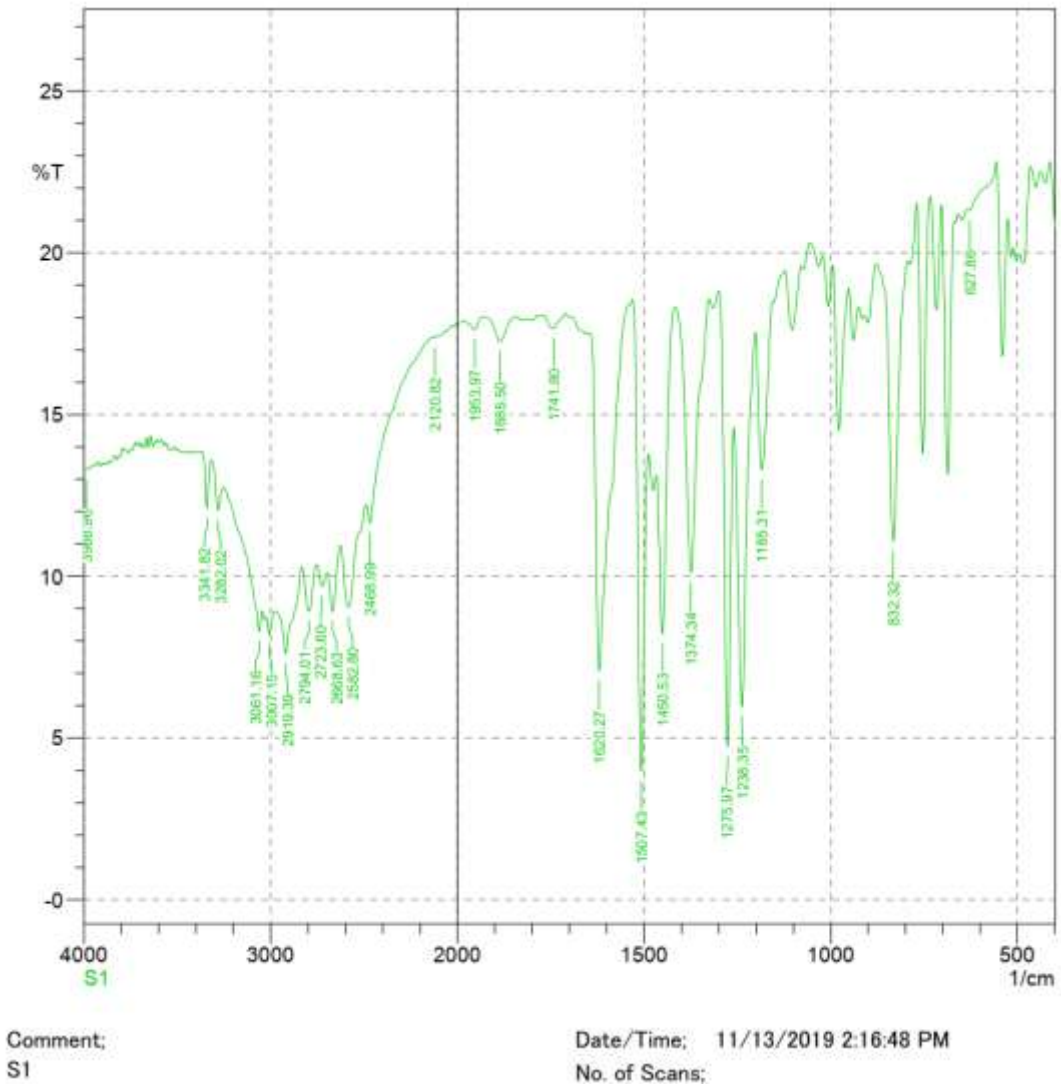

Figure 4.1: Representative IR spectrum for Schiff base S_1

4.3 Electronic Spectra Analysis

All the six Schiff bases showed four main peaks as shown in Table 4.3. On the higher energy side, two band at 201.80- 209.00 nm and 221.40- 236.80 nm corresponding to π–π∗ transitions of the aromatic rings (Cinarli *et al.*, 2011, Gichumbi *et al.*, 2016). A band at 261.40- 287.60 nm was observed corresponding to the n–π∗transitions of the azomethine C=N bond (Cinarli *et al.*, 2011, Ejidike and Ajibade, 2016, Gichumbi *et al.*, 2016). Intramolecular charge transfer corresponds to a band at higher wavelength at 331.80- 330.90 nm (Cinarli *et al.*, 2011, Ejidike and Ajibade, 2016).

Table 4.3: Absorbance wavelengths ($\lambda_{max\ (nm)}$) of the Schiff bases

Transition	S_1 [$\lambda_{max\ (nm)}$]	S_2 [$\lambda_{max\ (nm)}$]	S_3 [$\lambda_{max\ (nm)}$]	S_4 [$\lambda_{max\ (nm)}$]	S_5 [$\lambda_{max\ (nm)}$]	S_6 [$\lambda_{max\ (nm)}$]
π-π*	203.40	201.80	209.00	202.40	206.00	202.00
	236.80	233.20	229.60	222.80	221.40	223.80
n-π*	263.80	261.40	287.60	287.60	269.00	264.20
	333.00	330.90	331.80	331.80	336.40	374.40

Figure 4.2 is a representative UV spectrum. The rest of the spectra are shown in Appendix 2 (a) to 2(f)

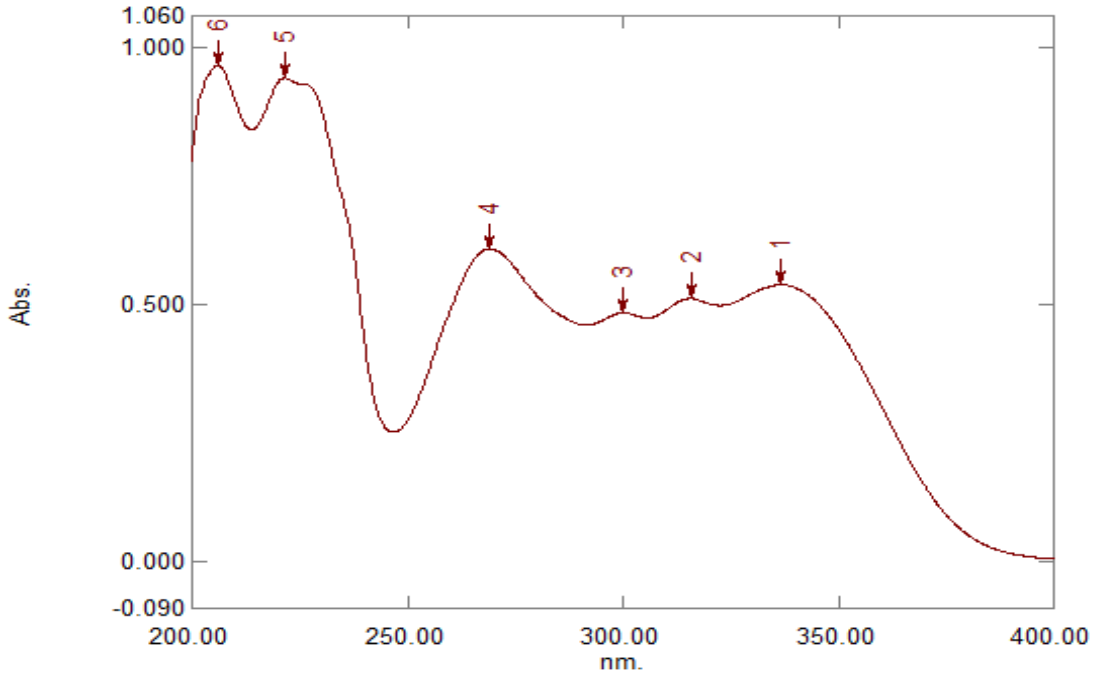

Figure 4.2: Representative UV-Vis spectrum for Schiff base S_1

4.4 NMR Spectra Analysis

The resonance spectra of the protons in ^{1}H NMR was assigned on the basis of their integration, chemical shifts and multiplicity patterns. The ^{1}H NMR spectrum for the Schiff base S_4 (Figure 4.3) showed a singlet peak at δ = 8.81 ppm corresponding to the azomethine proton (-N=CH-), an indication that the Schiff base was formed during the condensation reaction (Sherif, 2011, Munde *et al*., 2010).

Multiplets occurred in the range 7.29 ppm (multiplets, 3H, C-H (phenyl), 7.33 ppm (multiplets, 2H, C-H (phenyl), 7.44 ppm (multiplets, 2H, C-H (phenyl), 7.48 ppm

(multiplets, 2H, C-H (phenyl) corresponding to the aromatic hydrogens (Sherif, 2011, Munde *et al*., 2010).

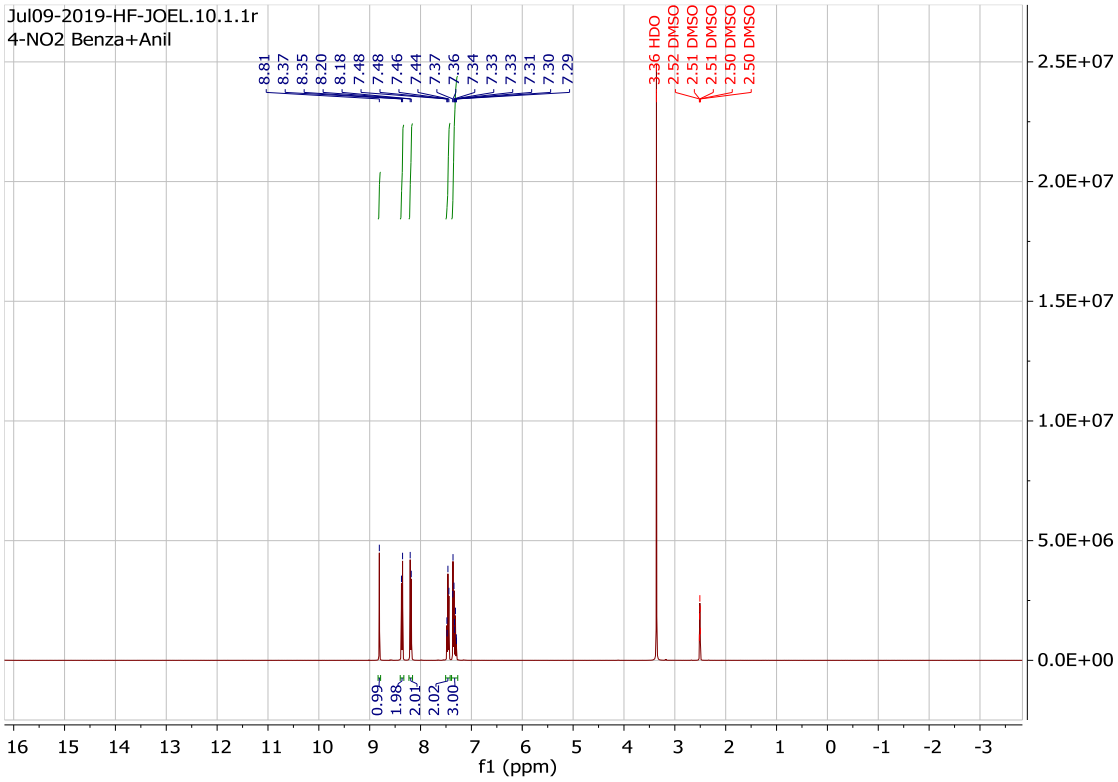

Figure 4.3: The ^{1}H NMR spectrum of the Schiff base S_4

In the ^{13}C NMR the azomethine carbon was observed at 159.35 ppm and the other phenyl carbons were observed in the range of 151.06 ppm to 121.73 ppm as shown in the Figure 8 (Sherif, 2011, Munde *et al*., 2010). This further confirms the formation of the Schiff base (Sherif, 2011, Munde *et al*., 2010).

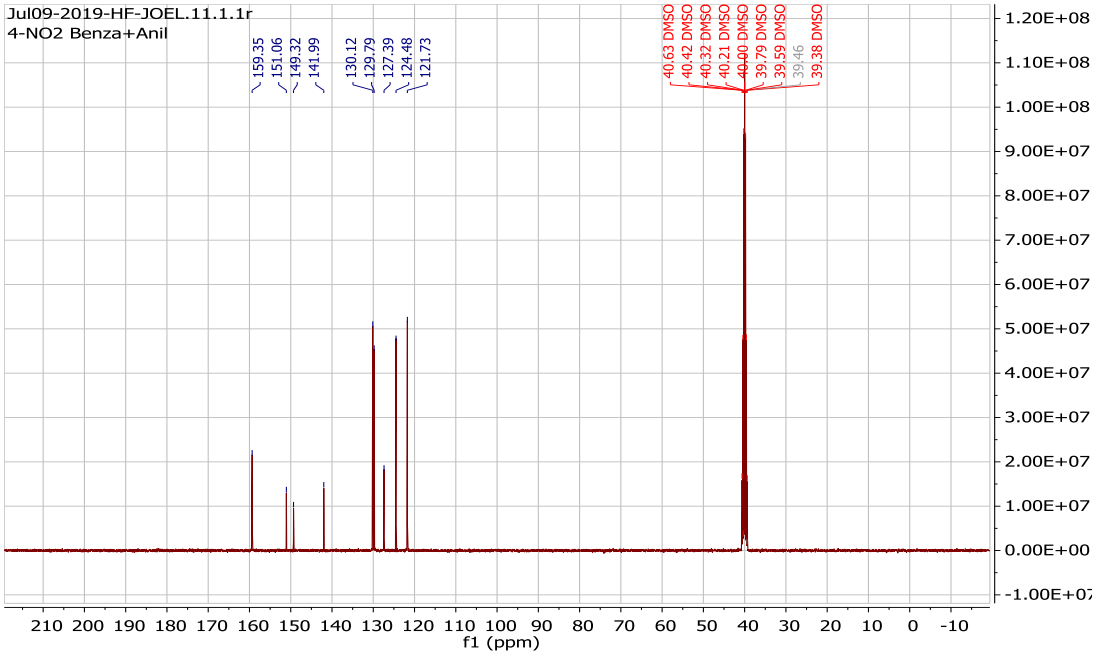

Figure 4.4: The ^{13}C NMR spectrum of the Schiff base S_4

For the Schiff base S_5 ^1H NMR spectrum, the azomethine proton peak was observed at 8.95 ppm and the OH peak from salicylaldehyde was observed at 13.12 ppm (Figure 4.5). The multiplets at 7.00 ppm, 7.29 ppm, 7.33 ppm, 7.40 ppm and 8.90 ppm corresponds to the phenylic C-H protons form the phenyl back bone of the aniline and salicyalaldehyde (Sherif, 2011, Munde *et al*., 2010).

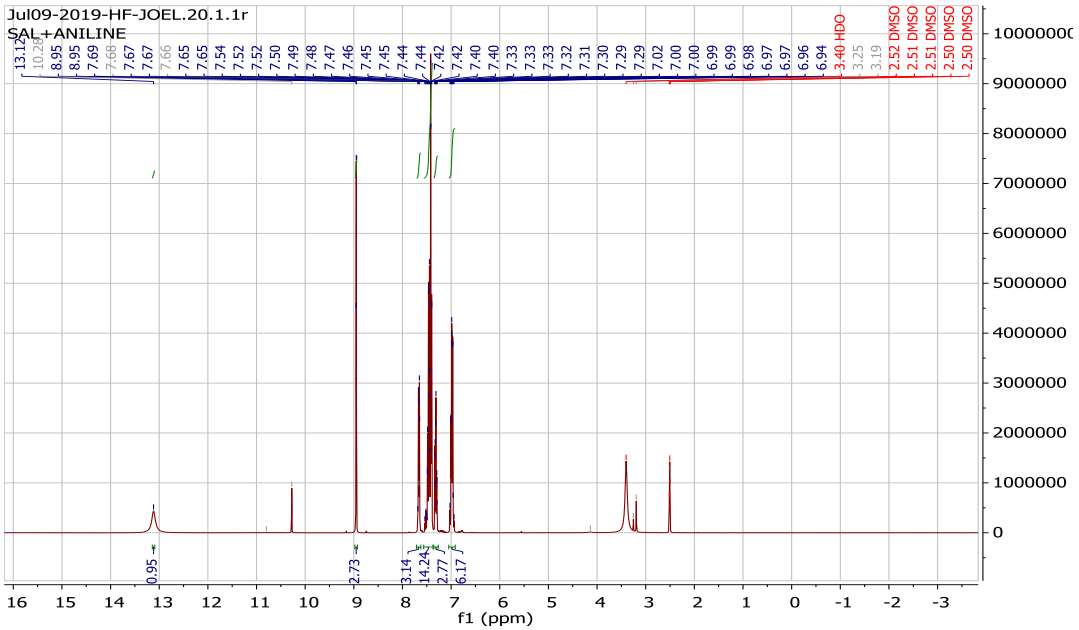

Figure 4.5: The ^1H NMR spectrum of the Schiff base S_5

The ^{13}C NMR spectrum of S_5 is shown in Figure 9. The peak at δ= 192.32 ppm corresponds to the azomethine carbon (-N=CH-) while the peaks in the range of 163.97 to 114.37 ppm corresponds to the aromatic carbons (Ommenya *et al.*, 2020).

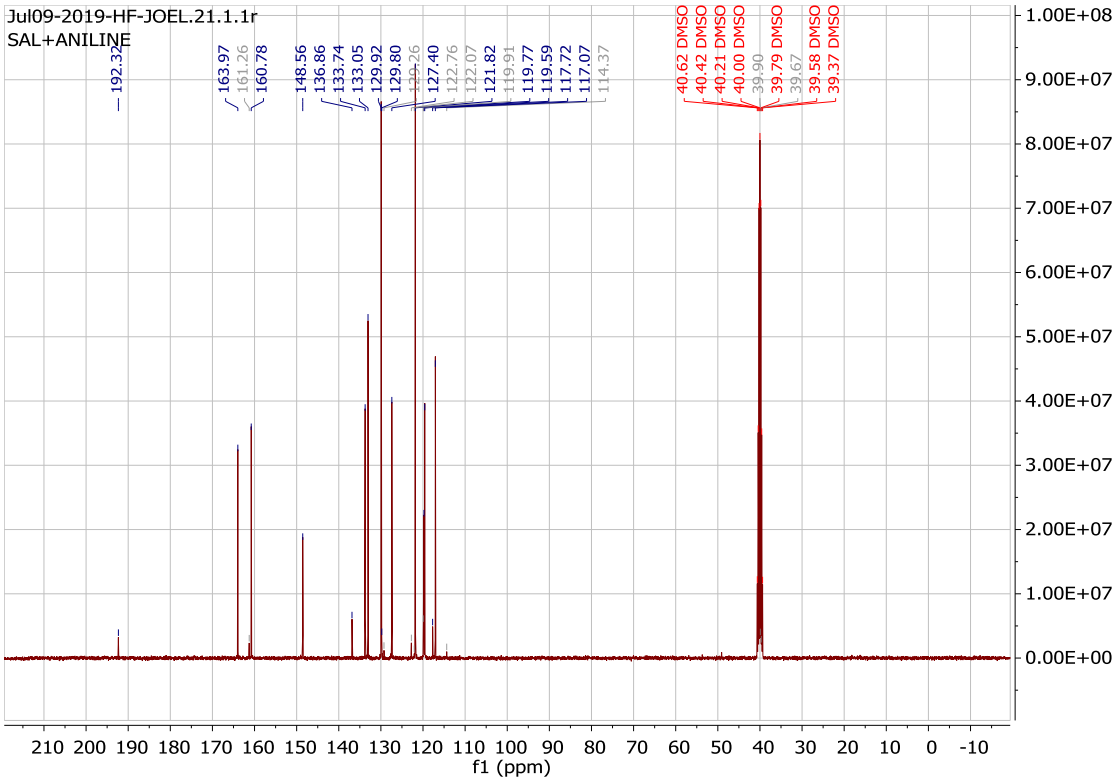

Figure 4.6: The ^{13}C NMR spectrum of the Schiff base S_5

The spectrum for the Schiff base S_6 (Figure 10) showed a singlet peak at δ =8.62 corresponding to the azomethine proton (-N=CH-) and multiplets in the range 7.26-7.96 ppm corresponding to the aromatic hydrogens in the benzene rings of the aldehyde and amine, an indication that the Schiff base was formed during the condensation reaction (Sherif, 2011, Munde *et al*., 2010).

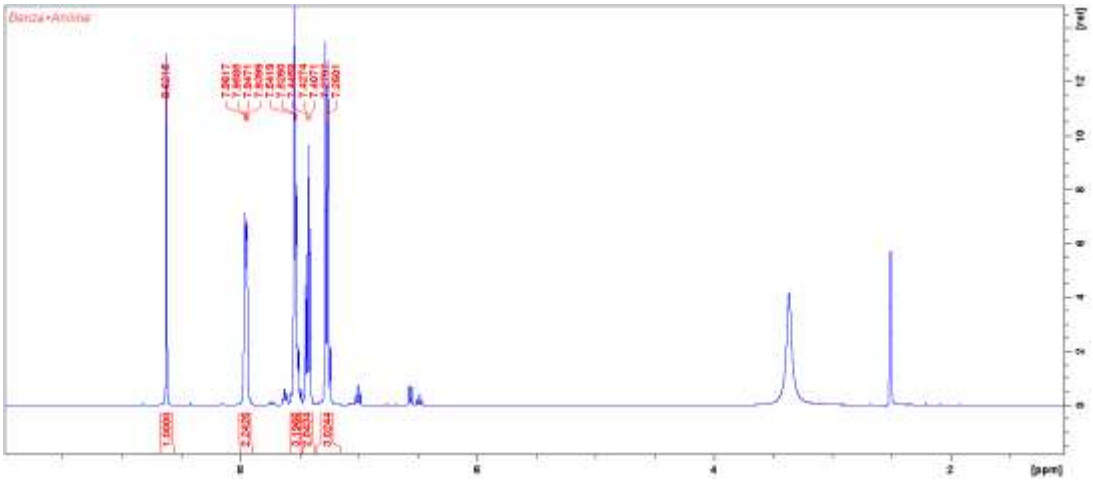

Figure 4.7: The ^{1}H NMR spectrum of the Schiff base S_6

The ^{13}C NMR spectrum of the Schiff base S_6 (Figure 11) exhibited the azomethine carbon at 161.16 ppm and other peaks due to the phenyl carbons in the aniline and aldehyde at 15.94, 136.49, 131.94, 129.67, 129.14, 126.44, 121.44 ppm and this agrees with the findings of other researchers (Ommenya *et al.*, 2020).

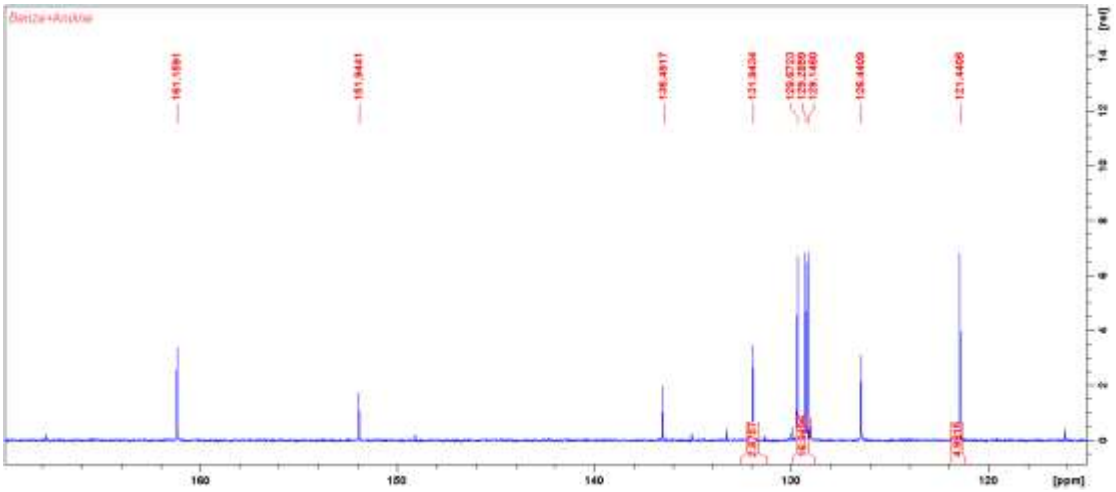

Figure 4.8: The^{13}C NMR spectrum of the Schiff base S_6

4.5 Antimicrobial Activities of the Synthesized Compounds

4.5.1Antimicrobial Activities Synthesized Compounds at different concentrations

The antimicrobial activities of the synthesized compounds at different concentrations at shown in Table 4. There was a significant ($p < 0.05$) difference in the bioactivity of compound S_1 against the tested microorganisms at the concentration of 500 ppm. *Salmonella typhi* exhibited the highest sensitivity (13.00 mm), followed by *Staphylococcus aureus* (11.62 mm), while *Escherichia coli* demonstrated the lowest sensitivity (7.12 mm). Similarly, compound S_2 displayed varying degrees of bioactivity against the micro-organisms. *Pseudomonas aeruginosa* was the most sensitive (13.66 mm), followed by *Escherichia coli* (11.29 mm), while *Candida albicans* showed the least sensitivity (5.83 mm). For compound S_3, *Salmonella typhi* was the most sensitive (14.92 mm), followed by *Escherichia coli* (14.46 mm), and *Candida albicans* was the least sensitive (4.58 mm).

Compound S_4 also exhibited significant ($p < 0.05$) differences in bioactivity against the micro-organisms. *Staphylococcus aureus* was the most sensitive (16.21 mm) followed by *Pseudomonas aeruginosa* (9.92 mm), while *Candida albicans* displayed the least sensitivity (7.16 mm). *Salmonella typhi* was the most sensitive in compound S_5 (14.66 mm), followed by *Staphylococcus aureus* (12.21 mm), and *Escherichia coli* exhibited the lowest sensitivity (6.04 mm). In addition to that, S_6 had varying levels of bioactivity. *Pseudomonas aeruginosa* and *Salmonella typhi* were the most sensitive at (15.33 mm) followed by *Candida albicans* (14.33 mm). The least sensitive was *Escherichia coli* (3.00 mm). Gentamycin, used as a reference, displayed significant ($p < 0.05$) bioactivity against all tested micro-organisms. It exhibited a mean zone of inhibition of 23.83 mm, while against *Candida albicans,* it showed a mean zone of inhibition of 3.67 mm (Table 4).

At the concentration of 250 ppm, there was a significant ($p < 0.05$) difference in the bioactivity of compound S_1 against the tested micro-organisms. *Salmonella typhi* exhibited the highest sensitivity (12.83 mm), followed by *Staphylococcus aureus* (11.66 mm), while *Escherichia coli* demonstrated the lowest sensitivity (6.91 mm). Compound S_2, had a significant ($p < 0.05$) variation in its bioactivity against the micro-organisms. *Pseudomonas aeruginosa* was the most sensitive (13.66 mm), followed by

Escherichia coli (11.08 mm), and *Candida albicans* exhibited the lowest sensitivity (5.66 mm). Compound S_3 also displayed significant ($p < 0.05$) differences in bioactivity against the micro-organisms. *Salmonella typhi* was the most sensitive (14.75 mm), followed by *Escherichia coli* (14.25 mm), while *Candida albicans* demonstrated the least sensitivity (4.41 mm) Compound S_4 exhibited significant ($p < 0.05$) variations in bioactivity against the micro-organisms. *Staphylococcus aureus* was the most sensitive (16.25 mm), followed by *Pseudomonas aeruginosa* (9.92 mm), and *Candida albicans* showed the least sensitivity (7.0 mm). Compound S_5 demonstrated significant ($p < 0.05$) differences in bioactivity against the micro-organisms as well. *Salmonella typhi* was the most sensitive (14.50 mm), followed by *Staphylococcus aureus* (12.25 mm), and *Escherichia coli* exhibited the lowest sensitivity (5.83 mm). Compound S_6 had quite significant activity against the micrioorganisms with *Staphylococcus aureus* showing the greatest sensitivity (17.67 mm) followed by *Candida albicans* (13.67 mm). The least activity was exhibited in *Escherichia coli* (2.33 mm). Gentamycin, used as a reference, displayed significant ($p < 0.05$) bioactivity against all tested micro-organisms. For example, against *Staphylococcus aureus*, it exhibited a mean zone of inhibition of (24.0 mm), while against *Candida albicans*, it showed a mean zone of inhibition of 3.0 mm (Table 4).

There was a significant ($p < 0.05$) difference in the bioactivity of compound S_1 against the tested micro-organisms at the concentration of 125 ppm. *Salmonella typhi* exhibited the highest sensitivity (12.50 mm), followed by *Staphylococcus aureus* (11.16 mm), while *Escherichia coli* demonstrated the lowest sensitivity (6.87 mm). For compound S_2, *Pseudomonas aeruginosa* was the most sensitive (13.75 mm), followed by *Escherichia coli* (11.04 mm), and *Candida albicans* exhibited the lowest sensitivity (5.33 mm). Compound S_3 also displayed significant ($p < 0.05$) differences in bioactivity against the micro-organisms. *Salmonella typhi* was the most sensitive (14.42 mm), followed by *Escherichia coli* (14.21 mm), while *Candida albicans* demonstrated the least sensitivity (4.0 mm).

Similarly, Compound S_4 exhibited significant ($p < 0.05$) variations in bioactivity against the micro-organisms. *Staphylococcus aureus* was the most sensitive (15.75 mm), followed by *Pseudomonas aeruginosa* (10.00 mm), and *Candida albicans*

showed the least sensitivity (6.67 mm). Compound S_5 also demonstrated significant ($p < 0.05$) differences in bioactivity against the micro-organisms as well. *Salmonella typhi* was the most sensitive (14.17 mm), followed by *Staphylococcus aureus* (11.75 mm), and *Escherichia coli* exhibited the lowest sensitivity (5.79 mm).

Table 4.4: Antimicrobial activities of the synthesized compounds against selected micro-organisms

		Compounds						
		At the concentration of 500ppm						
Organism	N	S_6	S_5	S_4	S_3	S_2	S_1	Gentamycin
S. aureus	12	15.33^{a}	12.21^{b}	16.21^{a}	12.62^{b}	10.45^{b}	11.62^{a}	23.83^{ab}
P. aeruginosa	12	13.33^{c}	10.92^{b}	9.92^{b}	10.91^{b}	13.66^{a}	10.17^{b}	21.33^{b}
E. coli	12	3.00^{d}	6.04^{c}	8.63^{bc}	14.46^{a}	11.29^{b}	7.12^{d}	22.17^{ab}
S. typhi	12	15.33^{b}	14.66^{a}	7.75^{bc}	14.92^{a}	6.25^{c}	13.0^{a}	24.0^{a}
C. albicans	12	14.33^{bc}	12.16^{b}	7.16^{d}	4.58^{c}	5.83^{c}	9.92^{b}	3.67^{c}
CV (%)		8.298	18.81	25.40	19.19	25.82	16.31	7
Mean		13.2	11.2	9.933	11.5	9.5	10.36	19
LSD (α=0.05)		1.993	1.728	2.352	1.809	2.011	1.386	2.55
		At the concentration of 250ppm						
S. aureus	12	17.67^{a}	12.25^{b}	16.25^{a}	12.66^{bc}	10.5^{b}	11.66^{a}	24.0^{a}
P. aeruginosa	12	9.33^{c}	10.91^{b}	9.92^{b}	10.91^{c}	13.66^{a}	10.16^{b}	21.33^{b}
E. coli	12	2.33^{d}	5.83^{c}	8.41^{bc}	14.25^{ab}	11.08^{b}	6.91^{c}	21.33^{b}
S. typhi	12	12.67^{b}	14.50^{a}	7.58^{bc}	14.75^{a}	6.08^{c}	12.83^{a}	23.33^{a}
C. albicans	12	13.67^{b}	12^{b}	7.0^{d}	4.41^{d}	5.66^{c}	9.75^{b}	3^{c}
CV (%)		7.691	18.48	28.75	18.89	25.58	15.79	4.81
Mean		11.133	11.10	9.83	11.40	9.40	10.26	18.60
LSD (α=0.05)		1.557	1.682	2.318	1.765	1.971	1.329	1.627
		At the concentration of 125ppm						
S. aureus	12	14.67^{a}	11.75^{b}	15.75^{a}	12.17^{b}	10.0^{b}	11.16^{a}	22.0^{a}
P. aeruginosa	12	10.00^{b}	11.0^{b}	10.0^{b}	11.0^{b}	13.75^{a}	10.25^{bc}	21.67^{b}
E. coli	12	2.00^{e}	5.79^{c}	8.38b^{c}	14.21^{a}	11.04^{b}	6.87d	21.16^{b}
S. typhi	12	16.67^{b}	14.17^{a}	7.25^{c}	14.42^{a}	5.75^{c}	12.50^{a}	22.0^{a}
C. albicans	12	12.00^{ab}	11.66^{b}	6.67^{c}	4.0^{c}	5.33^{c}	9.416^{c}	1.67^{b}
CV (%)		19.582	18.66	29.26	19.08	26.00	15.86	3.34
Mean		9.866	10.87	9.61	11.18	9.18	10.04	17.7
LSD (α=0.05)		3.515	1.664	2.305	1.748	1.956	1.306	1.076

^{a,b,c,d,e,cd} Means followed by the same letter in columns is not significantly different at $\alpha = 0.05$ Compound S_6 showed almost similar bioactivity levels as the rest of the compounds with *Staphylococcus aureus* being the most sensitive (14.67 mm) followed by *Candida albicans* (12.00 mm). The least activity was observed in *Escherichia coli*

(2.00 mm). Gentamycin, used as a reference, displayed significant ($p < 0.05$) bioactivity against all tested micro-organisms. For example, against *Staphylococcus aureus*, it exhibited a mean zone of inhibition of 22.0 mm, while against *Candida albicans*, it showed a mean zone of inhibition of 1.67 mm (Table 4).

4.5.2 Antimicrobial Activities of different Synthetic Compounds on Individual Microorganisms

There was a significant ($p < 0.05$) effect of different synthetic compounds against the tested microorganisms at 500 ppm concentration. For *Staphylococcus aureus,* the commercial antibiotic Gentamycin exhibited the highest inhibition zone with a diameter of 23.83 mm, indicating strong antimicrobial activity. Following Gentamycin, Compound S_6 displayed an inhibition zone of 20.0 mm, demonstrating significant inhibitory effects. The lowest inhibition zone in this category was observed in Compound S_2, with a measurement of 9.0 mm. Against *Pseudomonas aeruginosa*, Gentamycin once again demonstrated the highest inhibition zone, measuring 21.33 mm, indicating its excellent antimicrobial activity. Following Gentamycin, Compound S_2 exhibited an inhibition zone of 14.67 mm, showing a significantly lower inhibitory effect. Compound S_2 exhibited the lowest inhibition zone in this category, measuring 7.67 mm.

For *Escherichia coli*, Gentamycin displayed the highest inhibition zone of 22.17 mm, reaffirming its strong antimicrobial activity. Following Gentamycin, Compound S_3 exhibited an inhibition zone of 15.00 mm, indicating a considerably lower inhibitory effect. The lowest inhibition zone in this category was observed in Compound S_5, measuring 0.67 mm. Against *Salmonella typhi*, Gentamycin once more displayed the highest inhibition zone, measuring 24 mm, signifying its strong antimicrobial activity. Following Gentamycin, Compound S_6 exhibited an inhibition zone of 15.33 mm, showing a considerably lower inhibitory effect. Compound S_4 had no inhibitory effect while the lowest inhibition zone in this category was observed in Compound S_2, with a measurement of 0.33 mm. Finally, for *Candida albicans*, Gentamycin exhibited the highest inhibition zone with a diameter of 3 mm, indicating very low activity, although notably lower compared to the other tested microorganisms. Following Gentamycin,

Compound S_5 displayed an inhibition zone of 15.33 mm, indicating a considerably higher inhibitory effect.

Table 4.5: Antimicrobial Activities of synthesized compounds against selected micro-organisms at 500ppm

Compound	*S. aureus*	*P. aeruginosa*	*E. coli*	*S. typhi*	*C. albicans*
Gentamycin	23.83^{a}	21.33^{a}	22.17^{a}	24^{a}	3^{d}
S_6	20.0^{b}	13.33^{b}	3^{e}	15.33^{b}	14.33^{a}
S_5	9.67^{c}	10^{c}	0.67^{e}	13.67^{b}	15.33^{a}
S_4	17.0^{b}	8.33^{cd}	7^{d}	0^{d}	8.33^{bc}
S_3	11.0^{d}	10^{c}	15^{b}	14.33^{b}	6^{c}
S_2	9^{c}	14.67^{b}	9.67^{c}	0.33^{d}	10^{b}
S_1	9.33^{c}	7.67^{cd}	3^{e}	10.33^{c}	15^{a}
Means	14.261	12.19	8.64	11.14	10.72
Cv (%)	15.17	10.59	15.61	8.75	16.59
lsd (α=0.05)	3.787	2.261	2.363	1.709	3.165

^{a,b,c,d,e,cd} Means followed by the same letter in columns is not significantly different at α = 0.05

There was a significant ($p < 0.05$) effect of the different synthetic compounds against all tested microorganisms at 250ppm. For *Staphylococcus aureus*, the commercial antibiotic Gentamycin demonstrated the highest inhibition zone of 24 mm, signifying the most effective antimicrobial activity. Compound S_6 exhibited an inhibition zone of 17.67 mm, which was notably lower than Gentamycin but still displayed considerable inhibitory effects. Compounds S_2 displayed the lowest inhibition zones in this category, measuring 5.33 mm. Against *Pseudomonas aeruginosa*, Gentamycin again displayed the highest inhibition zone of 21.33 mm, underscoring its strong antimicrobial activity.

Compound S_2 exhibited an inhibition zone of 9.67 mm, indicating a considerably lower inhibitory effect while compound S_4 showed a lower inhibition zone of 5.67 mm. For *Escherichia coli*, Gentamycin demonstrated the highest inhibition zone of 21.33 mm, reaffirming its potent antimicrobial activity. Compound S_3 showed an inhibition zone of 12.33 mm, indicating a considerable inhibitory effect while compounds S_5 displayed a lower inhibition zones of 0.67 mm. Against *Salmonella typhi*, Gentamycin displayed the highest inhibition zone of 23.33 mm, signifying its strong antimicrobial activity followed by compound S_6 which exhibited an inhibition zone of 12.67 mm, indicating a considerable inhibitory effect while compound S_2 exhibited the lowest inhibition zone

in this category, measuring 0.33 mm. Finally, for *Candida albicans*, Gentamycin exhibited the highest inhibition zone of 3 mm, signifying its antimicrobial activity, although notably lower compared to the other tested microorganisms. Compound S_5 displayed an inhibition zone of 14.33 mm, indicating a considerably higher inhibitory effect while compound S_3, displayed a lower inhibition zones of 5.67 mm.

Table 4.6: Antimicrobial Activities of synthesized compounds against selected micro-organism at 250ppm

Compound	*S. aureus*	*P. aeruginosa*	*E. coli*	*S. typhi*	*C. albicans*
Gentamycin	24^{a}	21.33^{a}	21.33^{a}	23.33^{a}	3^{d}
S_6	17.67^{b}	9.33^{b}	2^{d}	12.67^{b}	13.67^{a}
S_5	7.33^{d}	7^{c}	0.67^{e}	11.33^{bc}	14.33^{a}
S_4	14.33^{c}	5.67^{b}	2.67^{d}	0	8.33^{bc}
S_3	7.33^{d}	6.67^{c}	12.33^{b}	11^{bc}	5.67^{cd}
S_2	5.33^{d}	9.67^{b}	6.67^{c}	0.33^{d}	7.33^{bc}
S_1	7^{d}	6.33^{c}	1.67^{de}	9.67^{c}	11^{ab}
Means	11.85	9.43	6.81	9.76	8.95
Cv (%)	14.14	13.29	13.96	9.99	28.14
lsd (α=0.05)	2.935	2.195	1.665	1.709	4.184

^{a,b,c,d,e,cd} Means followed by the same letter in columns is not significantly different at $\alpha = 0.05$

There was a significant ($p < 0.05$) effect of different synthetic compounds against *Staphylococcus aureus* the concentration of 125 ppm. Compound S_6 exhibited a higher inhibition zone (14.67 mm), ranking second only to the commercial antibiotic Gentamycin, which produced an inhibition zone of 22 mm. Conversely, compound S_2 demonstrated a significantly lower inhibition zone (3.67 mm). Similarly, for *Pseudomonas aeruginosa*, there was a significant ($p < 0.05$) effect of the synthetic compounds. Compound S_6 demonstrated an inhibition zone of (10.00 mm), while Gentamycin exhibited the highest inhibition zone (21.66 mm). Compound S_4, on the other hand, displayed the lowest inhibition zone (4.33 mm). Regarding *Escherichia coli*, a significant ($p < 0.05$) effect of the synthetic compounds was observed. Compound S_3 recorded an inhibition zone of (8.33 mm), while Gentamycin displayed the highest inhibition zone (21.17 mm). Compound S_5 exhibited the lowest inhibition zone (0.66 mm). For *Salmonella typhi*, there was a significant ($p <0.05$) effect of the synthetic compounds. Gentamycin demonstrated the highest inhibition zone (22.00 mm), followed by compound S_6 (10.67 mm). Compound S_2 exhibited the lowest inhibition zone (0.33 mm). Lastly, in the case of *Candida albicans*, there was a

significant ($p < 0.05$) effect of the synthetic compounds. Gentamycin showed an inhibition zone of 1.67 mm whereas compound S_5 displayed an inhibition zone of (15.33 mm). Compound S_2 had the lowest inhibition zone (2.33 mm).

Table 4.7: Antimicrobial Activities of different synthetic compounds against selected micro-organism at 125ppm

Compound	*S. aureus*	*P. aeruginosa*	*E. coli*	*S. typhi*	*C. albican*
Gentamycin	22^{a}	21.66^{a}	21.17^{a}	22^{a}	1.67^{d}
S_6	14.67^{b}	10^{b}	2^{cd}	10.67^{b}	12^{b}
S_5	8^{cd}	5.33^{cd}	0.66^{d}	9.67^{bc}	15.33^{a}
S_4	9.67^{b}	4.33^{d}	2.67^{c}	7^{c}	8.33^{c}
S_3	8.33^{cd}	5.67^{cd}	8.33^{b}	10.33^{bc}	3^{d}
S_2	3.67^{e}	9^{bc}	6.67^{c}	0.33^{d}	2.33^{d}
S_1	6.33^{d}	5.33^{cd}	1.67^{cd}	8^{bc}	10^{bc}
Means	10.38	8.76	6.16	9.71	7.52
Cv (%)	14.41	24.27	14.69	21.43	15.34
lsd (α=0.05)	2.62	3.72	1.587	3.645	2.022

^{a,b,c,d,e,cd} Means followed by the same letter in columns is not significantly different at $\alpha = 0.05$

The urgent need for more active compounds against pathogenic microorganisms has been a longstanding concern in the field of antimicrobial research. With the increasing prevalence of drug-resistant strains and the limitations of currently available antibiotics, there is a critical demand for novel and effective antimicrobial agents (Liu et al., 2023). The obtained results demonstrate significant variations in the bioactivity of the synthesized compounds (S_1- S_6) against a panel of clinically relevant microorganisms at different concentrations (500ppm, 250ppm, and 125ppm). At 500ppm, *Staphylococcus aureus*, a gram positive bacteria was better inhibited by compound S_6. The compound, prepared from aniline and benzaldehyde does not have significant substitution which could have contributed to better activity. Compound S_2, which was prepared from 4-aminophenol and 4-nitrobenzaldehyde did not have significant activity against *Staphylococcus aureus* a factor which can be attributed to the double substitution. Better activity however was observed from S_2, a compound having OH and NO_2 substituents against *Pseudomonas aeruginosa*, a gram negative bacteria.

The least activity was observed from compound S_1 which had an OH substitution only. S_3, containing two –OH substituents showed higher activity against *Escherichia coli*, a Gram negative bacteria compared to S_5 which had the least activity. S_5 had a single OH

substitution confirming that better activity was observed in compounds with multiple OH substitution. In addition to that, *Salmonella typhi*, a Gram negative bacteria were better inhibited by S_6. *Candida albicans* was best inhibited by S_5. Clearly, more substituted compounds had better activity against gram negative bacteria compared to the Gram positive bacteria. The compounds had significant antifungal activity against *Candida albicans* at different concentration. The trend in antimicrobial activity was replicated at all concentrations with the highest activity observed at 500 ppm followed by 250 ppm and finally 125 ppm. Among the bacteria, *Staphylococcus aureus* was the most susceptible to the synthesized compounds while *Escherichia coli* was the least susceptible.

The observed escalation in antimicrobial efficacy with increasing compound concentrations mirrors the results previously reported (Li *et al.,* 2015), with a similar trends in the antimicrobial activity of Cu nanoparticles against *Escherichia coli* and *Staphylococcus aureus* being noted. Additionally, akin to this present investigation, *Escherichia coli* exhibited greater resilience to synthetic compounds compared to *Staphylococcus aureus* (Li *et al.,* 2015). This variation in sensitivity could be attributed to differences in the cell wall structures and metabolic pathways among the tested microorganisms. For instance, *Staphylococcus aureus*, known for its thick peptidoglycan layer, may provide a more robust barrier against certain compounds compared to other Gram-negative bacteria like *Escherichia coli* (Zhang *et al.,* 2021; Pokhrel *et al.,* 2022).

Comparing to other synthetic compounds, compound S_4 displayed significant bioactivity against *Staphylococcus aureus*, indicating its potential as an effective antimicrobial agent. These observations align with previous studies (Srivastva *et al.,* 2016) that have reported varying degrees of sensitivity among different microorganisms to synthetic compounds. These findings emphasize the importance of evaluating antimicrobial agents against a diverse panel of microorganisms to assess their broad-spectrum potential.

The variations in bioactivity of different compounds against individual microorganism may be attributed to several factors, including differences in cell wall composition,

membrane permeability, and the presence of specific resistance mechanisms within each microorganism (Khameneh *et al.*, 2019). Additionally, the chemical properties of the synthetic compounds, such as molecular weight, solubility, and charge, can influence their interactions with microbial targets necessitating mechanistic studies (Gold *et al.*, 2018, Li and Zhuang, 2020).

This study contributes to the very important mission of finding novel bioactive compounds by testing synthesized compounds against clinically relevant microorganisms. The findings are relevant to solving the need for development of novel antimicrobial agents that can help combat antimicrobial resistance since the research aligns with the broader scientific community's dedication to discovering novel compounds that can combat emerging drug-resistant strains (Liu *et al.*, 2023).

CHAPTER FIVE

SUMMARY, CONCLUSIONS AND RECOMMENDATIONS

5.1 Summary

In this study, a 1:1 ratio of aldehydes (0.1 mole) and amines (0.1 mole) was used to prepare the Schiff bases in an average time of 20 minutes. Compound S_1 was prepared from 4-aminophenol and benzaldehyde. Compound S_2 was prepared from 4-aminophenol and 4-nitrobenzaldehyde. Compound S_3 was prepared from 4-aminophenol and salicylaldehyde. Compound S_4 was prepared from aniline and 4-nitrobenzaldehyde. Compound S_5 was prepared from aniline and salicylaldehyde and compound S_6 was prepared from aniline and benzaldehyde. Compounds S_2 was prepared by grinding technique while compounds S_1, S_3, S_4, S_5 and S_6 were prepared by stirring techniques. All the compounds were prepared in solvent and catalyst free procedures. Compounds S_1 and S_6 were amber yellow in colour, S_2 and S_3 were bright yellow while S_4 and S_5 were orange in colour. All the compounds were solids at room temperature except S_4 and S_6 which were liquids that solidified upon being left overnight. The compounds were soluble in ethanol.

The melting points of the compounds ranged from 110^{o}C 240^{o}C. Masses of the compounds obtained ranged from 13.8- 20.4 g corresponding to a 75- 89% yield. Infrared spectroscopy showed a peak at 1617.38- 1628.95 corresponding to the imine functional group. UV/Vis bands at 261.40- 287.60 corresponding to C=N bond were observed. ^{1}H NMR spectroscopy showed peaks at 8.62- 10.28 ppm corresponding to imine protons while ^{13}C NMR showed peaks at 159.35- 192.32 ppm corresponding to imine carbon atoms.

Selected bacteria and fungus showed different susceptibility to the synthesized compounds *in vitro* at different concentrations (500 ppm, 250 ppm and 125 ppm). At the three concentration levels, *Staphylococcus aureus*, *Salmonella typhi* and *Pseudomonas aeruginosa* were the most susceptible. *Salmonella typhi* was the most susceptible to S_1, S_3, S_5 and S_6. *Staphylococcus aureus* was the most susceptible to S_4 at the three concentrations. At 500 ppm and 250 ppm, *Staphylococcus aureus* was the most susceptible to compound S_6. Generally, *Candida albicans* showed the least activity against all the synthesized compounds. In all concentrations, S_6 was found to

be the most active. The activity exhibited by S_6 was against *Salmonella typhi* and *Staphylococcus aureus.*

5.2 Conclusions

Stochiometrically, primary aromatic amines and aromatic aldehydes condense in a 1:1 ratio to form Schiff bases. Solvent and catalyst free approach in the synthesis of Schiff bases prevent environmental pollution which was one of the main abjectives of this study. High yields are achieved in solvent and catalyst free grinding and stirring synthetic approaches. Reaction time is highly reduced compared to reflux method. However, the reaction times are longer than those involved in microwave irradiation. Production of by products is highly minimized through these procedures.

The compounds had moderate (110^{o}C) to high (240^{o}C) meting points. Infrared peaks at around 1620 cm^{-1}, UV/Vis bands at around 261 nm, ^{1}H NMR peaks at around 8.62 ppm and ^{13}C NMR at around 159 ppm confirm the presence of C=N bond. This confirms conversion of the amines and aldehydes to Schiff bases in solvent and catalyst procedures. In the IR spectra, the absence of the C=O band at around 1675 cm^{-1} further supports the conclusion that the aldehydes were converted to Schiff bases.

The antimicrobial activity of the synthesized compounds was moderate, slightly lower than that of the standard drug (gentamycin). Significant activity was observed in *Salmonella typhi* (gram negative), *Pseudomonas aeruginosa* (gram negative) and *Staphylococcus aureus* (gram positive). *Candida albicans* and *Escherichia coli* showed the least susceptibity towards the Schiff bases. The compounds had more antibacterial activity than antifungal activity.

5.3 Recommendations of the Study

Based on the results obtained, the following recommendations are made:

i. The characterization of the Schiff bases should be completed by including mass spectrometry and elemental analysis.

5.4 Recommendation for Further Studies

i. Further investigations to elucidate the underlying mechanisms of action for the synthetic compounds, including their mode of interaction with microbial cells should be carried out.

ii. The potential synergistic effects of combining different synthetic compounds should be explored, as this may enhance their antimicrobial efficacy.

iii. The study should investigate structural modifications of the synthetic compounds to enhance their antimicrobial activity while minimizing potential toxicity.

REFERENCES

Abdussalam-Mohammed, W., Ali, A. Q. and Errayes, A. O. (2020). Green chemistry: principles, applications, and disadvantages. *Chemical Methodologies*, 4(4), 408-423.

Abirami, M. and Nadaraj, V. (2014). Synthesis of Schiff base under solvent-free condition: As a green approach. *International Journal of ChemTech Research.* 6(4) 2534-2538.

Achutha, L., Parameshwar, R., Reddy, B.M. and Babu, V.H. (2013). Microwave-Assisted Synthesis of Some Quinoxaline-Incorporated Schiff Bases and their Biological Evaluation. *Journal of Chemistry.* 2013(1) 578438.

Al Zoubi., W., Al-Hamdani, A.A.S., Ahmed, S.D. and Ko, Y.G. (2017). A new azo-Schiff base: Synthesis, characterization, biological activity and theoritical studies of its complexes. *Applied Organometallic Chemistry*. 32(1), e3895.

Alharthi, S.S., Gomathi, T., Joseph, J.J., Rakshavi, J., Florence, J.A.K., Sudha, P.N., Rajakumar, G. and Thirunengadam, M. (2022). Biological activities of chitosan-salicylaldehyde Schiff base assisted silver nanoparticles. *Journal of King Saud University-Science.* 34(6) 102177.

Aljamali, N.M., Alasady, D. and Hassen, H.S. (2021). Review on Azomethine-Compounds with Their Applications. *International Journal of Chemical Synthesis and Chemical Reactions.*7(2) 1-10.

Al-Omar, M.A. and Amr, A.E.G.E. (2010). Synthesis of some new pyridine-2,6-carboxamide-derived Schiff bases as potential antimicrobial agents. *Molecules.* (15) 4711-4721.

Anacona, J.R., Santaella, J., Al-shemary, R.K.R, Amenta, J., Otero, A., Ramos, C. and Celis, F. (2021). Ceftriaxone-based Schiff base transition metal (II) complexes. Synthesis, characterization, bacterial toxicity and DFT calculations. Enhanced antibacterial activity of a novel Zn(II) complex against *S. aureus* and *E. coli. Journal of Inorganic Biochemistry.* 223(2021) 111519.

Anastas, P. and Eghbali, N. (2010). Green chemistry: principles and practice. *Chemical Society Reviews.* 39(1) 301- 312.

Arafa, W.A. and Shaker, R.M. (2016). A facile green chemistry approaches towards the synthesis of bis-Schiff bases using ultrasound versus microwave and conventional method without a catalyst. A*rkivoc.* 3 (187), 10-3998.

Aragon-Muriel, A., Reyes-Marquez, V., Canavera-Buelvas, F., Parra-Unda, J.R., Cuenu-Cabezas, F., Polo-Ceron, D., Colorado-Peralta, R., Suarez-Moreno, G., Aguilar-Castillo, B. and Morales-Morales, D. (2022). Pincer complexes derived from tridentate Schiff bases for their use as antimicrobial metallopharmaceuticals. *Inorganics.* 10(9), 134.

Aslam, M., Anis, I., Afza, N., Hussain, A., Iqbal, L., Iqbal, J., Ilyas, Z., Chaudhry, A. and Niaz, M. (2012). Structure-activity relationships study: synthesis, characterization and biological investigation of Schiff bases derived from 2-aminophenol and 4-haloacetophenones. *International Journal of Current Pharmaceutical Research.* 4(4), 42-46.

Bajpai, V.K., Sharma, A. and Baek, K.H. (2013). Antibacterial mode of action of *Cudrania tricuspidata* fruit essential oil affecting membrane permeability and surface characteristics of food-borne pathogens. *Food Control.* 32(2), 582-590.

Barbosa, H.F., Attjioui, M., Leitao, A., Moerschbacher, B.M. and Cavalheiro, E.T. (2019). Characterization, solubility and biological activity of amphihilic biopolymeric Schiff bases synthesized using chitosans. *Carbohydrate Polymers.* 220, 1-11.

Becker, K., Van Allen, S., Idelevich, E., Schleimer, N., Seggewiβ, J., Mellmann, A. and Peters, G. (2018). Plasmid-encoded transferable mec-B-mediated methicillin resistance in *Staphylococcus aureus. Emerging Infectious Diseases.* 24(2), 242.

Bedi, P., Pramanik, G and Pramanik, T. (2020). Garlic catalyzed and grindstone assisted solvent free green synthesis of pharmaceutically important Schiff bases. *Research Journal of Pharmacy and Technology.*13(1), 152- 156.

Bello-Lopez, J.M., Cabrero-Martinez, O.A., Ibanez-Cervantes, G., Hernandez-Cortez, C., Pelcastre-Rodriguez, L.I., Gonzalez-Avila, L.U. and Castro-Escarpulli G. (2019). Horizontal gene transfer and its association with antibiotic resistance in the genus *Aeromonas spp. Microorganisms.* 7(9), 363.

Bendale, A.R., Bhatt, R., Nagar, A., Jadhav, A.G. and Vidyasagar, G. (2011). Schiff base synthesis by unconventional route: An innovative green approach. *Der Pharma Chemica.* 3(2), 34-38**.**

Berhanu, A., Mohiuddin, G., Malik, A., Aulakh, J., Kumar, V. and Kim, K.(2019). A Review of the Applications of Schiff Bases as Optical Chemical Sensors.*TrAC Trends in Analytical Chemistry.*116(2019) 74-91

Bharti, S.K., Nath, G., Tilak, R. and Singh, S.K. (2010). Synthesis, anti-bacterial and anti-fungal activities of some novel Schiff bases containing 2,4-disubstituted thiazole ring. *European Journal of Medicinal Chemistry.* 45(2), 651-660.

Bhusnure, O.G., Vibhute, Y.B., Giram, P.S. and Vibhute, A.Y. (2015). Innovative Green synthesis of Schiff bases and their Antimicrobial Activity. *Journal of Pharmavy Research.* 9(12), 670- 677.

Boruah, J.J., Bhatt, Z.S., Nathani, C.R., Bambhaniya, V.J., Guha, A.K. and Das, S.P. (2021). Green synthesis of a vanadium (V) Schiff base complex by grinding method: study on its catalytic and anti-bacteraial activity. *Journal of Coordination Chemistry.* 74(12)2055-2068.

Cai, Y. H. and Luo, W. (2014). Preparation of Schiff Base Derived from 3,4-Dimethoxybenzaldehyde and *p*-Aminobenzoic acid by Supersonic Speed Gas Impacting Method. *Journal of Chemistry*.2014(1) 218376.

Cai, Y.H., Ma, D.M., Peng, R.F. and Chu, S.J. (2008). Preparation of Ultra-fine calcium carbonate by a solvent-free reaction using supersonic airflow and low temperatures. *South African Journal of Chemistry*. 61, 112-114.

Camara, G.A and Isawati, T.(2005). Parallel pathways of ethanol oxidation: The effect of ethanol concentration. *Journal of Electroanalytical Chemistry*. 578(2), 315-321.

Ceramella, J., Iacopetta, D., Catalano, A., Cirillo, F., Lappano, R. and Sinicropi, M.S. (2022). A review on the antimicrobial activity of Schiff bases: Data collection and recent studies. *Antibiotics.* 11(2), 191.

Chakraborty, M., Baweja, S., Bhagat, S. and Chundawat, T. (2012). Microwave assisted synthesis of Schiff bases: A green approach. *International Journal of Chemical Reactor Engineering.*10(1).

Chalmers, J. D. and Pletz, M. W. (2017).Antibiotic Stewardship in the Hospital Setting.*European Respiratory Society.*127-149.

Chemchem M., Menacer R., Merabet N., Bouridane H., Yahiaoui S., Moussaoui S. and Belkhiri L. (2020). Green synthesis, antibacterial evaluation and QSAR analysis of some isatin Schiff bases. *Journal of Molecular Structure.* 1208, 127853.

Chigurupati, S. (2015). Designing new vanillin schiff bases and their antimicrobial studies. *Journal of Medical and Bioengineering.* 4, 363-366.

Cinarli, A., Gurbuz, D., Tavman, A. and Birteksoz, A. (2011). Synthesis, spectral characterizations and antimicrobial activity of some Schiff bases of 4-chloro-2-aminophenol. *Bulletin of the Chemical Society of Ethiopia.* 25(3).

Cincic, D. and Kaitner, B. (2010). Schiff base derived from 2-hydroxy-1-napthaldehyde and liquid-assisted mechanochemical synthesis of isostructural Cu(II) and Co(II) complexes. *CrystEngcomm*. 13(13), 4351-4357.

Coates, A.R., Halls, G. and Hu, Y. (2011). Novel classes of antibiotics or more of the same? *British Journal of Pharmacology*. 163(1), 184-194.

Dadgostar, P. (2019). Antimicrobial resistance: implications and costs. *Infection and Drug Resistance*. 3903-3910.

De Francesco, V., Giorgio, F., Hassan, C., Manes, G., Vannella, L., Panella, C., Lerardi, E. and Zullo, A. (2010). Worldwide *Helicobacter pylori.* Antibiotic Resistance: a systematic review. *Journal of Gastrointestinal and Liver Diseases.* 19(4), 409-419.

Dianat, O., Saedi, S., Kazem, M. and Alam, M. (2015). Antimicrobial activity of nanoparticle calcium hydroxide against *Enterococcus faecalis*: in vitro study. *Iranian Endodontic Journal.* 10(1), 39.

Dos Santos Abrantes, P.M., McArthur, C.P. and Africa, C.W.J. (2014). Multi-drug resistant oral *Candida spps* isolated from HIV-positive patients in South Africa and Cameroon. *Diagonistic Microbiology and Infectious Diseases.* 79(2), 222-227.

Dowling, A., O'Dwyer, J. and Adley, C. (2017). Antibiotics: mode of action and mechanisms of resistance. *Antimicrobial research: Novel bioknowledge and educational programs*. 1, 535- 545.

Ebrahimi, H.P., Hadi, J.S., Abdulnabi, Z.A. and Bolandnazar, Z. (2014). Spectroscopic, thermal analysis and DFT computational studies of salen-type Schiff base complexes. *Spectrochimica Acta Part A: Molecular and Biomolecular Spectroscopy.* 117, 485-492.

Eftekhari, S., Foroughifar, N., Hallajian, S. and Khajeh-Amiri, A. (2020). Green Synthesis of Some Novel Imidazole Schiff base Derivatives Under Microwave Irradiation/Reflux Conditions and Evalluations of the Antibacterial Activity. *Current Microwave Chemistry.* 7(3), 207- 215.

Ejidike, I.P. and Ajibade, P.A. (2016). Synthesis, characterization, anticancer and antioxidant studies of Ru(III) complexes of monobasic tridentate Schiff bases. *Bioinorganic Chemistry and Applications.* 2016(1) 9672451.

El-Gammal, O.A., Mohamed, F.S., Rezk, G.N. and El-Bindary, A.A. (2021). Structural characterization and biological activity of a new metal complexes based on Schiff base. *Journal of Molecular Liquids.* 330, 115522.

El-Garch, F., Lismond, A., Piddock, L.J,, Courvalin, P., Tulkens, P.M. and Bambeke, F. (2010). Fluoroquinolones induce the expression of patA and patB, which encode ABC efflux pumps in *Streptococcus pneumoniae. Journal of Antimicrobial Chemotherapy.* 65(10), 2076-2082.

El-Sayed, W.M., Hussin, W.A., Mahmoud, A.A. and AlFredan, M.A. (2013). The *Conyza triloba* extracts with high chlorophyll content and free radical scavenging activity had anticancer activity in cell lines. *BioMed Research International*. 2013(1), 945638.

Fabbrizzi, L. (2020). Beauty in chemistry: making artistic molecules with Schiff bases. *The Journal of Organic Chemistry.* 85(19), 12212-12226.

Ferrari, E., Saladini, M., Pignedoli, F., Spagnolo, F. and Benassi, R. (2011). Solvent Effect On Keto-Enol Tautomerism in A New B-Diketone: A Comparison Between Experimental Data and Different Theoretical Approaches. *New Journal of Chemistry*, (35), 2840-2847.

Fugu, M.B., Ndahi, N.P., Paul, B.B. and Mustapha, A.N. (2013). Synthesis, characterization and antimicrobial studies of some vanillin schiff base metal (II) complexes. *Journal of Chemical and Pharmaceutical Research*. 5(4), 22-28.

Gavalyan, V.B. (2016). Synthesis and characterization of new chitosan-based Schiff base compounds. *Carbohydrate Polymers.* 145, 37-47.

Gichumbi, J.M., Friedrich H.B., Omondi, B., Singh M., Naicker K. and Chenia, H.Y. (2016). Synthesis, characterization and cytotoxic and antimicrobial activities of ruthenium(II) arene complexes with N,N-bidentate ligands. *Journal of Coordination Chemistry*. 69(23), 3531-3544.

Glaser, P., Martins-Simones, P., Villain, A., Barbier, M., Tristan, A., Bouchier, C., Vandenesch, F. (2016). Demography and intercontinental spread of the USA 300 community acquired methicillin-resistant *Staphylococcus aureus* lineage. *mBio.* 7(1), 10-1128.

Gold, K., Slay, B., Knackstedt, M. and Gaharwar, A. K. (2018). Antimicrobial activity of metal and metal- oxide based nanoparticles. *Advanced Therapeutics.* 1(3), 1700033.

Gopalakrishnan, M., Sureshkumar, P., Kanagarajan, V., Thanusu J. and Govindaraju, R. (2006). A simplified green chemistry approaches to organic synthesis in solid media. Activated fly ash, an industrial waste (pollutant) as an efficient and novel catalyst for some selected organic reactions in solvent free conditions under microwave irradiation. *ARKIVOC*. 13, 130-141.

Guardabassi, L. and Courvalin, P. (2005). Modes of antimicrobial action and mechanisms of bacterial resistance. *Antimicrobial Resistance in Bacteria of Animal Origin*. 1-18).

Guo, Z., Zhang, Q., Cheng, Z., Liu, Q., Zuo, J., Jin, B. and Peng, R. (2020). Airflow impacting synthesis of metal organic frameworks: a continuous highly efficient large-scale mechanochemical synthetic method. *ACS Sustainable Chemistry and Engineering.* 8(10) 4037-4043.

Hackel, M., Lascols, C., Bouchillon, S., Hilton, B., Morgenstern, D. and Purdy, J. (2013). Serotype prevalence and antibiotic resistance in *Streptococcus pneumoniae* clinical isolates among global populations. *Vaccines.* 31(42), 4881-4887.

Hisaindee, S., Al-Kaabi, L., Ajeb, S., Torky, Y., Iratni, R., Saleh, N. and AbuQamar, S. (2015). Antipathogenic effects of structurally-related Schiff base derivatives. Structure-activity relationship. *Arabian Journal of Chemistry.* 8(6), 828- 836.

Holthoff, E.L., Farrell, M.E. and Pellegrino, P.M. (2012). Investigating a drop-on-demand microdispenser for standardized sample preparation. *In Chemical Biological, Radiological, Nuclear and Explosives (CBRNE) Sensing XIII*. 8358, 234-241.

Issa, R.M., Khedr, A.M. and Rizk, H. (2008). ^{1}H NMR, IR and UV/VIS Spectroscopic Studies of Some Schiff Bases Derived from 2-Aminobenzothiazole and 2-Amino-3-Hydroxypyridine. *Journal of the Chinese Chemical Society*. 55(4), 875-884.

Jain, A., De, S. and Barman, P. (2022). Microwave-assisted synthesis and notable applications of Schiff-base and metal complexes: a comparative study. *Research On Chemical Intermediates.* 48(5), 2199- 2251.

Jaka, H., Rhae, J., Oustlundh, L., Peck, R., Mueler, A., Kassang, C. and Mshana, S. (2018). The Magnitude of Antibiotic Resistance to *H. pylori* in Africa and Identified Mutants which confer Resistance to Antibiotics: Systematic Review and Meta-analysis. *BMC Infectious Diseases.*18(1), 8876-8898.

Kangogo, M.C., Wanyoike, W., Revathi, G., Wakibia, J.G. and Bii, C. (2011). Emerging azole resistance among *Candida albicans* from clinical sources in Nairobi, Kenya. *Journal of Agriculture, Science and Technology.* 13(2), 108-114.

Kapadnis, K.H., Jadhar, S.P., Patil A.P. and Hiray, A.P. (2016). Four synthetic methods of Schiff base ligands and preparation of their metal complexes with infrared and antimicrobial investigation. *World Journal of Pharmacy and Pharmaceutical Sciences.* 5(2), 1055-1063.

Kar, S., Mohapatra, P. and Mohanty, D. (2023). Green synthesis, characterization and antibacterial activity studies of new multifunctional nano polymeric material, which may have multidimensional application in water purification. *Polymer Bulletin.* 80(1), 703-723.

Keller, L.E., Robinson, D.A. and McDaniel, L.S. (2016). Nonencapsulated *Streptococcus pneumoniae:* emergence and pathogenesis. *mBio.* 7, 1792- 1815.

Kesah, C., Ben Redjeb, S., Odugbemi, T.O., Boye, C.B., Dosso, M., Ndinya Achola, J.O., Koulla, S., Benbachir, M., Rahal, K. and Borg, M. (2003). Prevalence of methicillin-resistant *Staphylococcus aureus* in eight African hospitals and Malta. *Clinical Microbiology and Infection.* 9(2), 153-156.

Khalil, M.M., Ismail, E.H., Mohamed, G.G., Zayed, E.M. and Badr, A. (2012). Synthesis and characterization of a novel schiff base metal complexes and their application in determinination of iron in different types of natural water. *Open Journal of Inorganic Chemistry*.2(2) 13.

Khameneh, B., Iranshahy, M., Soheili, V. and Fazly Bazzaz, B. S. (2019). Review on plant antimicrobials: a mechanistic viewpoint. *Antimicrobial Resistance & Infection Control. 8*, 1-28.

Kim J., Lee J., Park J. and Gho Y. (2015). Gram-negative and Gram-positive bacterial extracellular vesicles. *Seminars in Cell & Developmental Biology.* 40, 97-104.

Klein, D. (2012). *Organic Chemistry* (pp. 915-1089). John Wiley and Sons Inc.

Kumar S. and Varela M. (2013). Molecular mechanisms of bacterial resistance to antimicrobial agents. *Chemotherapy*. 14(18) 522- 534.

Kumar, S., Dhar, D.N. and Saxena, P.N. (2009). Applications of metal complexes of Schiff bases-A review. *Journal of Scientific & Industrial Research*, 68, 181-187.

Lemilemu, F., Bitew M., Demissie, T.B., Eswaramoorthy, R. and Endale, M. (2021). Synthesis, antibacterial and antioxidant activities of Thiazole-based Schiff base derivatives: a combined experimental and computational study. *BMC Chemistry.* 15(1), 67.

Li, H., Chen, Q., Zhao, J., & Urmila, K. (2015). Enhancing the antimicrobial activity of natural extraction using the synthetic ultrasmall metal nanoparticles.*Scientific Reports*. 5(1), 11033.

Li, J. and Zhuang, S. (2020). Antibacterial activity of chitosan and its derivatives and their interaction mechanism with bacteria: Current state and perspectives. *European Polymer Journal.* 138, 109984.

Liu, H., Xing, F., Zhou, Y., Yu, P., Xu, J., Luo, R. and Ritz, U. (2023). Nanomaterials-based photothermal therapies for antibacterial applications. *Materials and Design.* 11223.

Liu, X. and Hamon, J.R. (2019). Recent developments in penta-, hexa- and heptadentate Schiff base ligands and their metal complexes. *Coordination Chemistry Reviews.* 389, 94-118.

Liu, Y., Yang, L., Yin, D., Dang, Y., Yang, L., Zou, Q., Jie, L. and Sun, J. (2019). Solvent-free synthesis, characterization, biological activity of Schiff bases and their metal (II) complexes derived from ferrocenyl chalcone. *Journal of Organometallic Chemistry.* 899, 120903.

Majeed, N.M., Obaid S.M.H., Raheema M.H., Al-Noor T.H., Al-Ayash S.R. and Abdou A. (2023). Preparation, Characterization and Biologial Activity of Mixed Schiff Base Ligand Complexes with Amino Acid L-Proline.*Rusian Journal of General Chemistry.* 93(Suppl 4), S1016- S1025.

Mane, A., Vidhate, P., Kusro, C., Waman, V., Saxena, V., Kulkarni-Kale, U. and Risbud, A. (2016). Molecular mechanisms associated with fluconazole resistance in clinical *Candida albicans* isolates from India. *Mycoses.* 59(2), 93-100.

McManus, M. (1997). Mechanisms of bacterial resistance to antimicrobial agents. *American Journal of Health-System Pharmacy.* 54(12), 1420- 1433.

Mermer, A., Demirbas, N., Uslu, H., Demirbas, A., Ceylan, S. and Sirin, Y. (2019). Synthesis of novel Schiff bases using green chemistry techniques; antimicrobial, antioxidant, antiurease activity screening and molecular docking studies. *Journal of Molecular Structure.* 1185, 412-422.

Miar, M., Shiroudi, A., Pourshamsian, K., Oliaey, A. and Hatamjafari, F., (2021). Theoritical investigations on the HOMO-LUMO gap and global reactivity descriptor studies, natural bond orbital and nucleus-independent chemical shifts analyses of 3-phenylbenzo[*d*]thiazole-2(3H)-imine and its *para*-substituted derivatives: Solvent and substituent effects. *Journal of Chemical Research.* 45(1-2), 147-158.

Miceli, M.H., Diaz, J.A. and Lee, S.A. (2011). Emerging opportunistic yeast infections. *The Lancet Infectious Diseases.* 11(2), 142-151.

Mohamed, G.G., Omar, M.M. and Hindy, A.M. (2006). Metal complexes of Schiff bases: preparation, characterization and biological activity. *Turkish Journal of Chemistry*. 30(3) 361- 382.

Mounika, K., Pragathi, J. and Gyanakumari, C. (2010). Synthesis, characterization and biological activity of a Schiff base derived from 3-ethoxy salicylaldehyde and 2-amino benzoic acid and its transition metal complexes. *Journal of Scientific Research.* 2(3), 513- 513.

Muhammad Kaleem, K., Muhammad Asghar, J., Muhammad Jawad, S., Majid, M., ur Rehman, F., Muhammad, F., Hafiz, M.S., Muhammad, S. and Shabnam, H. (2015). Synthesis, Spectra investigation [[1H], [13C]] and Anti-microbial screening of benzophenone imines. *Parkistan Journal of Pharmaceutical Sciences.* 28 (6), 2167-2171.

Munde, A.S., Jagdale, A.N., Jadhav, S.M. and Chondhekar, T.K. (2010). Synthesis, characterization and thermal study of transition metal complexes of an asymmetrical tetradentate Schiff base ligand. *Journal of the Serbian Chemical Society.* 75(3), 349-359.

Naeimi, H., Salimi, F. and Rabiel, K. (2006). Mild and convinient one pot synthesis of Schiff bases in the presence of P_2O_5 / Al_2O_3 as new catalysts under solvent-free conditions. *Journal of Molecular Catalysis*. 260(1-2), 100-104.

Nagesh, G. Y. and Mruthyunjayaswamy, B. H. M. (2015). Synthesis, characterization and biological relevance of some metal (II) complexes with oxygen, nitrogen and oxygen (ONO) donor Schiff base ligand derived from thiazole and 2-hydroxy-1-naphthaldehyde. *Journal of Molecular Structure*. 1085, 198-206.

Naghavi, M., Vollset, S.E., Ikuta K.S., Swetschinski L.R., Gray A.P., Wool E.E., Aguilar G., Mestrovic T., Smith G., Han C., Hsu R., Chalek J., Araki D., Chung E. and Raggi C. (2024). Global burden of bacterial antimicrobial resistance 1990-2021: a systematic analysis and forecast to 2050. *The Lancet.* 404(10459) 1199-1226.

Naik, B. and Desai, K.R. (2006). Novel approach for the rapid and efficient synthesis of heterocyclic Schiff bases and azetidinones under microwave irradiation. *Indian Journal of Chemistry.* 45B, 267-271.

Nakano, S., Fujisawa, T., Ito, Y., Chang, B., Matsumura, Y., Yamamoto, M. and Ichiyamo, S. (2018). Spread of meropenem-resistant *Streptococcus pneumoniae*

serotype 15A-ST63 clone in Japan, 2012-2014. *Emerging Infectious Diseases.* 24(2), 275.

Naqvi, A., Shahnawaaz, M., Rao, A.V., Seth, D.S. and Sharma, N.K. (2009). Synthesis of Schiff Bases via Environmentally Benign and Energy-Efficient Greener Methodologies. *Journal of Chemistry.* 6, S75-S78.

Nordmann, P., Naas, T. and Poirel, L. (2011).Global spread of carbapenemase-producing *Enterobacteriaceae. Emerging Infectious Diseases.* 17(10), 1791-1798.

Nunez, M.G., Farley A.J. and Dixon D.J. (2013). Bifunctional iminophosphorane organocatalysts for enantioselective synthesis: application to the ketimine nitro-Mannich reaction. *Journal of the American Chemical Society.* 135(44), 16348-16351.

Nys, S., Okeke, I.N., Kariuki, S., Dinant, G.J., Driessen, C. and Stobberingh, E.E. (2004). Antibiotic resistance of faecal *Escherichia coli* from healthy volunteers from eight developing countries. *Journal of Antimicrobial Chemotherapy*. 54(5), 952-955.

Okeke, I.N., Aboderin, O.A., Byarugaba, D.K., Ojo, K.K. and Opintan, J.A. (2007). Growing problem of multidrug-resistant enteric pathogens in Africa. *Emerging Infectious Diseases.* 13(11), 1640.

Ommenya, F.K., Nyawade, E.A., Andala, D.M. and Kinyua, J. (2020). Synthesis, Characterization and Antibacterial Activity of Schiff Base, 4-Chloro-2-{(E)-[(4-Fluorophenyl)imino] methyl}phenol Metal (II) Complexes. *Journal of Chemistry.* 2020(1) 1745236.

Ooi, T., Tayama, E., Doda, K., Takeuchi, M. and Maruoka, K. (2000). Dramatic rate enhancement by ultrasonic irradiation in liquid-liquid phase-transfer catalytic reactions. *Synlett.* 2000(10) 1500-1502.

Pal, R., Kim, K.H., Hong, Y.J. and Jeon,E.C. (2008). The pollution status of atmospheric carbonyls in a highly industrialized area. *Journal of Hazardous Materials.* 153(3), 1122- 1135.

Panda, J., Patro, V.J., Sahoo, B.M. and Mishra, J. (2013). Green Chemistry Approach for Efficient Synthesis of Schiff Bases of Isatin Derivatives and Evaluation of their Antibacterial Activities. *Journal of Nanoparticles.* 2013(1), 549502.

Parekh, J., Inamdhar, P., Nair, R., Baluja, S. and Chanda, S. (2005). Synthesis and antibacterial activity of some Schiff bases derived from 4-aminobenzoic acid. *Journal of the Serbian Chemical Society*. 70(10), 1155-1162.

Perkampus, H. H. and Perkampus, H. H. (1992). Recent developments in UV-VIS spectroscopy. *UV-Vis Spectroscopy and Its Applications*. 81-130)

Perlin, D.S., Rautemaa-Richardson, R. and Alastruey-Izquierdo, A. (2017). The global problem of antifungal resistance: prevalence, mechanisms and management. *The Lancet Infectious Diseases.* 17(12), e383-e392.

Petty, N. K., Ben Zakour, N. L., Stanton-Cook, M., Skippington, E., Totsika, M., Forde, B. M., ...& Beatson, S. A. (2014). Global dissemination of a multidrug resistant *Escherichia coli* clone. *Proceedings of the National Academy of Sciences*. 111(15), 5694-5699.

Pfaller, M.A., Messer, S.A., Woosley, L.N., Jones, R.N. and Castanleira, M. (2013). Echinocandin and triazole antifungal susceptibility profiles for clinical opportunistic yeast and mold isolates collected from 2010 to 2011: application of new CLSI clinical breakpoints and epidemiological cutoff values for characterization of geographic and temporal trends of antifungal resistance. *Journal of Clinical Microbiology*. 51(8), 2571-2581.

Pokhrel, R., Shakya, R., Baral, P., & Chapagain, P. (2022). Molecular modeling and simulation of the peptidoglycan layer of Gram-positive bacteria *Staphylococcus aureus*. *Journal of Chemical Information and Modeling.* 62(20), 4955-4962.

Pratiwi R.A. and Nandiyanto A.B.D. (2022). How to read and interpret UV-Vis spectrophotometric results in determining the structure of chemical compounds. *Indonesian Journal of Educational Research and Technology.* 2(1), 1-20.

Raafat, M. I., Abdalla, M. K. and Helen, F. R. (2005). UV-Vis, IR and ^{1}H NMR Spectroscopic Studies of some Schiff Bases of Derivatives of 4-aminoantipyrine. *Science Direct.* 62(2005), 621-629.

Rani, A., Kumar, M., Khare, R. and Tuli, H.S. (2015). Schiff base as an antimicrobial agent: A review. *Journal of Biological and Chemical Sciences.* 2, 62-91.

Sachdeva, H., Saroj, R., Khaturia, S., Dwivedi, D. (2012). Operationally simple green synthesis of some Schiff bases using grinding chemistry technique and evaluation of antimicrobial activities. *Green Processing and Synthesis*. 1(5), 469-477.

Sachdeva, H., Saroj, R., Khaturia, S., Dwivedi, D. and Prakash Chauhan, O. (2014). Green route for efficient synthesis of novel amino acid Schiff bases as potent antibacterial and antifungal agents and evaluation of cytotoxic effects. *Journal of Chemistry.* 2014(1), 848543.

Salama, H.E., Saad, G.R. and Sabaa, M.W. (2015). Synthesis, characterization and biological activity of Schiff bases based on chitosan and aryl pyrazole moiety. *International Journal of Biological Macromolecules.* 79, 996-1003.

Sanguinetti, M., Posteraro, B. and Lass-Florl, C. (2015). Antifungal drug resistance among *Candida* species: mechanisms and clinical impact. *Mycoses.* 58, 2-13.

Santos, J.E., Dockal, E.R. and Cavalheiro, E.T. (2005). synthesis and characterization of Schiff bases from chitosan and salicylaldehyde derivatives.*Carbohydrate Polymers.* 60(3), 277-282.

Savalia, R.V., Patel, A.P., Trivedi, P.T., Gohel, H.R. and Khetani, D.B. (2013). rapid and economical synthesis of Schiff bases of salicylaldehyde by microwave irradiation. *Research Journal of Chemical Sciences.* 3(10), 97-99.

Secka, O., Berg, D.E., Antonio, M., Corrah, T., Tapgun, M., Walton, R., Thomas, V., Galano, J., Saucho, J., Adegbola, R. and Thomas, J. (2013). Antimicrobial susceptibility and resistance patterns among *Helicobacter pylori* strains from Gambia, West Africa. *Antimicrobial Agents and Chemotherapy*. 57(3), 1231-1237.

Shah, S., Lubeck, E., Zhou, W. and Cai, L. (2016). *In Situ* transcription profiling of single cells reveals spartial organization of cells in the mouse hippocampus. *Neuron.* 92(2), 342-357.

Shanty, A.A. and Mohanan, P.V. (2018). Heterocyclic Schiff bases as non-toxic antioxidants: Solvent effect, structure activity relationship and mechanism of action. *Spectrochimica Acta Part A*: *Molecular and Biomolecular Spectroscopy*. 192, 181- 187.

Sharaby, C.M., Amine, M.F. and Hamed, A.A. (2017). Synthesis, structure characterization and biological activity of selected metal complexes of sulfonamide schiff base as a primary ligand and some mixed ligand complexes with glycine as a secondary ligand. *Journal of Molecular Structure.* 1134, 208-216.

Sharif, H.M.A., Ahmed, D. and Mir, H. (2015). Antimicrobial salicylaldehyde Schiff bases: Synthesis, characterization and evaluation. *Pakistan Journal of Science.* 28(2), 449-455.

Sherif, E.S.M. (2011). Corrosion and corrosion inhibition of pure iron in neutral chloride solutions by 1,1'-thiocarbonyldiimidazole. *International Journal of Electrochemical Science.* 6(8), 3077- 3092.

Shinde, A., Zangade, S., Chavan, S. and Vibhute, Y. (2014). Microwave induced synthesis of bis-Schiff bases from propane-1,3-diamine as promising antimicrobial analogs. *Orgnanic Communications.* 7(2), 60-67.

Shinde, M.P., Toche, R.B., Chavan, S.M. and Tambde, P.J. (2018). Synthesis, Characterization and Antimicrobial Screening of Fe(II)-Glycine Schiff Base. *Chemical Science.* 7(1), 47-54.

Shittu, A.O. and Lin, J. (2006). Antimicrobial suscepibility patterns and characterization of clinical isolates of *Staphylococcus aureus* in Kwazulu-Natal province South Africa. *BMC Infectious Diseases.* 6, 1-13.

Simon, M.O. and Li, C.J. (2012). Green chemistry oriented organic synthesis in water. *Chemical Society Reviews*. 41(4), 1415-1427.

Singh, K., Kumar, Y., Puri, P., Sharma, C. and Aneja K.R. (2017). Antimicrobial spectra and thermal studies of divalent cobalt, nickel, copper and zinc complexes with triazole Schiff bases. *Arabian Journal of Chemistry*. 10, S978-S987.

Sinicropi M., Ceramella J., Iacopetta D., Catalano A., Mariconda A., Rosano C., saturnine C., El-Kashef H. and Longo P.(2022). Metal Complexes with Schiff Bases: Data Collection and Recent Studies of Biological Activities. *International Journal of Molecular Science.*23(23), 14840.

Smith, S., Fowora, M. and Pellicano, R. (2019). Infections with *Helicobacter pylori* and challenges encountered in Africa. *World Journal of Gastroenterology.* 25(25), 3183.

Sridevi, C. (2015). Designing New Vanillin Schiff bases and their Antimicrobial Studies.*Journal of Medical and Bioengineering.*4(5), 1-5.

Srivastva, A. N., Singh, N. P. and Shriwastaw, C. K. (2016). *In Vitro* antibacterial and antifungal activities of binuclear transition metal complexes of ONNO Schiff base and 5-methyl-2, 6-pyrimidine-dione and their spectroscopic validation. *Arabian Journal of Chemistry.* 9(1), 48-61.

Strauβ, L., Stegger, M., Akpaka, P.E., Alabi, A., Breurec, S., Coombs, G. and Mellmann, A. (2017). Origin, evolution and global transmission of community acquired *Staphylococcus aureus* ST8. *Proceedings of the National Academy of Sciences.* 114(49), E10596-E10604.

Stuart, B.H. (2004). Infrared spectroscopy: fundamentals and applications. *John Wiley & Sons, Inc.*

Sun, W.H., Li, K.H., Liu, H., Gu, Y.T., Zhang, Y., You, Z.L. and Li, W. (2017). Synthesis, characterization, crystal structures and antibacterial activity of polynuclear nickel (ii) and copper (ii) complexes with similar tridentate Schiff bases. *Russian Journal of Coordination Chemistry*. 43, 693-699.

Taj, T., Kamble, R.R., Gireesh, T.M., Hunnur, R.K. and Margankop, S.B. (2011). One-pot synthesis of pyrazoline derivatised carbazoles as antitubercular, anticancer agents, their DNA cleavage and antioxidant activities. *European Journal of Medicinal Chemistry.* 46(9), 4366-4373.

Talaviya, S. and Majmudar, F. (2012). Green chemistry: A tool in pharmaceutical chemistry. *NHL Journal of Medical Sciences.* 1(1), 7-13.

Tanih, N.F., Dube, C., Green, E., Mkwetshana, N., Clarke, A.M., Ndip, L.M. and Ndip, R.N. (2009). An African perspective on *Helicobacter pylori:* prevalence of human infection drug resistance and alternative approaches to treatment. *Annals of Tropical Medicine and Parasitology.* 103(3), 189-204.

Tanih, N.F., Okeleye, B.I., Naidoo, N., Clarke, A.M., Mkwetshana, N., Green, E., Ndip, L. and Ndip, R. (2010). Marked susceptibility of South African *Helicobacter pylori* strains to ciprofloxacin and amoxicillin: clinical implications. *South African Medical Journal.* 100(1), 45-48.

Terreni, M., Taccani, M. and Pregnolato, M. (2021). New antibiotics for multidrug-resistant bacterial strains: latest research developments and future perspectives. *Molecules.* 26(9), 2671.

Thung, I.H., Aramin, V., Vavinskaya, S., Gupta, S., Park, J.Y., Crowe, S.E. and Valasek, M.A. (2016). The global emergence of *Helicobacter pyroli* antibiotic resistance. *Alimentary Pharmacology &Theraputics.* 43(4), 514-533.

Thystrup C., Majowicz S.E., Kitila D.B., Desta B.N., Fayemi O.E., Ayolabi C.I., Hugho E., Buys E., Akanni G., Machava N., Monjane C., Hald T. and Pires S.M. (2024). Etiology-specific incidence and mortality of diarrheal diseases in the African region: a systematic review and meta-analysis. *BMC Public Health.* 24(1), 1864.

Uddin, M.N., Ahmed, S.S. and Alam, S.R. (2020). Biomedical applications of Schiff base metal complexes. *Journal of Coordination Chemistry.* 73(23), 3109-3149.

Uddin, N., Rashid, F., Ali, S., Tirmizi, S., Ahmad, I., Zaib, S. and Haider, A. (2020). Synthesis, characterization and anticancer activity of Schiff bases. *Journal of Biomolecular Structure and Dynamics*, 38(11), 3246- 3259.

Upmanyu, N. and Malviya, V.N. (2020). Antibiotics: Mechanisms of action and modern challenges. *In Microorganisms for Sustainable Environment and Health.* 2020, 367-382.

Uzma, N., Khaja, B., Salar, M., Kumar, B., Aziz, N., David, M. and Reddy, V. (2008). Impact of Organic Solvents and Environmental Pollutants on the Physiological Function in Petrol Filling Workers.*International Journal of Environmental Research and Puvlic Health.* 139- 146.

Venkatesan, K., Satyanarayana, V.S.V. and Sivakumar, A. (2011). Ultrasonic assisted synthesis of napthalene substituted Schiff base derivatives and their antioxidant activity studies. *Journal of the Chinese Chemical Society.*58(5), 583-589.

Vibhute, A.Y., Mokle, S.S., Nalwar, Y.S., Vibhute, Y.B. and Gurav, V.M. (2009). An efficient and operationally simple synthesis of some new Schiff bases using grinding technique. *Bulletin of the Catalysis Society of India*. 8, 164-168.

Vicha, J. (2014). Applications of NMR Spectroscopy to Study Transition-Metal Complexes with Nitrogen-based Ligands. *Science Direct.* 25(3), 12-59.

Will, A., Natalia, M. and Frank, R. (2017). Vancomycin Resistance in *S. aureus.Yale Journal of Biology and Medicine.*90(2), 269-281.

Xavier, A. and Srividhya, N. (2014). Synthesis and Study of Schiff base ligands. *ISOR Journal of Applied Chemistry.* 7(11), 6-15.

Yadav, G. and Mani, J.V. (2015). Green synthesis of Schiff bases by using natural acid catalysts. *International Journal of Science and Research.* 4(2) 121-127.

Yusuf, T.L., Oladipo, S.D., Olagboye, S.A., Zamisa, S.J. and Tolufashe, G.F. (2020). Solvent-free synthesis of nitrobenzyl Schiff bases. Characterization, antibacterial studies, density function theory and molecular docking studies. *Journal of Molecular Structure.* 1222, 128857.

Zaidan, M.R., Noor Rain, A., Badrul, A.R., Adlin, A., Norazah, A. and Zakiah, I. (2005). In vitro screening of five local medicinal plants for antibacterial activity using disc diffusion method. *Tropical Biomedicine.* 22(2), 165-170.

Zhang, R., Shebes, M.A., Kho, K., Scaffidi, S.J., Meredith, T.C. and Yu, W. (2021). Spatial regulation of protein A in *Staphylococcus aureus*. *Molecular Microbiology*. 116(2), 589-605.

Zulfiqar, A., Ahmed, D., Fatima, R. and Yousuf, S. (2020). Green synthesis, urease inhibitory activity and antioxidant potential of 4-bromo-2-(((2'-chloro-4'-nitrophenyl)imino)methyl)phenol Schiff base. *Journal of Molecular Structure.* 1202, 127263.

APPENDICES

Appendix 1: Infrared spectra of compounds S_2-S_6

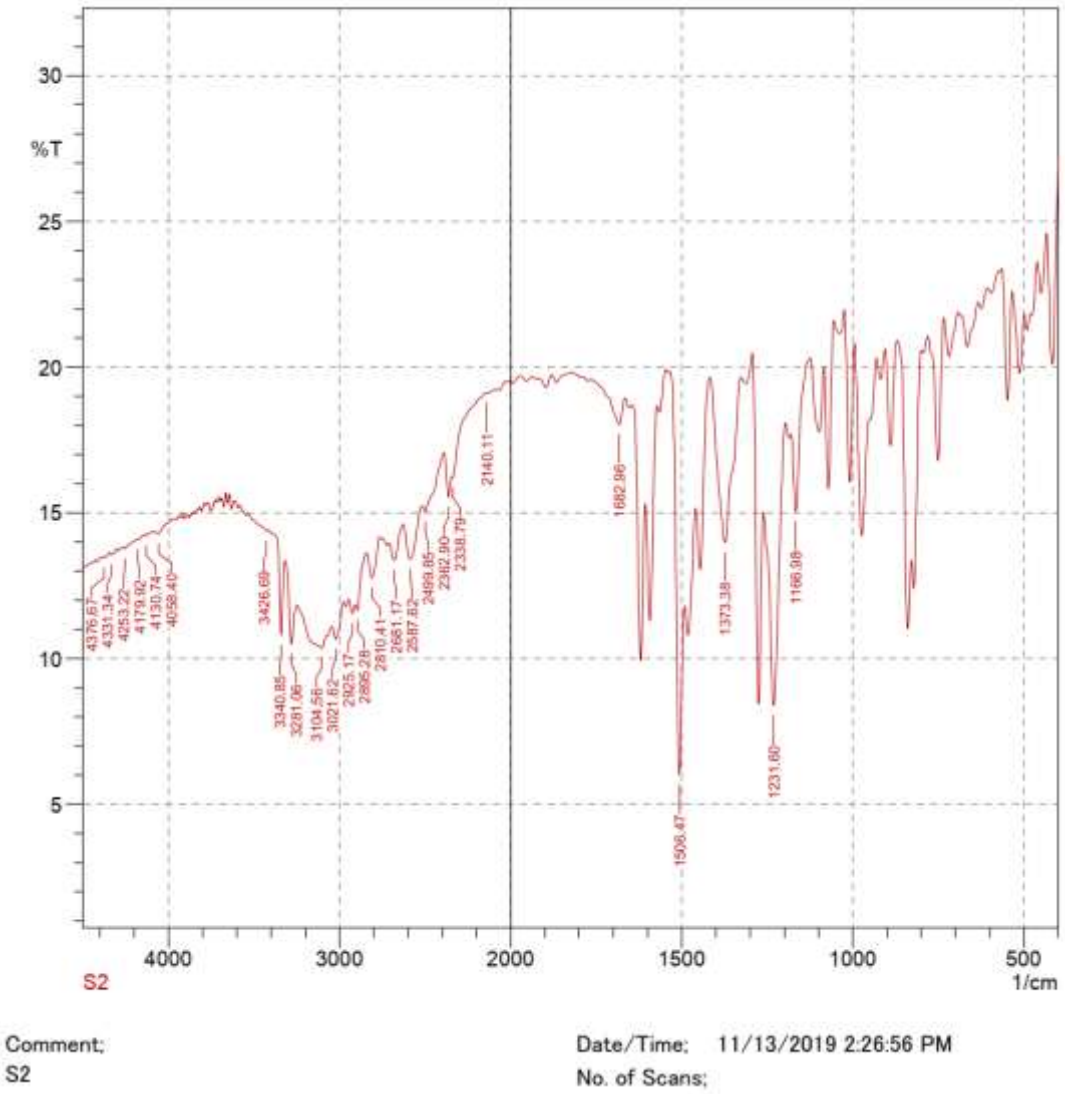

Figure 1(a): Infrared spectrum of Schiff base S_2

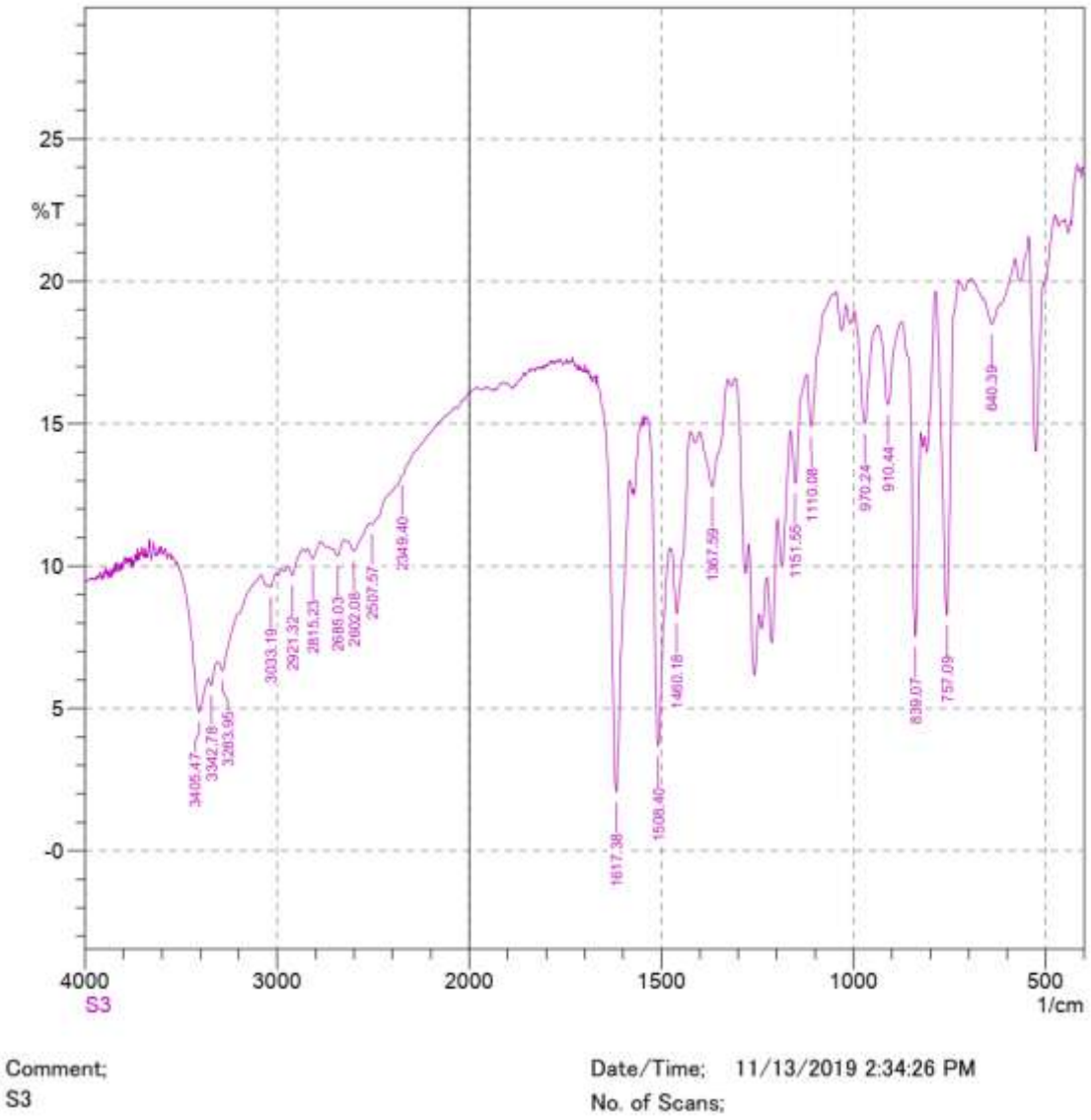

Figure 1(b): Infrared spectrum of Schiff base S_3

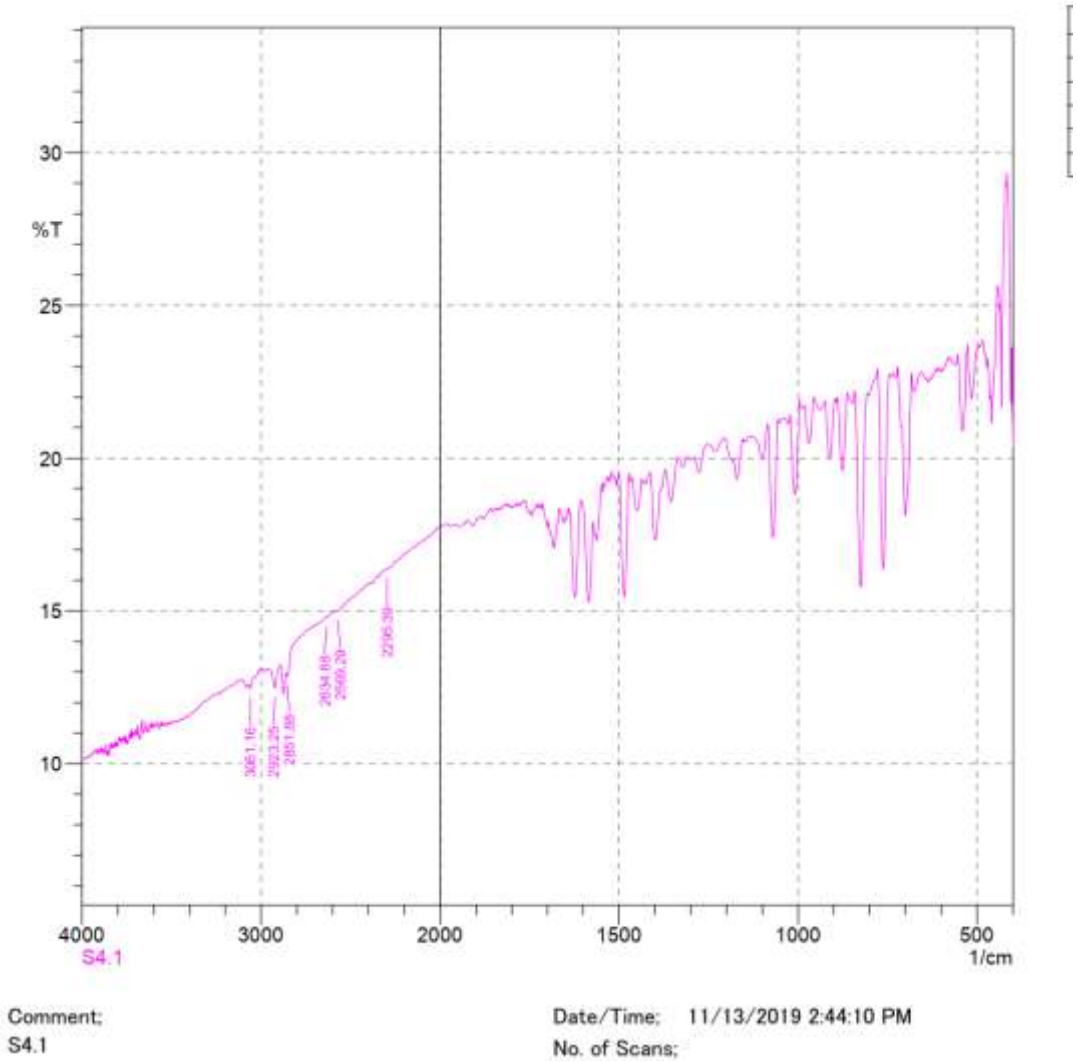

Figure 1(c): Infrared spectrum of Schiff base S_4

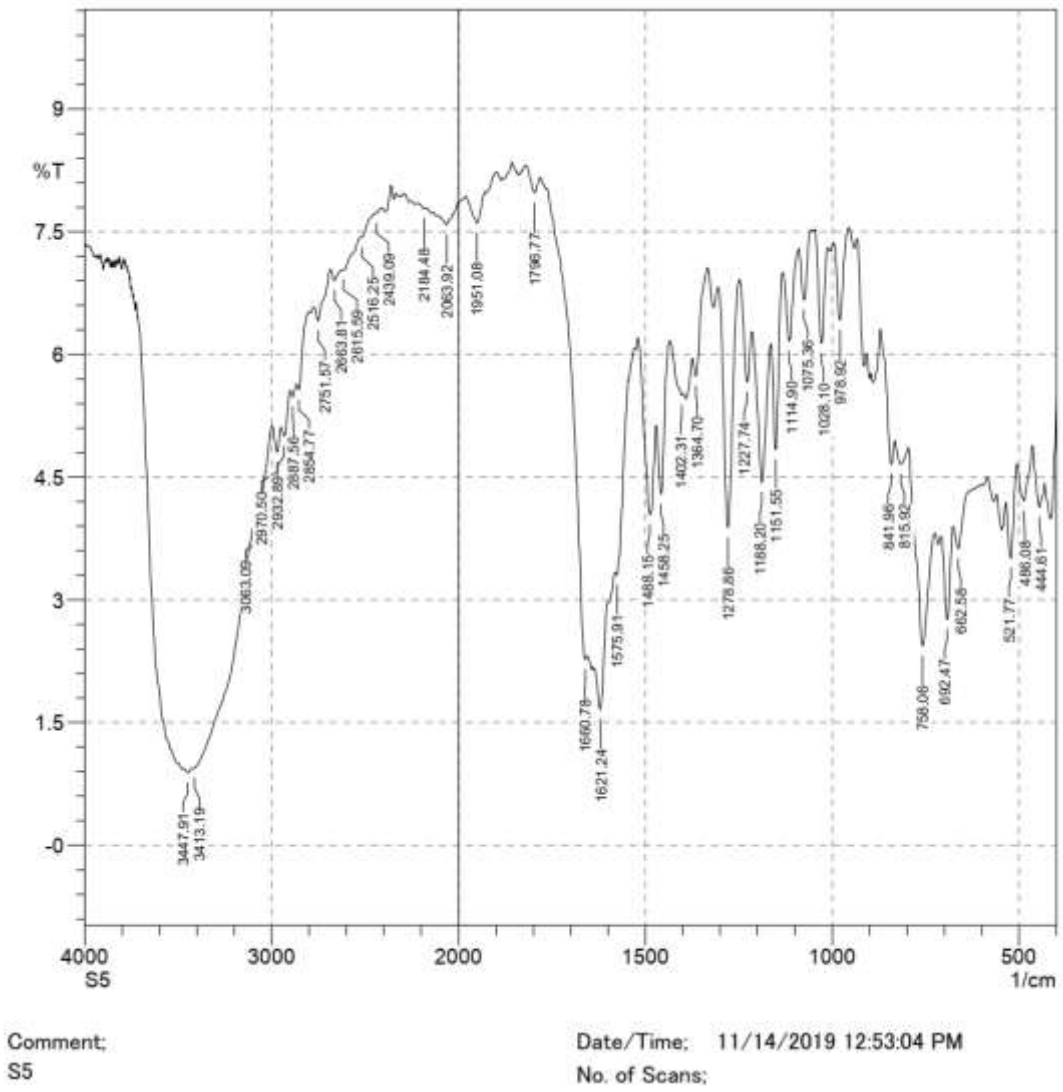

Figure 1(d): Infrared spectrum of Schiff base S_5

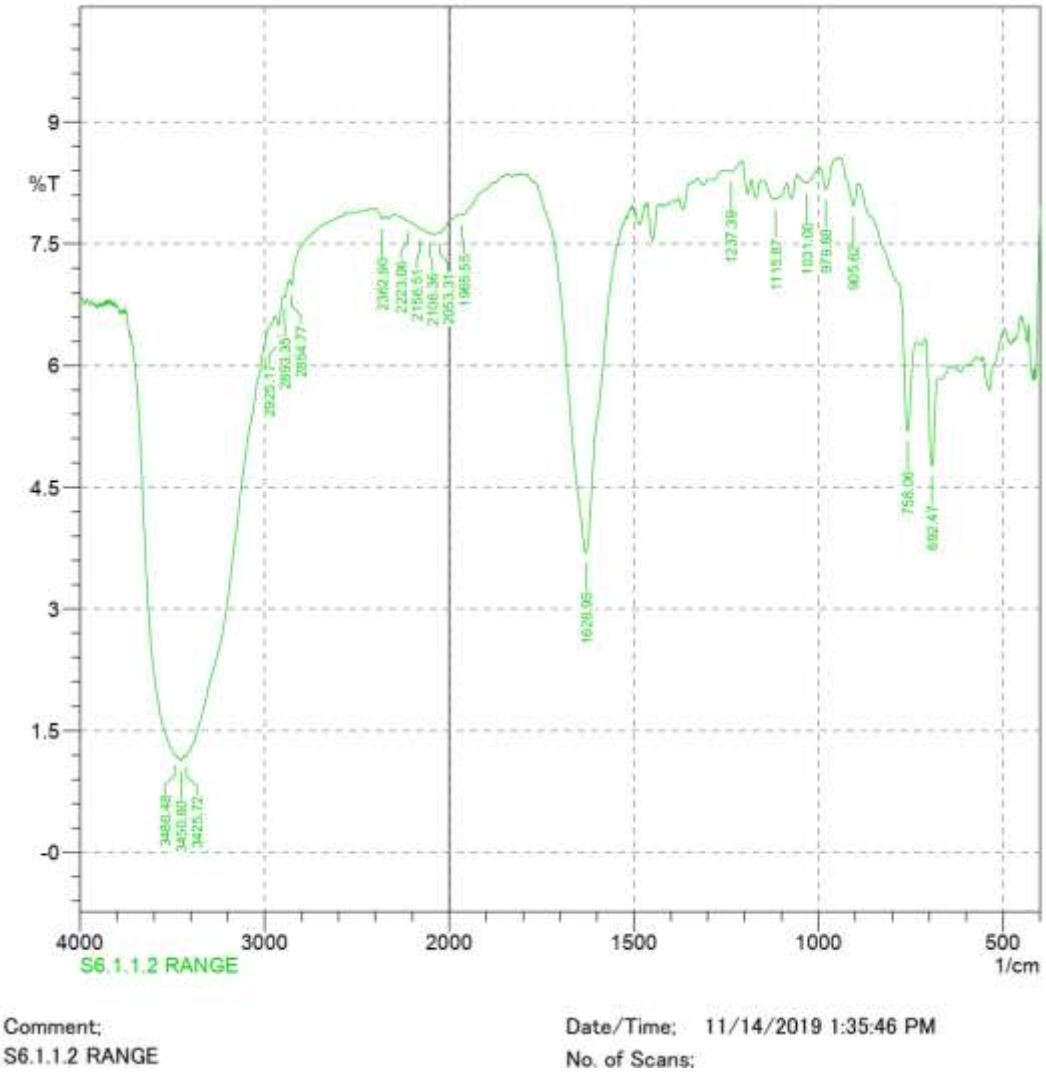

Figure 1(e): Infrared spectrum of Schiff baseS_6

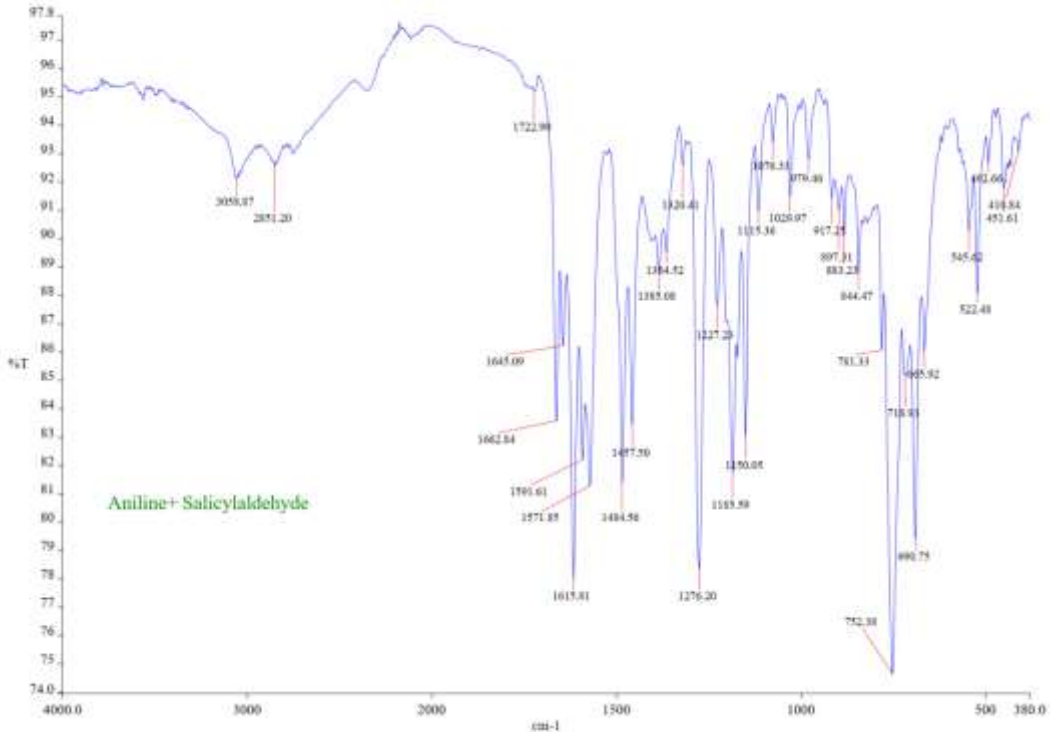

Figure 1(f): Infrared spectrum of Schiff base S_5

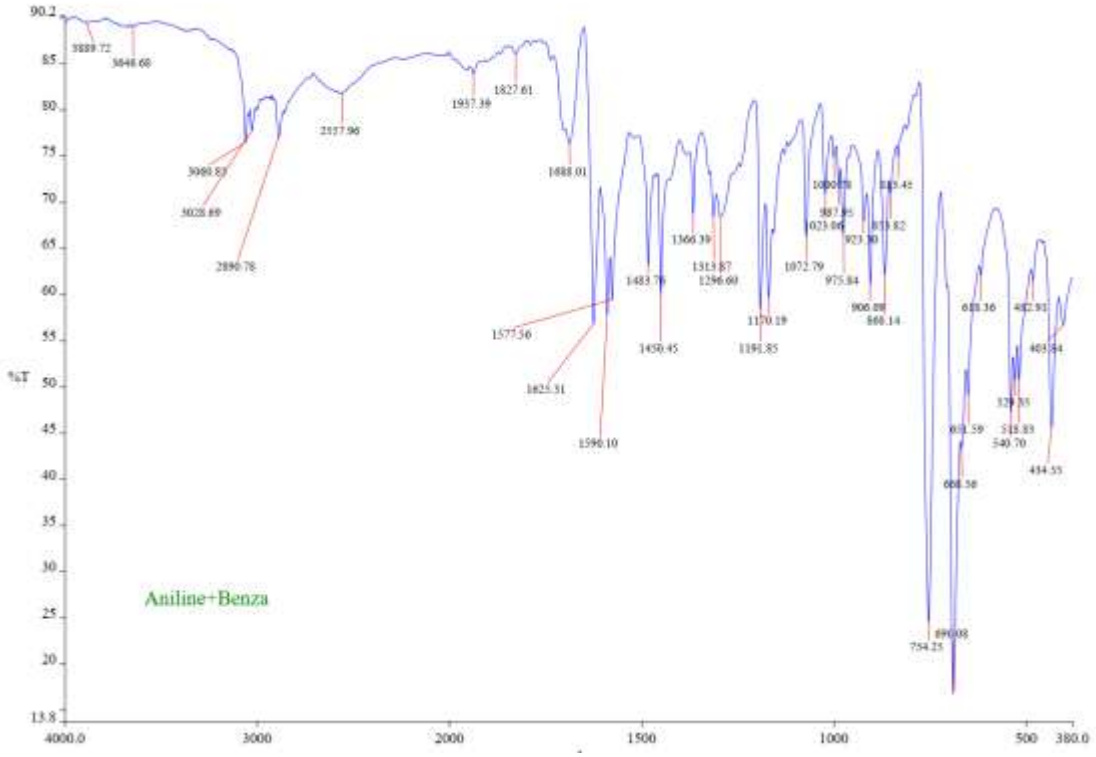

Figure 1(g): Infrared spectrum of Schiff base S_6

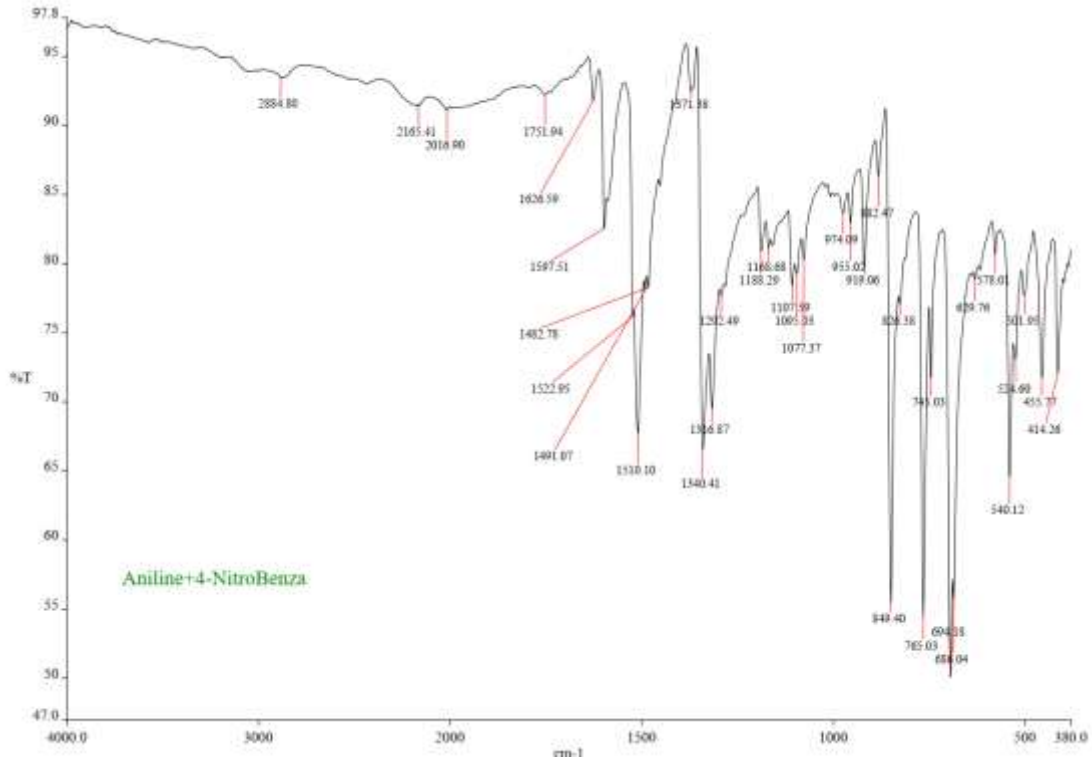

Figure 1(h): Infrared spectrum of Schiff base S_4

Appendix 2: UV-Vis Spectra of compounds S_2- S_6

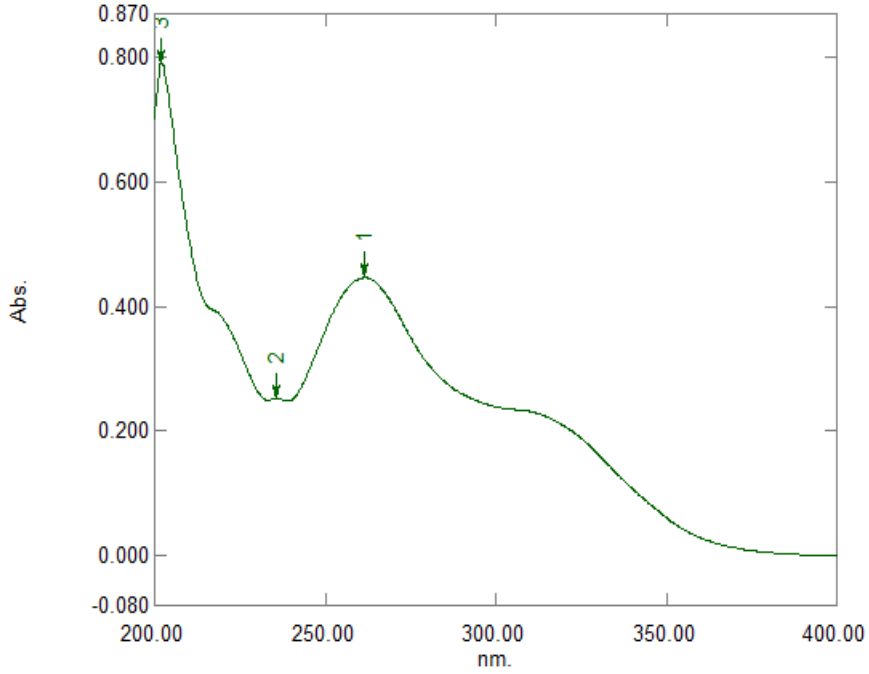

Figure 2(a): UV/Vis spectrum of Schiff base S_2

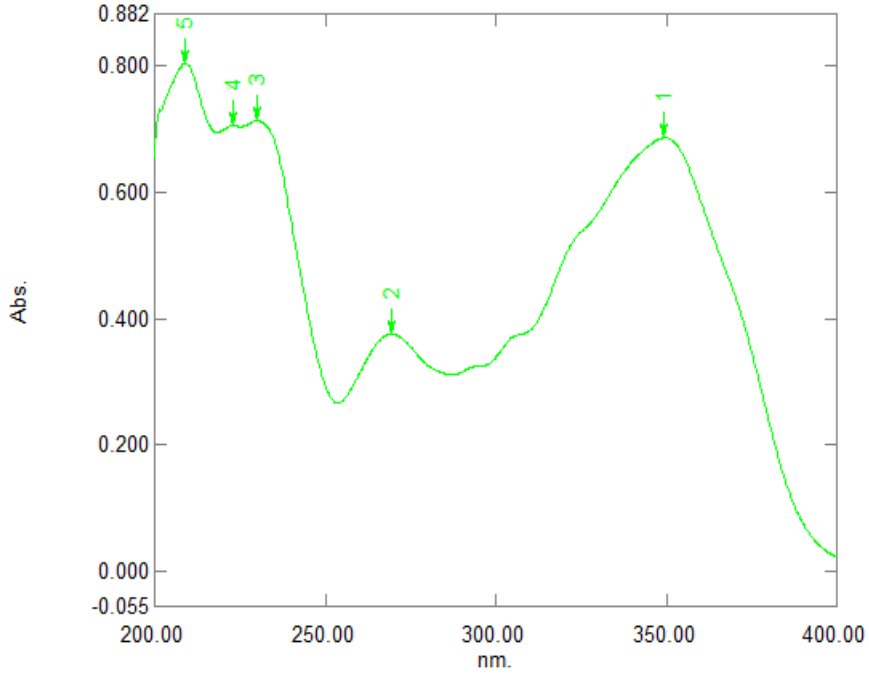

Figure 2(b): UV/Vis spectrum of Schiff base S_3

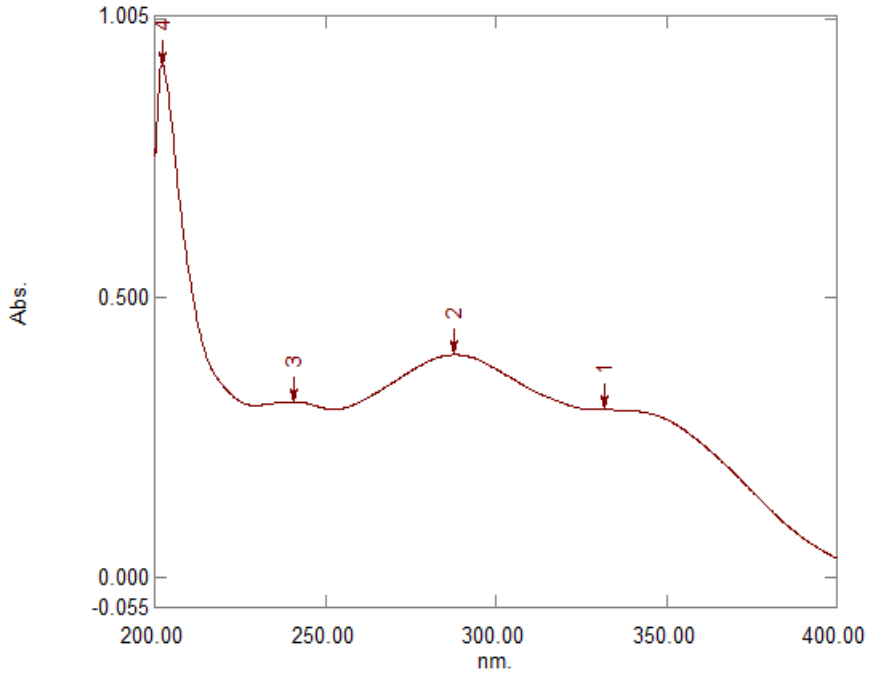

Figure 2(c): UV/Vis spectrum of Schiff base S_4

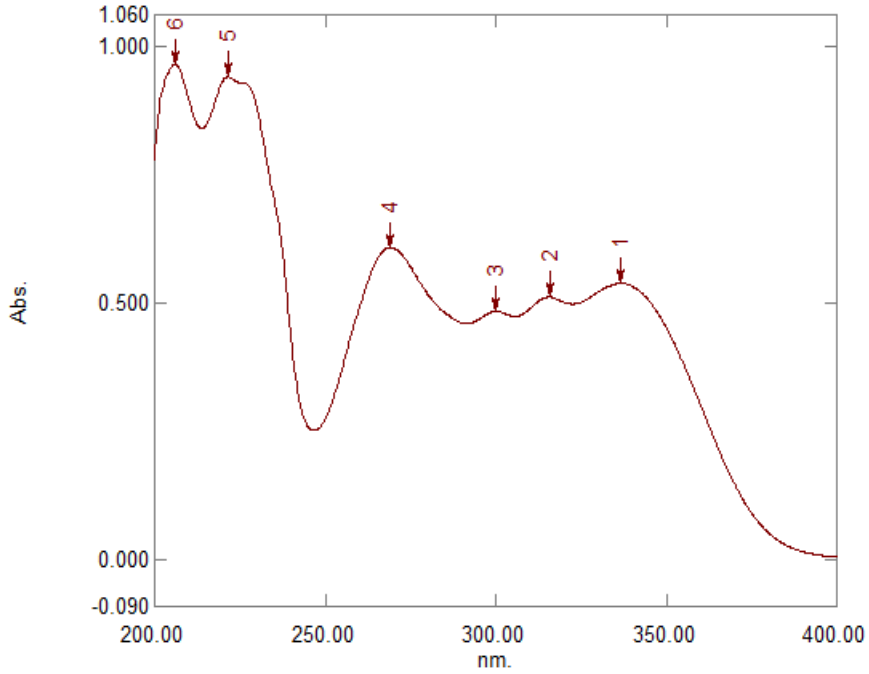

Figure 2(d): UV/Vis spectrum of Schiff base S_5

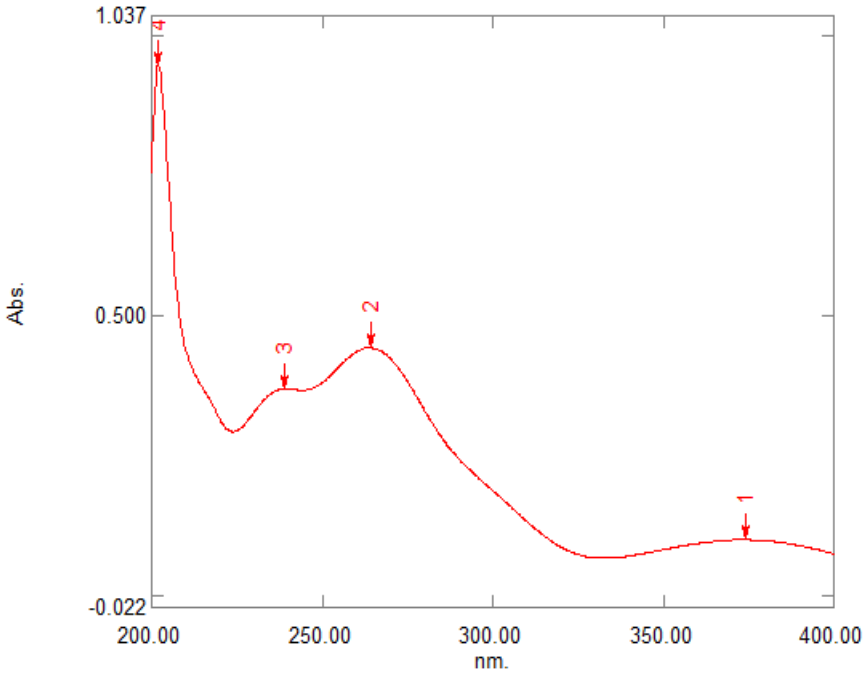

Figure 2(e): UV/Vis spectrum of Schiff base S_6

Appendix 3: Chuka University Ethics Review Letter

Appendix 4: NACOSTI Authorization